535
8-10-78

Dh. 364

ORO-4944-7

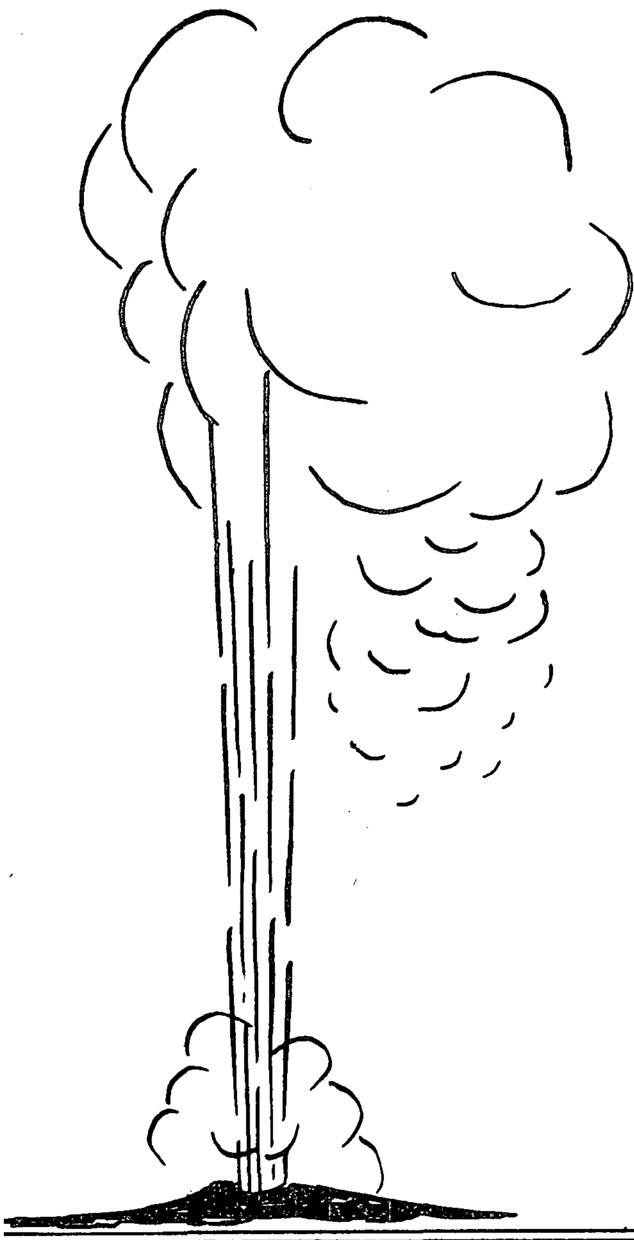

RESOURCE UTILIZATION EFFICIENCY IMPROVEMENT
OF GEOTHERMAL BINARY CYCLES, PHASE II

Final Report, June 15, 1976—December 31, 1977

By
Kenneth E. Starling
Harry West
Khan Zafar Iqbal
C. C. Hsu
Z. I. Malik
L. W. Fish
C. O. Lee

Work Performed Under Contract No. EY-76-S-05-4944

School of Chemical Engineering and Materials Science
University of Oklahoma
Norman, Oklahoma

MASTER

U. S. DEPARTMENT OF ENERGY
Geothermal Energy

ORO-4944-7
Distribution Category UC-66d

REPORT ORO-4944-7

RESOURCE UTILIZATION EFFICIENCY IMPROVEMENT OF GEOTHERMAL BINARY CYCLES - PHASE II

Final Report

Prepared by

Kenneth E. Starling,
Harry West,
Khan Zafar Iqbal,
C.C. Hsu,
Z.I. Malik,
L.W. Fish,
C.O. Lee

The University of Oklahoma
School of Chemical Engineering and Materials Science
202 West Boyd
Norman, Oklahoma 73019

June 15, 1976 - December 31, 1977

PREPARED FOR THE U.S. ENERGY RESEARCH AND
DEVELOPMENT ADMINISTRATION
UNDER CONTRACT NO. E-(40-1)-4944

ABSTRACT

During Phase II of this research program, the following elements of research have been performed: (1) improvement in the conventional geothermal binary cycle simulation computer program, (2) development of a direct contact brine heat exchanger algorithm for the cycle simulation program, (3) development of a preheater algorithm for the cycle simulation program, (4) modification of the basic simulation program to incorporate the staged flash binary cycle, (5) development of a parameter optimization algorithm to aid cycle evaluation studies (6) sensitivity analysis of cost factors, (7) comparison of pure hydrocarbon and binary mixture cycles.

TABLE OF CONTENTS

Table of Contents (continued)

1. OVERVIEW

1.1 Statement of Objectives

This research project addresses the problem of the selection of a working fluid and suitable operating conditions for optimal geothermal binary cycle performance and minimum capital cost per kilowatt of plant generating capacity. It is believed that mixtures offer possible advantages over pure compounds for use as working fluids in geothermal binary cycles. Therefore, both pure fluids and mixtures are being considered as working fluids in the evaluation of alternative cycles.

To satisfactorily carry out the evaluation engineering studies required to evaluate the potential of mixtures as working fluids in geothermal binary cycles and consider the effects of varying operating conditions on resource utilization for alternative cycles, a computer simulation of geothermal binary cycles capable of using <u>both</u> pure fluids and mixtures as working fluids must be utilized. The evaluation of mixture cycles requires that the simulator utilize a thermodynamic and physical properties package capable of accurate prediction of not only pure fluid but mixture properties.

The ongoing research, which is Phase II of a planned three-phase overall geothermal project at the University of Oklahoma includes the following elements: (1) development of a geothermal binary cycle simulation computer program capable of mixture and pure fluid cycle simulation, (2) incorporation in the simulator of an accurate thermodynamic properties computer program package (including hydrocarbon mixtures and pure fluids), (3) development of alternate cycle operational strategies, including a preheater, staged flash binary cycle, and direct contact heat exchangers, (4) development of design criteria for maximizing geothermal resource utilization in binary cycles, (5) evaluation of the advantages and disadvantages of the use of mixtures as working fluids in geothermal binary cycles, (6) comparison of mixture and pure fluid cycles, including relative equipment sizing and economics.

1.2 Simulation Capabilities

In order to accomplish the aforementioned objectives, a computer simulation of the geothermal binary cycle energy conversion process was developed. Since a variety of cycle alternatives were included in the investigation, a series of simulation system options were designed to permit cost-effective utilization of available computer facilities and to allow system flexibility for the changing requirements of a research-oriented investigation. Development of the simulation system options was also directed toward computer program accessibility in order to prepare for eventual use by geothermal system design engineers.

The geothermal simulation system options can be classified into five principal categories; (1) Cycle Process System, (2) Thermodynamic Property Estimation, (3) Equipment Size Determination, (4) Optimization of Process Operating Conditions, and (5) Economic Estimation.

Table I presents an overview of the primary features of the geothermal process simulation. The solid circles indicate current operational features. The open circles indicate additions originally planned for Phase III. The Phase III plan originally contained the documentation of all of the GEO simulation options, as noted by the open circles in Table I.

1.2.1 <u>cycle process system</u>

The major elements of the conventional geothermal binary power plant are shown in Figure 1.1. The process consists of the following major units:

1. Brine Heat Exchanger
2. Turbine-generator
3. Condenser and Cooling System
4. Cycle Pump
5. Wells and Gathering System
6. Auxiliary Plant Equipment

The nodal points indicated in Figure 1.1 correspond to the process state points calculated in the simulation system. However, due to the possibility of temperature pinch points within the heat transfer units, each heat exchanger is subdivided during the calculation.

The direct contact brine heat exchanger option noted in Table 1 utilizes the same basic cycle. Rather than indirect heat transfer using a shell-and-tube heat exchanger, the working fluid is vaporized in direct contact with the geothermal brine.

The use of a working fluid preheater is suggested when excessive superheat remains in the turbine exhaust. Simulation

TABLE I

PRIMARY FEATURES OF THE GEOTHERMAL PROCESS SIMULATION SYSTEM

SIMULATOR SYSTEM OPTION	GEO 1	GEO 2	GEO 3	GEO 4	GEO 5	GEO 6	GEO 7	GEO 8	GEO 9	GEO 10
CYCLE PROCESS SYSTEM										
1. Conventional	●	●	●	●	●					○
2. With preheater						●				
3. Direct contact brine heat exchanger							●			
4. Staged flash binary								●		
5. Dual boiler									○	
THERMODYNAMIC PROPERTIES										
1. Pure working fluid	●	●	●	●	●	●	●		○	○
2. Mixtures	●	●	●	●	●	●	●		○	
EQUIPMENT SIZE										
1. Selected heat transfer coefficients and pressure drops				○	●	○	○	○	○	○
2. Heat exchanger design		●	●	●	●	●	●	●	○	
OPTIMIZATION										
1. Sequential search				●	●					
2. Flexible tolerance (multiparameter)					●					
ECONOMICS										
1. Capital cost model			●	●	●	●	●	●	●	○
2. Unit energy cost				○	○	○	○	○	○	○
Listing Available				●	○	○	○	○	○	○
Card Deck Available				●	○	○	○	○	○	○
Documentation Available				○	○	○	○	○	○	○

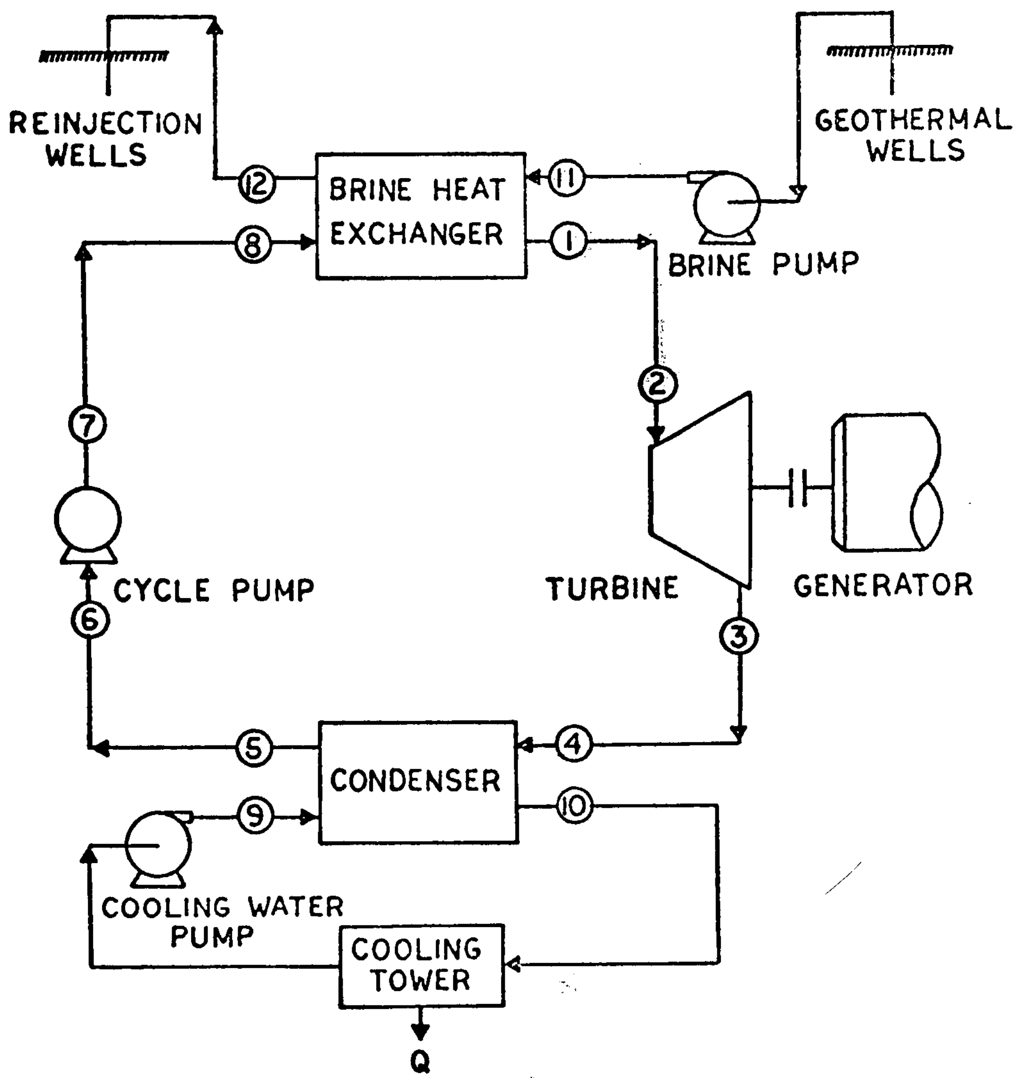

Figure 1.1 Geothermal Binary Cycle Streams and Nodes

of this system requires a modification of the basic cycle as shown in Figure 1.3.

For particularly corrosive or high salinity geothermal brines, the staged flash binary cycle has been proposed to use only the flashed vapor portion of the geothermal brine to heat the working fluid, as shown in Figure 1.2 The cascade or staged heat exchangers can accept the energy transfer from the brine with a reduced fouling potential and more efficient heat transfer.

The dual boiler system shown in Figure 1.4 represents an attempt to increase the resource utilization of a moderately low temperature brine.

1.2.2 thermodynamic property estimation

The estimation of the thermodynamic properties of the working fluid as it progresses through the power cycle is an extremely important factor in process evaluation. The HSGC program, documented in Report ORO-4944-2 (1), uses the Starling-Benedict-Webb-Rubin equation of state. The HSGC program is capable of predicting the properties of mixed hydrocarbons.

Table II presents a list of the working fluids which are available in the thermodynamic estimation system and have been used as working fluid candidates in the cycle simulation system. The asterisk indicates that the component can be used in a mixture working fluid. The components in parentheses may be available at a later date.

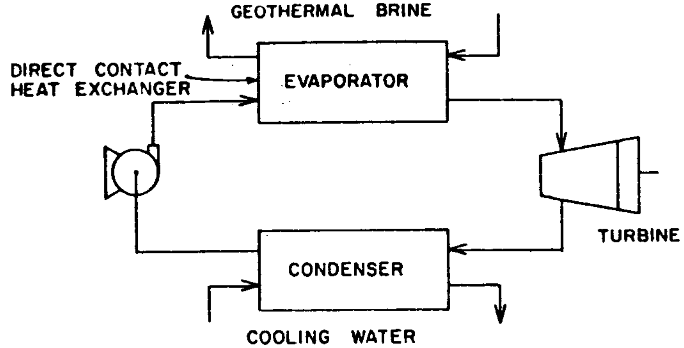

FIGURE 1.1 DIRECT CONTACT CYCLE

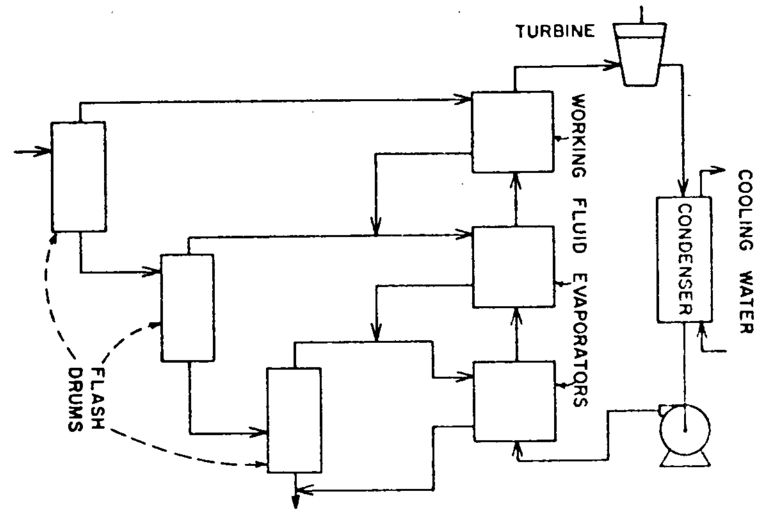

FIGURE 1.2 STAGED BINARY FLASH

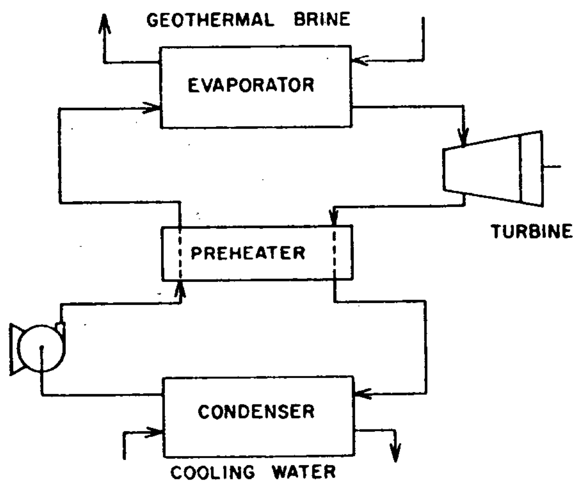

FIGURE 1.3 REGENERATIVE PREHEAT CYCLE

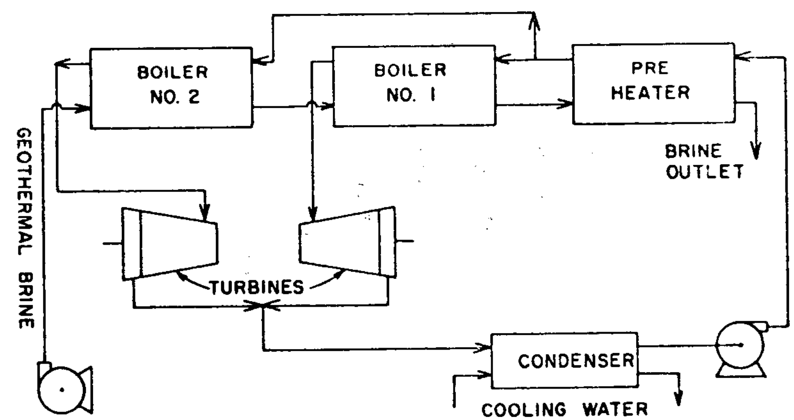

FIGURE 1.4 DUAL BOILER CYCLE

TABLE II

WORKING FLUIDS AVAILABLE
IN THE CYCLE SIMULATION

Propane *	R-11
n-Butane *	R-114
i-Butane *	R-113
n-Pentane *	R-152A
n-Hexane *	R-22
Ammonia	Toluene
Water	(Fluorinol)

1.2.3 equipment size selection

In order to simplify the task of detailed process unit specification, the selection of heat transfer coefficients and process pressure drops can be made apriori. This option permits the designer relative freedom from mechanical detail, yet furnishes sufficient data to make rational design decisions. A heat exchanger (shell-and-tube) design routine is also available in order to provide a more detailed description of the required process unit. The calculational details of the heat exchanger design routine are described in Report ORO-4944-3 (2).

1.2.4 optimization of process operating conditions

Using a performance function such as the minimum capital cost per unit generating capacity, the cycle simulation system can select the optimal process operating conditions for a selected brine inlet temperature and selected working fluid.

Two methods of optimization are available--the sequential search and the more complex flexible tolerance method. These methods are described in more detail in a subsequent section of this report.

1.2.5 economic estimation

The cost of each of the major process units is obtained by available process size/cost correlations. The total plant cost is then obtained through the use of the factored-estimate cost estimation system, as described in detail in Report ORO-4944-5 (3).

The unit energy cost model is currently under development. This methodology will permit an estimation of the unit energy cost by including energy accounting principles.

2.0 IMPROVEMENTS TO THE GEOTHERMAL BINARY CYCLE SIMULATOR

Based on engineering analysis of the preliminary results of the cycle studies using the geothermal binary cycle simulator, several improvements were made to increase the flexibility of the simulation program. The details concerning the simulator improvements were documented in report ORO-4944-5 (3). In addition to the aforementioned modifications, several computer system modifications were instituted to permit cost-effective evaluations.

The addition of several options, including a preheater, direct contact heat exchanger, staged flash binary, and optimization routines, are discussed in subsequent sections of this report.

The design basis parameters used with the conventional geothermal binary cycle simulator are detailed in Appendix A. A sample output of the cycle simulator is presented in Appendix B.

3.0 PREHEAT BINARY CYCLE SIMULATION

The preheat binary cycle simulation capability was accomplished by adding a preheater subroutine and by making some additional changes to the GEO4 simulator. The preheater serves as a medium for heat exchange between the superheated vapor from the turbine exhaust and compressed liquid from the cycle pump. Thus, the superheat of the working fluid from the turbine exhaust is used to preheat the working fluid before entry into the brine heat exchanger.

Figure 3.1 shows the process flow streams and nodes of a preheat geothermal binary cycle. The preheater design presently utilized is a shell and tube heat exchanger with vapor on the shell side and liquid on the tube side. An objective of preheat cycle simulation is to define the working fluid state points numbered 1 through 8 on Figure 3.1, subject to the limitations of fluid properties and process unit capabilities. In order to do this, two additional pinch point temperature differences were added to the simulator input: one at the preheater inlet of the liquid from the cycle pump (i.e., ΔT between state points 4 and 7), DTPHI, and the other at the entrance to the preheater of the vapor from the turbine exhaust (ΔT between state points 3 and 8), DTPHO. Non-zero input values of DTPHI, and DTPHO key the simulator to make the preheat cycle calculations. Fixed (input) shell side pressure drops are utilized in the preheater and condenser with the tube pitch in the preheater and condenser calculated as a floating variable. Heat transfer coefficients for both the shell and tube sides of the preheater are calculated using the Dittus-Boelter correlation (4).

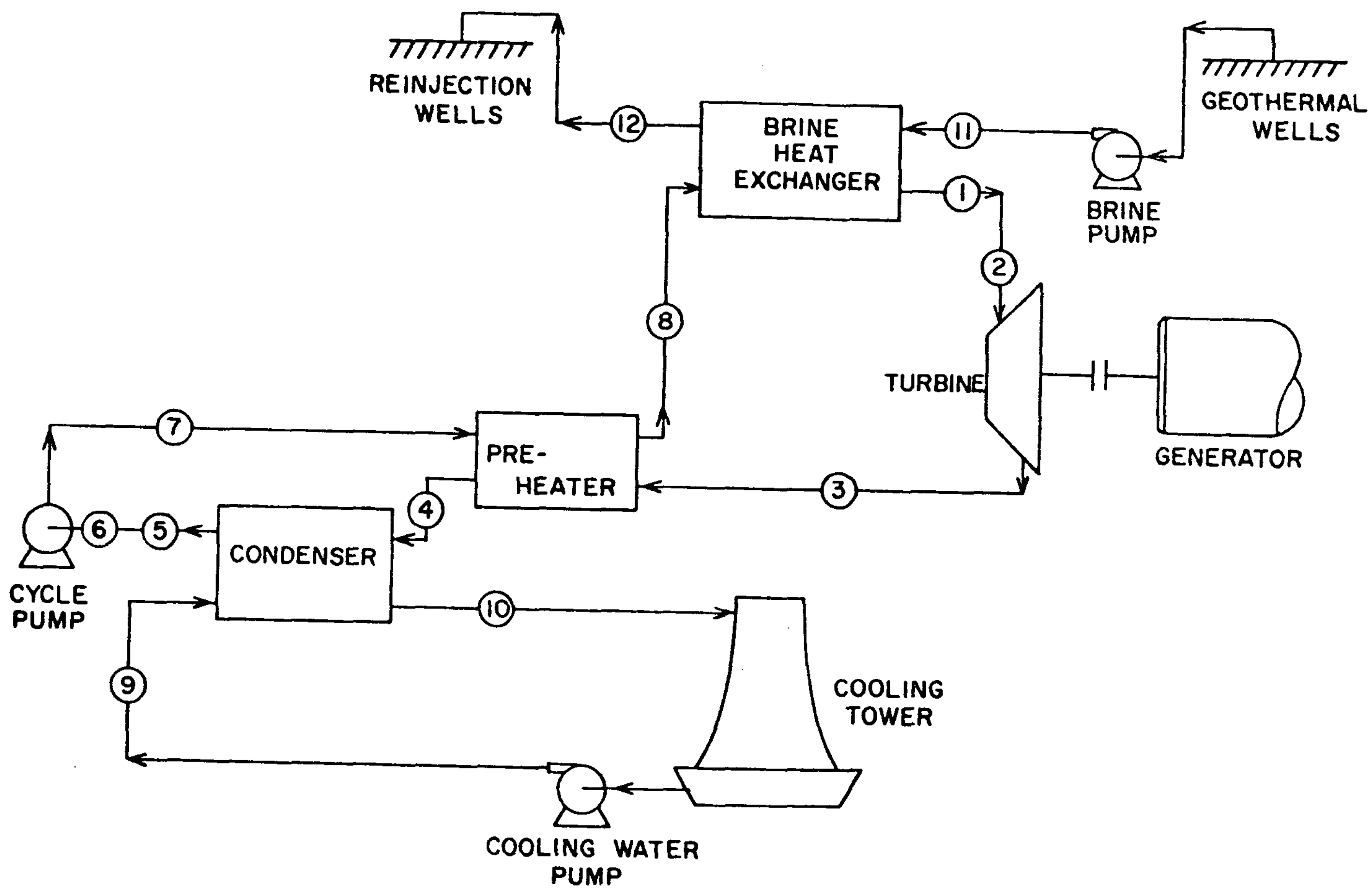

Figure 3.1 Preheat Geothermal Binary Cycle Simulator Streams and Nodes

In the process of developing the preheat geothermal binary cycle simulator, a preliminary evaluation of the preheat cycle was performed for the case of a net 25 MW plant with a 400°F georesource and isopentane as the working fluid. Isobutane was not considered as the working fluid because there is too little superheat at the turbine exit. In the calculations which were performed, attention was focused on the following factors which can contribute to an advantage of the preheat cycle over the conventional cycle.

(1) Decrease in total heat transfer surface area requirements.

(2) Decrease in cooling water flow rate and cooling tower duty.

(3) Increase in brine exit temperature (thereby reducing brine precipitation probability).

The results of the simulation of the preheat cycle are compared with the cycle without preheat in Table 3.1. It can be noted that with the preheat cycle there are reductions in the heat transfer surface area of 2.3%, cooling water flow rate of 3.6%, and the capital cost of 1.2%. The reduction in the cost of the cooling tower for the preheat cycle is 3.8%. Although the decrease in total system capital cost is only 1.2%, the decrease in electrical energy cost for the preheat cycle would be greater because of the reduction in the make-up water requirements. In addition, the preheat cycle was not optimized whereas the operating conditions for the cycle without preheat are optimized. Thus, although the margin is small for the 400°F georesource, the preheat cycle would offer definite promise if the turbine exit superheat were greater. Using isopentane as the working fluid, the

Table 3.1 Comparison of Isopentane Geothermal Binary Cycles With and Without Preheat for a 400°F Georesource.

	With Preheat	Without Preheat
Net Power Output, MW	25.	25.
Brine Inlet Temperature, °F	400.	400.
Brine Exit Temperature, °F	217.	212.
Cooling Water Inlet Temperature, °F	80.	80.
Cooling Water Exit Temperature, °F	102.	102.
Cooling Water Flow Rate, lb/hr $x10^{-6}$	26.8	27.8
Turbine Inlet Temperature, °F	272.	272.
Turbine Inlet Pressure, psia	200.	200.
Heat Transfer Surface Area, ft^2x10^{-2}		
(1) Brine Heat Exchanger	312.	317.
(2) Condenser	1216.	1309.
(3) Preheater	62.	0.
(4) Total	1590.	1627.
Preheater Minimum Approach Temperature, °F	55.	-
Net Thermodynamic Efficiency, %	13.4	13.0
Capital Cost, $/kw	755.	764.

amount of superheat at the turbine exit increases as the georesource temperature increases. Therefore, it is probable that the preheat cycle can offer clear economic advantages over the cycle without preheat at georesource temperatures approaching 500°F.

4.0 DIRECT CONTACT BRINE HEAT EXCHANGER

Direct contact heat exchangers can be classified as counter-current or co-current. The pipe mixer and free surface tray are both examples of co-current equipment. There are other variations of co-current devices such as agitated vessels and venturi type mixers. For geothermal power production, the co-current direct contact exchangers are economically unattractive (5, 6).

There are three general types of counter-current direct contact heat exchangers: (1) spray towers, (2) perforated tray towers and (3) packed columns. The perforated tray tower contains a series of trays which increase the efficiency of the heat transfer per unit height. The spray column is merely an empty shell. However, since the flow capacity of the perforated tray tower is smaller than that of spray column by a factor of 3 to 4, the column diameter of the tray tower will be as much as twice that of spray column. The packed column resembles the spray tower except that the interior of the shell is filled with packing to increase heat transfer efficiency. One disadvantage of the packed column in geothermal use is that the packing would rapidly become fouled by the brine.

In this study, the counter-current spray column was selected as the most promising type of direct contact heat exchanger on the basis of (1) higher flow capacity, (2) simple design and relatively inexpensive equipment, (3) low maintenance due to absence or reduction of scale formation, and (4) the obtainable close temperature approach.

A spray column of the Elgin-type is shown in Figure 4.1. It is designated the Elgin-type column because it was developed by Elgin

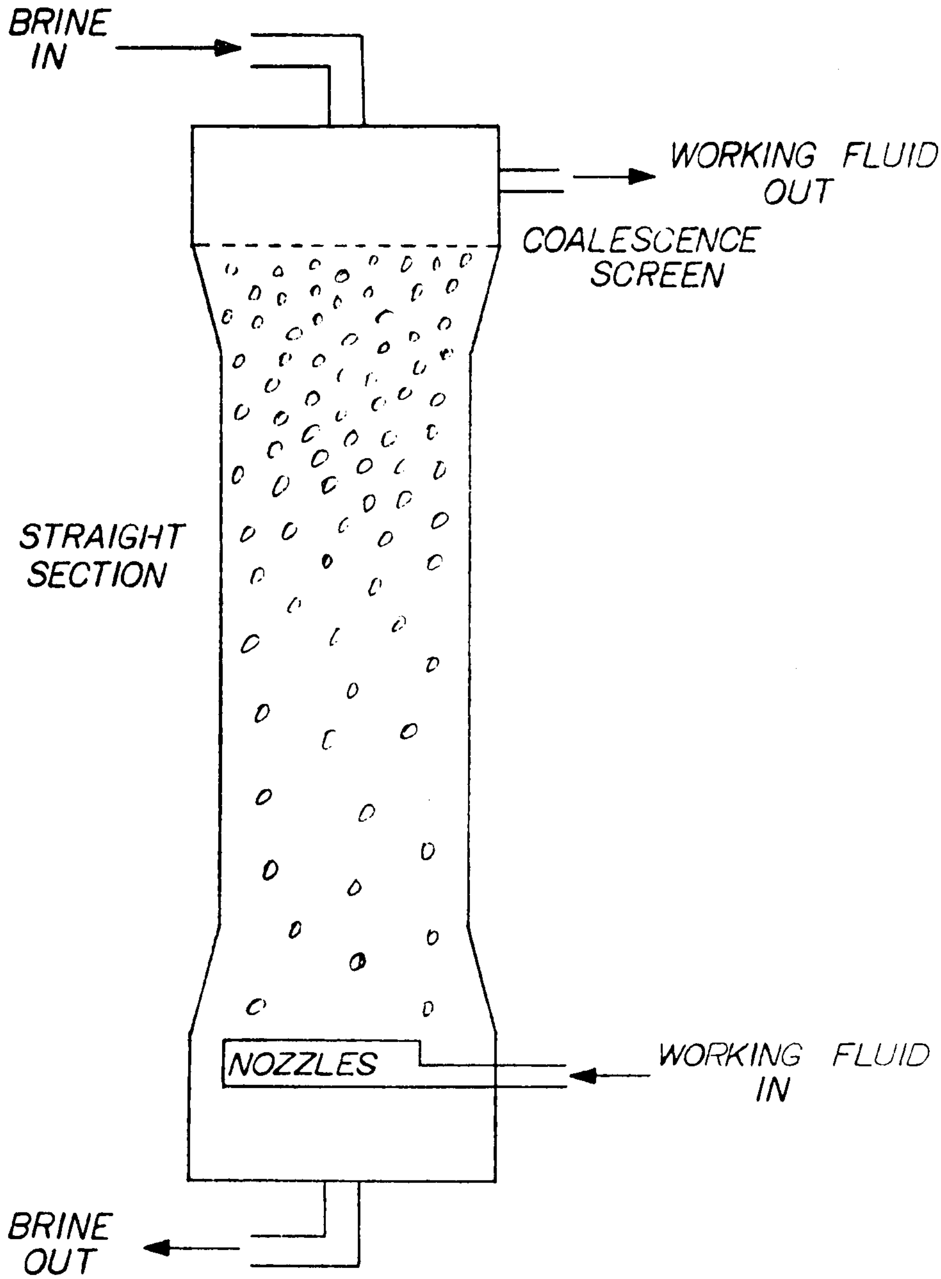

Figure 4.1 Direct Contact Brine Evaporator

and various co-workers. The paper of Blanding and Elgin (7) describes the details of its evolution. Originally, the spray column was designed for mass transfer operations such as liquid-liquid extraction. This operation depended on the immiscibility and difference in density of the two phases. Recently, the spray column has been successfully used as a heat exchanger in desalination processes.

Numerous theories have been proposed to describe the heat transfer mechanism between two phases. Sideman (8) has presented an excellent review of these theories. The objective of this report is not to explore all of these theories, but to size the spray column related to the geothermal cycle.

In the design of a spray column, two factors are particularly important; the height of column and the column diameter. The column diameter is determined by the maximum permissible velocity of the phases involved. The column height is determined from heat transfer considerations.

As shown in Figure 4.1, the heavier continuous phase, geothermal brine, is introduced into the column at the top, flows downward through a straight section and leaves at the bottom of the column. The working fluid is dispersed through nozzles as droplets at the bottom of the column and rises through the straight section to a coalescence screen at the top of the column. The brine is the continuous phase and the working fluid is the dispersed phase.

For a fixed flow rate of the continuous phase, as the flow rate of the dispersed phase is increased, the slowly rising droplets beneath the coalescence screen increase in concentration within the column to a point where more of the dispersed phase cannot be forced through the column. The column is completely filled with closely-packed droplets. Any additional increase in the flow rate of the dispersed phase results in the entrainment of droplets by the continuous phase at the bottom of the column with subsequent loss of working fluid. When the zone of concentrated droplets fills the column, the situation is referred to as a flooded column. The droplets cannot escape freely into the coalescence zone and tend to accumulate in the straight section with the characteristic appearance of closely packed spheres. The column can only operate satisfactorily at a lower flow rate. Further, the efficiency of heat transfer decreases at flooding. When there is a concentrated zone of droplets in one section of the column with the remainder of the column being less concentrated, the column is said to be at its flooding point.

The flooding correlation of Sakiadis and Johnson (9) was used as the basis for calculating the column diameter.

The temperature profile within the spray column was calculated using the mathematical model proposed by Letan and Kehat (10).

In the design of spray column heat exchangers for geothermal cycles, the direct contacting unit is divided into three different heat exchange zones, as shown in Figure 4.2. In each of the heat exchange zones, the heat is transferred from geothermal brine to the working fluid by a different heat transfer mechanism: liquid-liquid heat transfer (preheater); liquid-liquid-vapor heat transfer (boiler); and liquid-vapor heat transfer (superheater). With this arrangement, the working fluid enters the liquid zone as a subcooled liquid at t_1, leaves preheated and enters liquid-liquid-

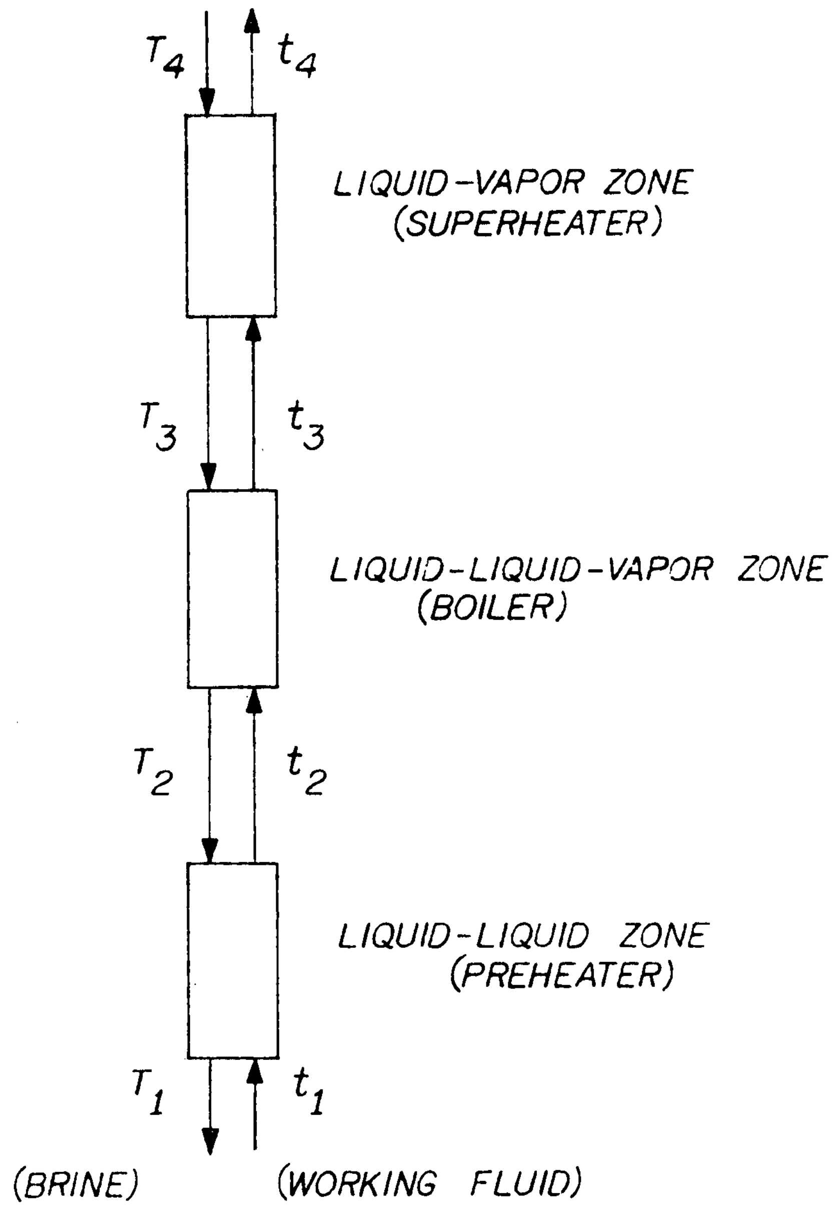

Figure 4.2 Primary Sections of Direct Contact Brine Evaporator

vapor zone at its bubble point temperature t_2, leaves the boiler and enters the liquid-vapor zone as saturated vapor at its dew point temperature t_3, and finally leaves the superheater as superheated vapor at the temperature t_4. The hot brine enters the superheater at temperature T_4, leaves the superheater and enters the boiler at the temperature T_3, leaves the boiler and enters the preheater at the temperature T_2, and finally leaves the preheater at temperature T_1. The outlet pressure of the working fluid is the same (approximately) as the inlet pressure of the turbine. Therefore, the operating pressure of the spray column is chosen to be the same as the inlet pressure of the turbine.

Several FORTRAN IV subroutine programs for designing spray column heat exchangers have been developed for inclusion into the geothermal simulation GEO-4 to perform the geothermal cycle calculations. The direct contact evaporation sizing module permits the use of parallel units in order to keep the tower diameters within realistic economic constraints. The cost model for the direct contact evaporation is based on standard pressure vessel sizing techniques.

The results obtained from the simulator are compared with the experimental data reported by DSS Engineers (11) in Table 4.1.

Table 4.1

Flow Rate of Brine	Flow Rate of Working Fluid	HEIGHT OF COLUMN		Heat Transfer		REGION or ZONE
		Experimental Ft.	Predicted Ft.	Calculated	Predicted	
3004	2547	6	6.4	4053	4018.58	Liquid-Liquid Region
--	--	6	0.009	17,000 Max.	22.4×10^5	Boiler
--	--	--	--	17,000 Max.	19.7×10^5	Superheater

5.0 STAGED FLASH BINARY CYCLE MODIFICATION

For particularly corrosive or extremely high salinity geothermal brines, the staged flash binary has been proposed to alleviate the problems associated with heat exchanger fouling.

The staged flash binary heat exchanger system consists of several flash drums and heat exchangers. In each flash drum, the pressure of the geothermal brine is reduced to yield saturated steam. This steam is then passed through a scrubber to reduce the dissolved solid contents which are carried over with the steam. The scrubbed steam passes through the heat exchanger on the tube side (condensing steam) with the working fluid on the shell side.

Figure 5.1 shows the flow sheet for the case of a four stage flash system. A minimum of two and a maximum of four stages can be used in the computer program. If five stages are chosen, then the first three stages will serve as preheaters, one as the boiling section, and the last one the superheating section of the working fluid. When no superheating is required, then a minimum of two stages can be used: one dealing with the boiling section of the working fluid and the other as a preheater.

To determine the heat transfer coefficient for the condensing steam, the Bokyo-Kruzhlin correlation (12) is used. For the single phase working fluid, the Seider-Tate correlation (13) is used. In case of the boiling section of the working fluid, Chen's boiling heat transfer correlation (14) is used.

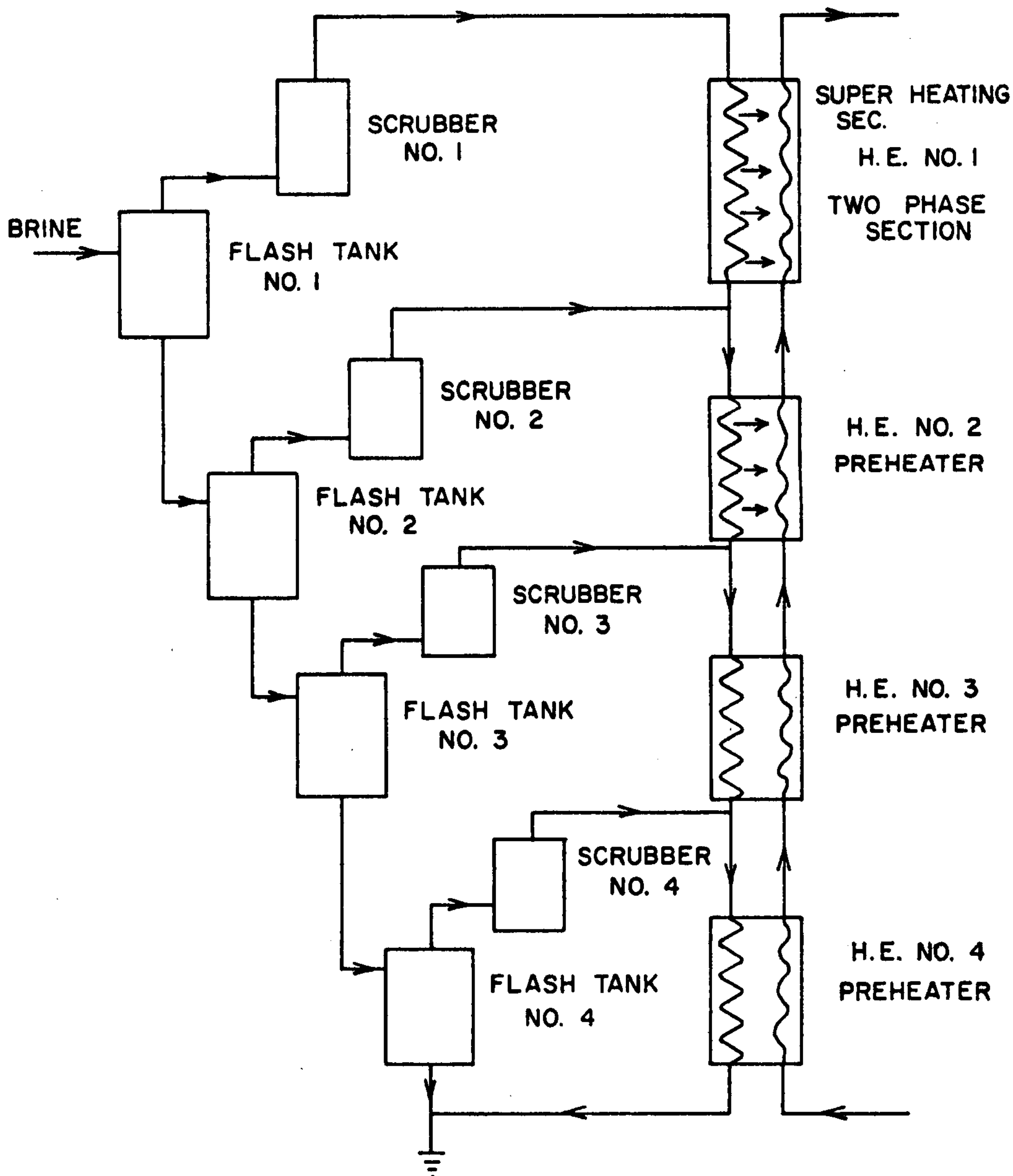

Figure 5.1. Staged Flash Brine Heat Exchanger System

6.0 DEVELOPMENT OF SEQUENTIAL OPTIMIZATION ROUTINE

The initial effort of optimizing geothermal binary cycles has included the development of a direct sequential search algorithm similar to that developed for ocean thermal energy conversion (OTEC) cycles by TRW, Inc. (15). This algorithm has been used in conjunction with the upgraded Phase I cycle simulator developed by the authors (16).

The objective function which was selected for minimization in the optimization algorithm is system capital cost per kilowatt of net plant capacity. Other objective functions which were to be added later include cost per kilowatt-hour of net plant output, negative of the net plant capacity per lb of brine used, negative of the net plant output, and negative of the net plant work divided by the availability.

The simulator can be used in three modes: (1) a "once-through" calculation wherein the net plant capacity is calculated from an input value of brine flow rate, and heat exchanger calculated fluid pressure drops may not be consistant with input values; therefore it is the responsibility of the cycle designer to resolve the heat exchanger pressure drops external to the simulation; (2) the heat exchanger pressure drops and the brine flow rate are adjusted to obtain a desired net plant capacity; (3) the selected objective function is minimized with respect to any one or more of six parameters while the steps of (2) are repeated for each perturbation of the parameters.

The parameters are varied by a fixed step direct search performed on the parameters one at a time. Parameters selected for analysis include: (1) evaporator working fluid exit approach temperature, (2) evaporator minimum pinch temperature, (3) condenser working fluid exit approach temperature, (4) condenser working fluid inlet approach temperature (5) turbine inlet pressure and (6) cooling water exit temperature. The difference in the objective function value is checked as each parameter is varied in a fixed increment which is an input value for each parameter. The incrementation will continue in the direction leading to a minimum until the objective begins to increase. If more than one parameter is to be varied, the parameter value which yields the minimum objective is used in subsequent calculations with the other parameters. The sequence of parameter variations is essentially in the order as listed above. The uncertainty region containing the local minimum with respect to each parameter can be reduced by decreasing the various input parameter increment values and repeating the search procedure.

The optimization routine is not a substitute for engineering judgement, but rather an effective tool which permits the design engineer to evaluate multiple cases with minimal effort.

7.0 DEVELOPMENT OF SIMULTANEOUS OPTIMIZATION ROUTINE

The basic limitation of the sequential optimization routine described previously is that the final optimum value of the objective function may be different, depending on the order of the optimization procedure. A simultaneous optimization routine, by definition, would not suffer from this restriction.

A multi-dimensioned steepest descent optimization routine based on the flexible tolerance method (17) was developed. This algorithm permits the optimization of the defined objective function without regard to parameter order. Details of this methodology, including computer algorithm flow charts, are available (18).

The objective function used in this optimization algorithm is the system capital cost per kilowatt of net plant generation capacity.

The variables used to minimize the objective function are:

(1) turbine inlet pressure

(2) brine inlet approach temperature

(3) brine heat exchanger pinch point temperature difference

(4) cooling water exit temperature

(5) condenser inlet approach temperature

(6) condenser exit approach temperature.

The composition of the working fluid and the georesource temperature are the major independent variables used in this study. However, it is not feasible or desirable to include these functions within an optimization routine.

8.0 COMPARISON OF PURE HYDROCARBON AND MIXTURE WORKING FLUIDS

Parameter sensitivity studies were conducted using the geothermal binary cycle simulator to compare pure hydrocarbon and mixture working fluids. The cycle working fluids considered in this study were isobutane, isopentane, and various binary mixtures of these compounds. The cycle operating conditions and performance for the working fluids evaluated in this study are discussed below.

The design basis parameters used to conduct this sensitivity study are listed in detail in Appendix A. The sequential search method was used to determine near optimal values of turbine inlet conditions, heat exchanger approach temperatures and cooling water exit temperature. The general trends which are noted should be correct, although the operating conditions obtained from the sequential search routine may be non-optimal in a few cases.

8.1 Total System Cost

Figure 8.1 illustrates the effect of variations in working fluid molecular weight and georesource temperature on the total system capital cost, in 1976 dollars. Tables 8.1 through 8.4 show the various cycle parameters for the 300° to 500°F georesource temperature range. At 300°, 350° and 400°F three different mixtures of iosbutane and isopentane exhibit the lowest total system costs compared to either isobutane or isopentane cycles. This is due primarily to the higher turbine inlet temperatures and/or larger enthalpy change in the turbine attainable for these mixtures compared to pure isobutane or isopentane. A related factor is that

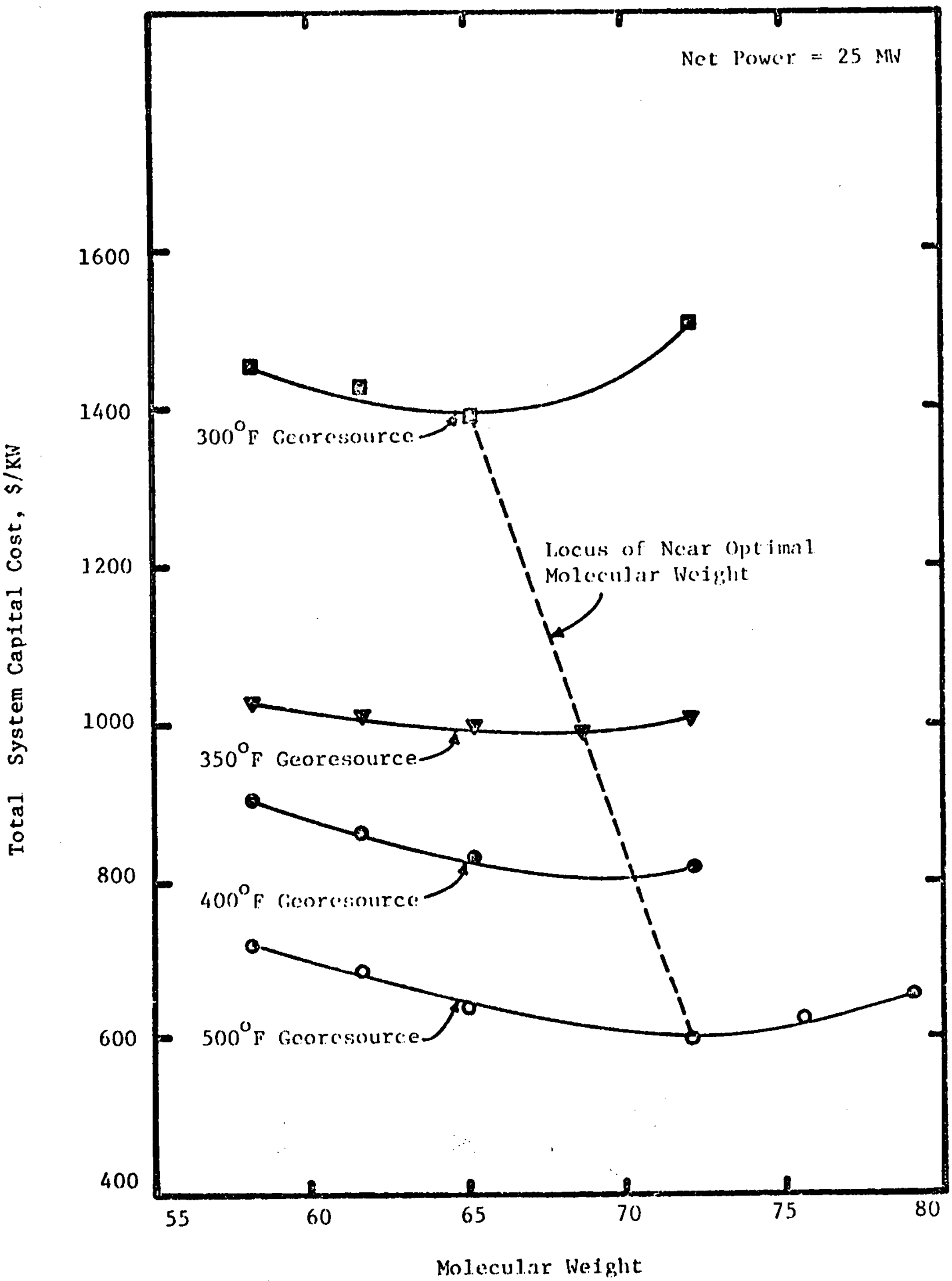

Figure 8.1 Total System Capital Cost Versus Georesource Temperature and Molecular Weight

Table 8.1 Comparisons of Cycle Parameters for the Georesource Temperature of 300°F.

Compound	iC_4H_{10}	iC_4H_{10} = 75% iC_5H_{12} = 25%	iC_4H_{10} = 50% iC_5H_{12} = 50%	iC_5H_{12}
Mol. Weight	58.12	61.626	65.133	72.146
Net Power, MW	25.00	25.00	25.00	25.00
Gross Power, MW	31.07	30.21	29.76	29.93
Plant Cost, $/KW	868	817	772	820
Total System Cost, $/KW	1453	1434	1398	1508
Turbine Inlet P, psia	300	250	200	100
Turbine Inlet T, °F	220	232	235	210
Turbine ΔH, Btu/lb	19.37	21.40	21.97	18.97
Condenser Superheat ΔT, °F	26.0	33.2	38.9	43.4
Cond. Superheat ΔH, Btu/lb	11.95	15.08	17.83	19.05
Condenser Dew Point P, psia	78.1	57.7	44.2	23.6
Condenser Dew Point T, °F	108.0	116.9	119.0	109.0
Heat Exch. Bubble Point T, °F	221.1	223.4	224.0	219.6
Brine Exit T, °F	182.4	191.8	193.0	192
Brine Flow, MM lb/hr	7.515	7.931	8.060	8.858
Working Fluid to Brine Ratio	0.728	0.607	0.573	0.608
Cool. Water to Brine Ratio	5.89	4.87	4.87	6.14
Net Work/Availability	0.3161	0.2997	0.2952	0.2682
Net Thermo Efficiency, %	10.80	11.10	11.10	10.23
Res. Thermal Util. Effic., %	5.81	5.47	5.38	5.02
Net Plant Work, Btu/lb Brine	11.35	10.76	10.60	9.63

Table 8.2 Comparisons of Cycle Parameters for the Georesource Temperature of 350°F

Compound	iC_4H_{10}	iC_4H_{10} = 50% iC_5H_{12} = 50%	iC_4H_{10} = 25% iC_5H_{12} = 75%	iC_5H_{12}
Mol. Weight	58.12	65.133	68.64	72.146
Net Power, MW	25.00	25.00	25.00	25.00
Gross Power, MW	31.14	29.27	28.85	28.49
Plant Cost, $/KW	673	620	606	593
Total System Cost, $/KW	1032	997	991	1003
Turbine Inlet P, psia	450	300	230	170
Turbine Inlet T, °F	260	273	269	256
Turbine ΔH, Btu/lb	21.94	27.10	26.75	25.1
Condenser Superheat ΔT, °F	17.5	48.8	58.30	61.0
Condenser Superheat ΔH, Btu/lb	8.24	22.5	26.60	27.40
Condenser Dew Point P, psia	86.3	45.6	34.6	26.2
Condenser Dew Point T, °F	115.0	122.0	120.0	115.0
Heat Exch. Bubble Point T, °F	260.2	263.1	262.5	261.7
Brine Exit T, °F	186.4	203.8	204.1	211.7
Brine Flow, MM lb/hr	4.623	4.856	4.947	5.276
Working Fluid to Brine Ratio	1.048	0.759	0.743	0.734
Cooling Water to Brine Ratio	7.33	6.510	6.516	6.196
Net Work/Availability	0.280	0.274	0.268	0.255
Net Thermo Efficiency, %	12.15	12.91	12.69	12.52
Res. Thermal Util. Efficiency, %	7.36	6.99	6.86	6.41
Net Plant Work, Btu/lb Brine	18.45	17.57	17.25	16.17

Table 8.3 Comparisons of Cycle Parameters for the Georesource Temperature of 400°F

Compound	iC_4H_{10}	iC_4H_{10} = 75% iC_5H_{12} = 25%	iC_4H_{10} = 50% iC_5H_{12} = 50%	iC_5H_{12}
Mol. Weight	58.12	65.133	61.626	72.146
Net Power, MW	25.00	25.00	25.00	25.00
Gross Power, MW	31.76	30.13	29.04	28.19
Plant Cost, $/KW	634	608	558	529
Total System Cost, $/KW	908	866	833	820
Turbine Inlet P, psia	550	450	350	200
Turbine Inlet T, °F	285	287	287	272
Turbine ΔH, Btu/lb	22.88	25.68	27.26	26.18
Condenser Superheat ΔT, °F	12.6	26.5	46.9	65.3
Condenser Superhear ΔH, Btu/lb	5.98	12.4	21.86	29.4
Condenser Dew Point P, psia	88.7	67.3	50.9	28.9
Condenser Dew Point T, °F	117.0	127.0	129.0	121.0
Heat Exch. Bubble Point T, °F	---	282.9	279.2	277.3
Brine Exit T, °F	195.7	191.5	206.9	215.4
Brine Flow, MM lb/hr	3.533	3.314	3.544	3.749
Working Fluid to Brine Ratio	1.34	1.21	1.03	0.980
Cooling Water to Brine Ratio	9.19	8.50	7.24	7.57
Net Work/Availability	0.271	0.294	0.284	0.266
Net Thermo Efficiency, %	12.52	12.96	12.99	12.84
Res. Thermal Util. Efficiency %	7.99	8.44	7.84	7.41
Net Plant Work, Btu/lb Brine	24.14	25.74	24.08	22.76

Table 8.4 Comparisons of Cycle Parameters for the Georesource Temperature of 500°F

Compound	iC_4H_{10}	iC_4H_{10} = 50% iC_5H_{10} = 50%	iC_5H_{12}
Mol. Weight	58.12	65.133	72.146
Net Power, MW	25.0	25.0	25.0
Gross Power, MW	32.72	29.29	27.99
Plant Cost, $/KW	519	455	411
Total System Cost, $/KW	720	639	598
Turbine Inlet P, psia	700	450	250
Turbine Inlet T, °F	314	315	294
Turbine ΔH, Btu/lb	23.4	28.0	25.89
Condenser Superheat ΔT, °F	19.8	44.9	67.3
Condenser Superheat ΔH, Btu/lb	9.73	21.27	31.42
Condenser Dew Point P, psia	106.3	58.4	36.7
Condenser Dew Point T, °F	130.2	138.0	136.0
Heat Exch. Bubble Point T, °F	--	306.7	299.8
Brine Exit T, °F	228.0	228.0	222.5
Brine Flow, MM lb/hr	2.582	2.366	2.408
Working Fluid to Brine Ratio	1.85	1.51	1.53
Cooling Water to Brine Ratio	10.54	9.65	8.62
Net Work/Availability	0.2798	0.3052	0.2997
Net Thermo Efficiency, %	12.27	13.25	12.64
Res. Thermal Util. Efficiency, %	7.95	8.55	8.35
Net Plant Work, Btu/lb Brine	33.05	36.06	35.4

the net thermodynamic cycle efficiencies of the mixture cycles are slightly larger than the pure fluid cycles as noted in Tables 8.1 through 8.4. The dotted line in Figure 8.1 between the 300°F and 500°F georesource temperature represents the locus of optimal working fluid molecular weight. This locus of optimal working fluid molecular weight is limited to the isobutane-isopentane system. Moreover, this locus is very sensitive to changes in the cost models. For example, if the particular site-specific brine system cost declines sharply, the locus of optimal molecular weight will shift towards the higher molecular weight working fluids. The reverse will be true if power conversion plant costs decrease sharply (e.g., due to advances in technology).

8.2 Power Conversion Plant Cost

Figure 8.2 shows the effect of variations in working fluid molecular wieght and georesource temperature on the power conversion plant capital costs. The power conversion plant includes all major plant equipment except the brine delivery and disposal systems. The power conversion plant capital cost exhibits a minimum for a particular molecular weight working fluid at each georesource temperature. For a 300°F georesource temperature, a 50% isobutane and 50% isopentane mixture(molecular weight of 65.13) has lower power conversion plant cost, primarily due to lower turbine and cooling tower cost, than the pure isopentane cycle. For the georesource temperature range of 350°-500°F isopentane seems to have a lower power conversion plant cost mainly due to lower brine heat exchanger, condenser and fluid pumping costs. Since brine heat exchanger and condenser costs decrease with increasing working fluid molecular weight, whereas turbine costs increase with increasing molecular weight, a trade-off

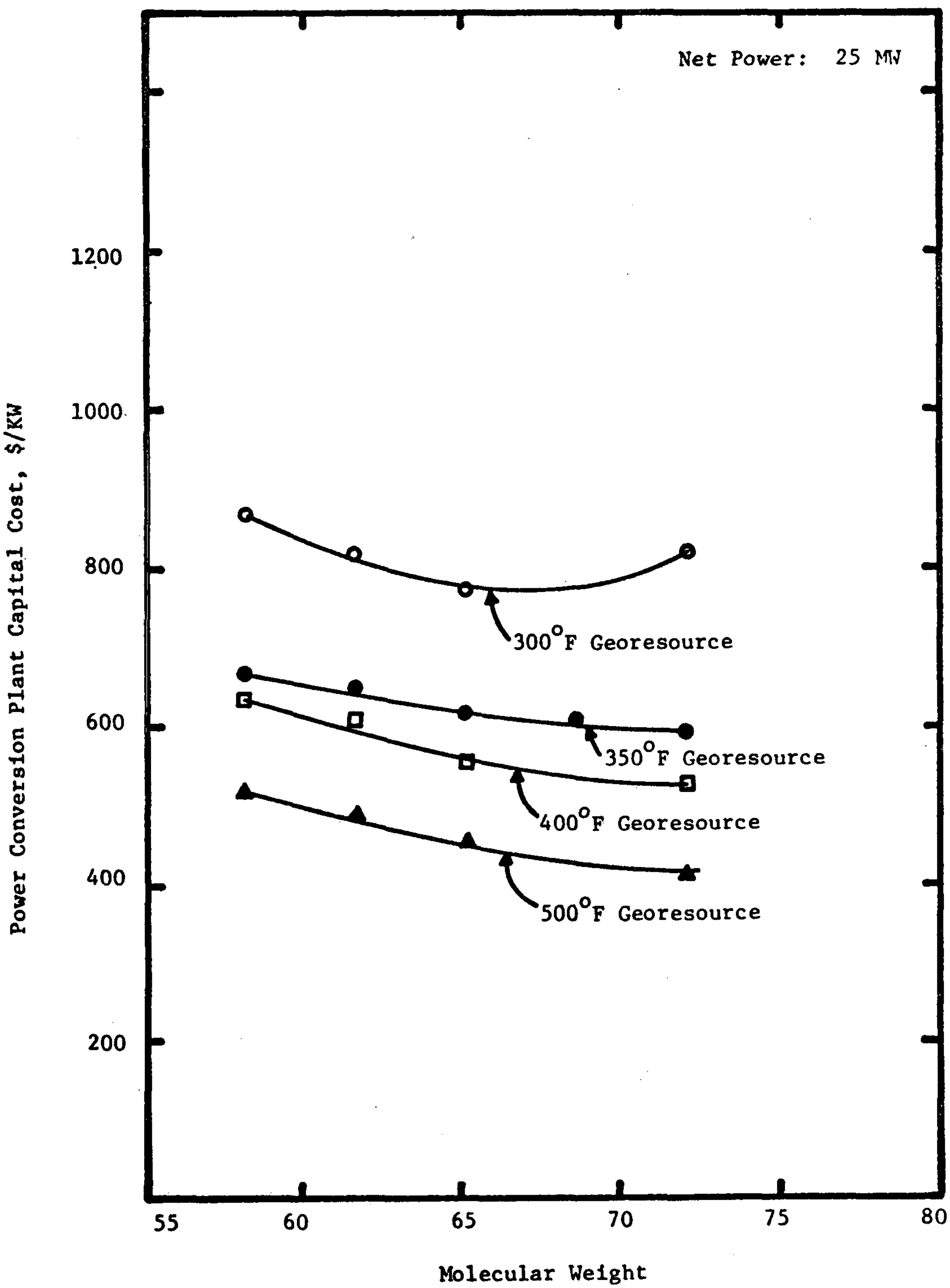

Figure 8.2 Power Conversion Plant Capital Cost Versus Georesource Temperature and Molecular Weight

exists between these major cost items in power conversion plant equipment.

8.3 Brine System Cost

Geothermal brine delivery costs are extremely site dependent, but for particular geothermal producing areas, the total cost of geothermal fluid delivery increases as the required flow rate increases. For process evaluation purposes, a typical cost of $500,000 to drill a geothermal well with a flow rate of 500,000 lb/hr was assumed for this study. Additional costs for well-to-plant piping, as well as indirect costs are added to the well cost to obtain the total brine system cost.

The brine system cost, which includes the cost of reinjection wells (equal number of production and reinjection wells) and pumping and piping system requirements, is shown in Figure 8.3 as a function of georesource temperature and molecular weight. The brine system cost increases with working fluid molecular weight for the georesource temperature range of 300°-400°F, but decreases with molecular weight for the 500°F georesource temperature.

8.4 Power Conversion Plant Capital Cost Elements

The cost of geothermal power is mainly affected by the capital investment requirement of the primary process units.

The primary cost elements are: (1) brine heat exchanger, (2) condenser, (3) turbine and generator, (4) fluid pumping equipment, and (5) auxiliaries. The cost of auxiliaries is proportional to the other cost elements. In this section, power conversion plant equipment costs will be detailed.

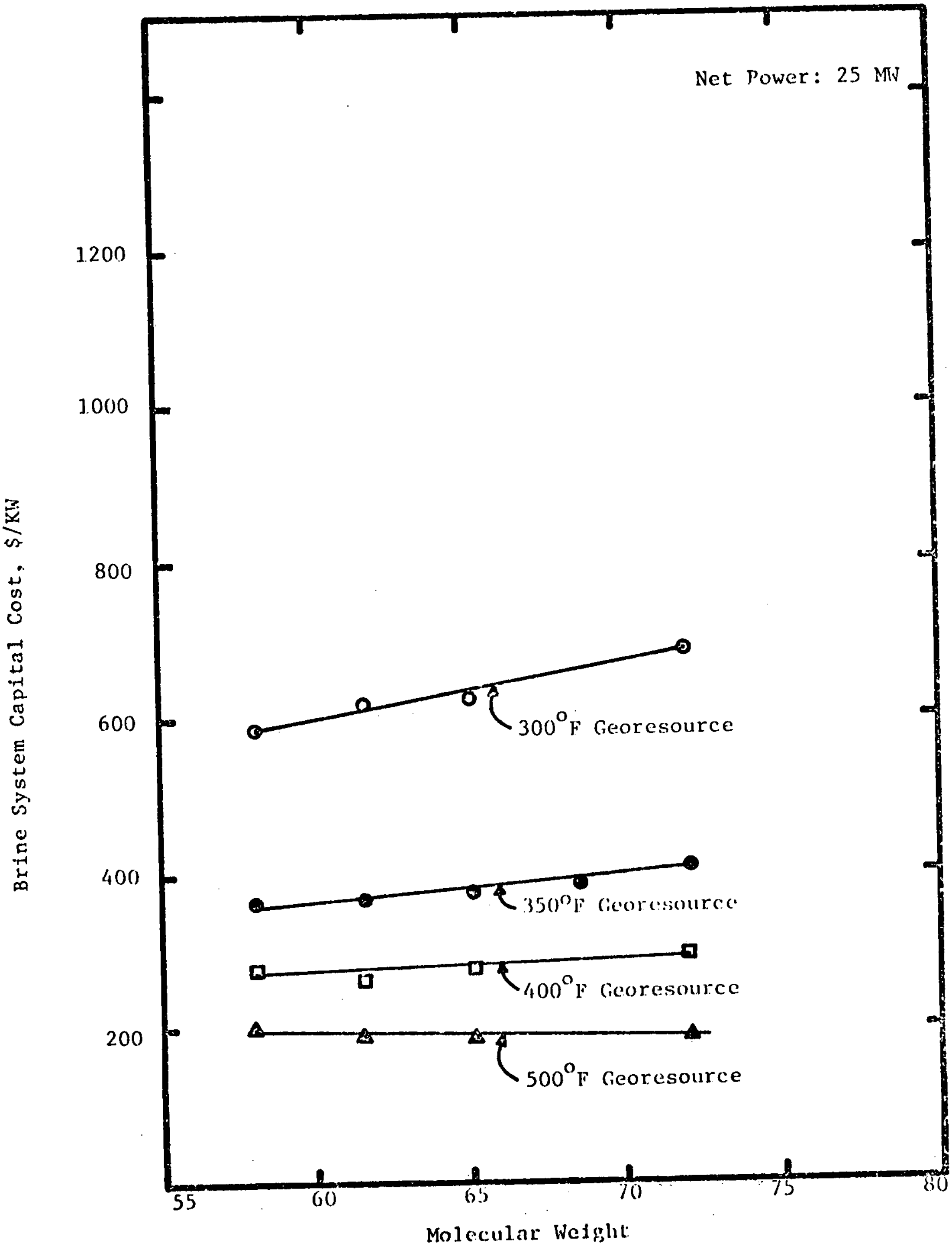

Figure 8.3 Brine System Capital Cost Versus Georesource Temperature and Molecular Weight

8.4.1 brine heat exchanger cost

Brine heat exchanger cost is primarily dependent on the heat transfer surface area required and the design pressure rating. Note the design pressure rating must be about 25% higher than the normal operating pressure in order to prevent relief valve operation during load variations. Heat exchangers designed to accomodate high pressure operation require thicker containment, hence substantially increased costs are incurred.

Figure 8.4 shows the effect of georesource temperature and working fluid molecular weight variations on the brine heat exchanger capital cost estimate. It can be seen from Figure 8.4 that brine heat exchanger costs decrease with increasing georesource temperature and/or increasing molecular weight. The costs for higher molecular weight fluids decrease mainly due to the lower operating pressures and hence lower cost per square foot of heat transfer area.

8.4.2 condenser cost

Like brine heat exchanger costs, the condenser costs depend primarily on the heat transfer surface area requirement and the design pressure rating. It has been assumed here that condensers with design pressures (1.25 x operating pressure) between 15-50 psia would have the same cost/ft^2 of heat transfer surface.

Figure 8.5 presents condenser costs at various georesource temperatures versus working fluid molecular weights. Condenser costs follow a pattern similar to that noted for the brine heat exchanger.

8.4.3 turbine and generator cost

Turbine cost is a direct function of the last stage diameter

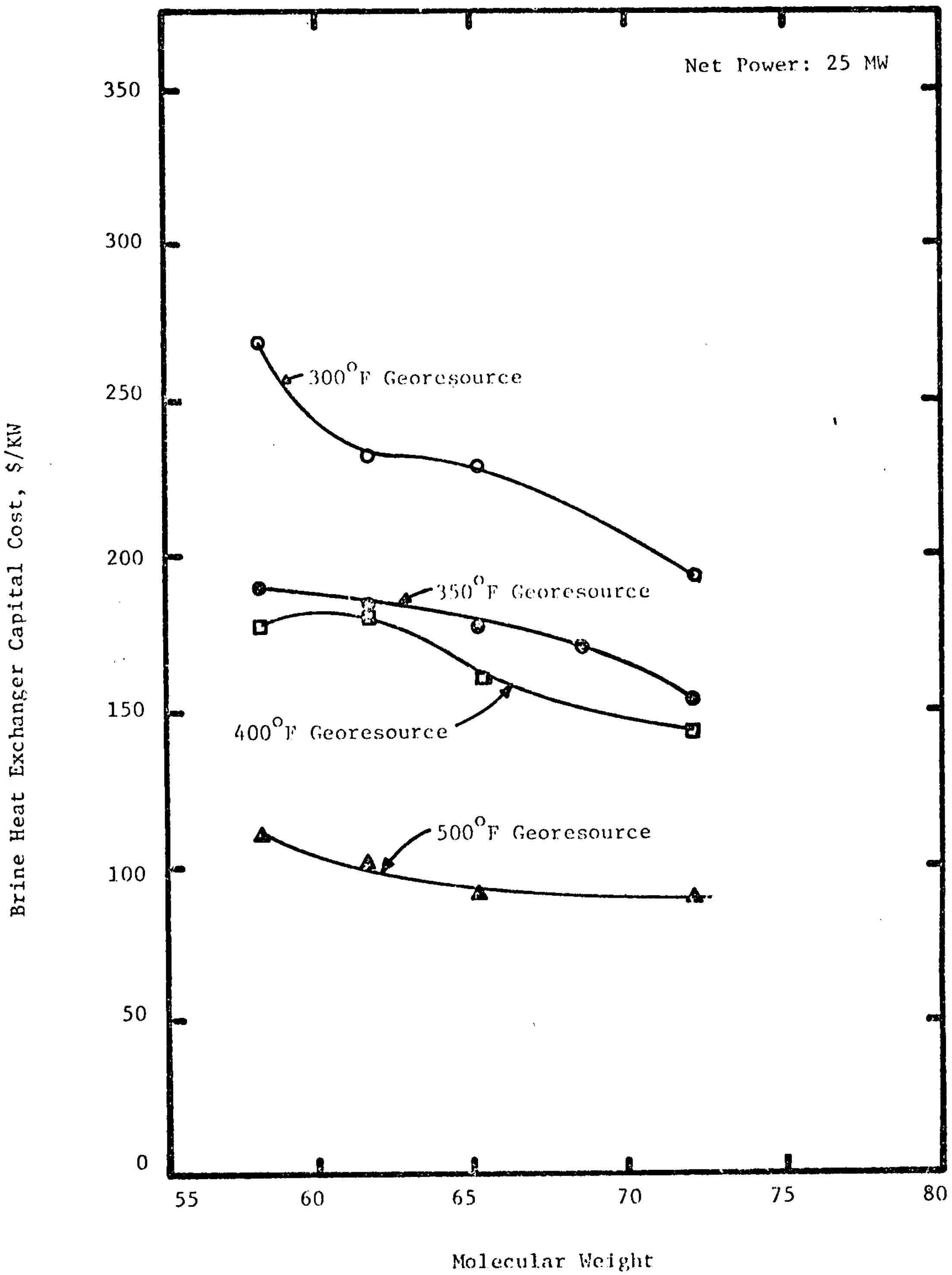

Figure 8.4 Brine Heat Exchanger Capital Cost Versus Georesource Temperature and Molecular Weight

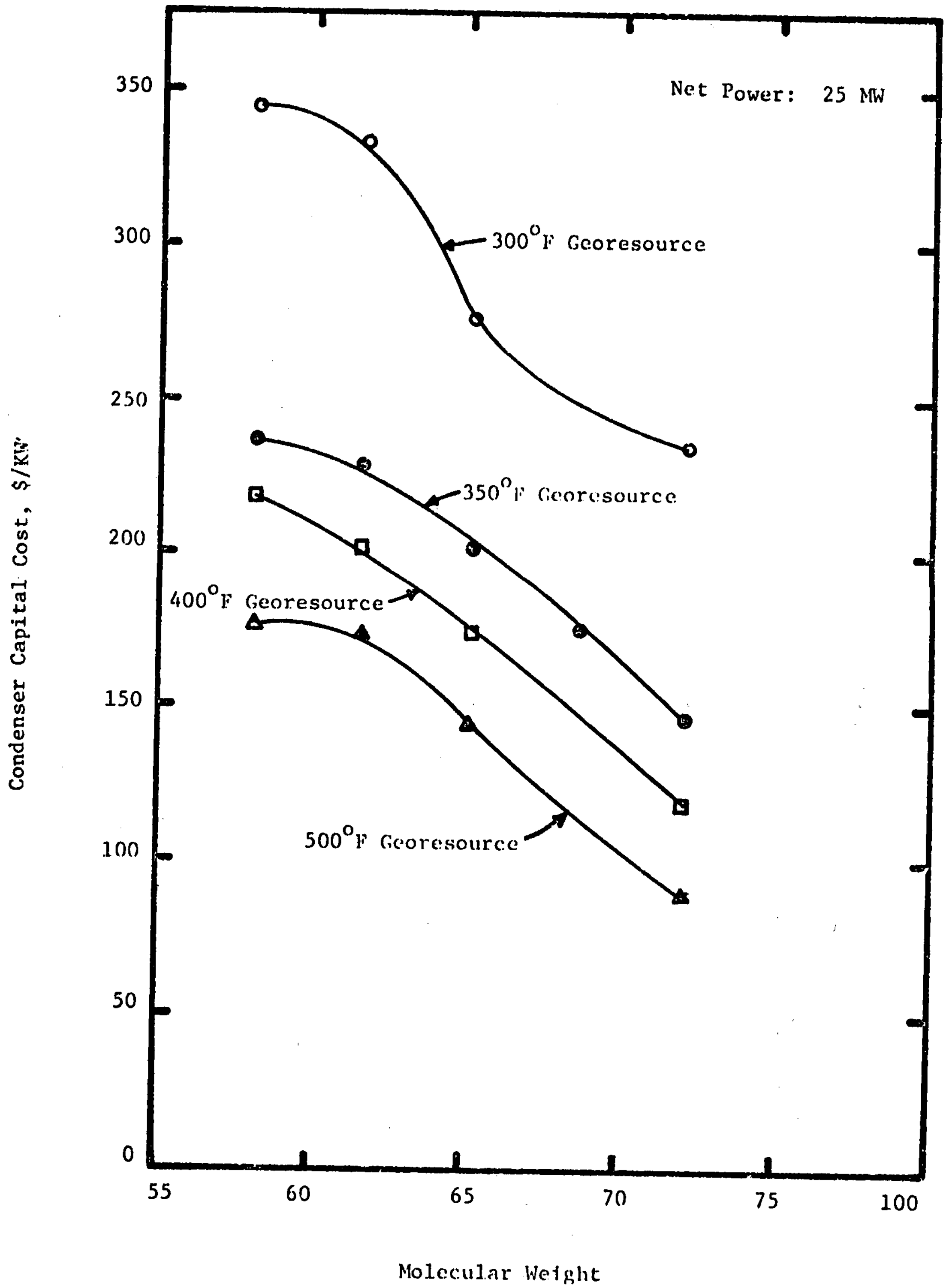

Figure 8.5 Condenser Capital Cost Versus Georesource Temperature and Molecular Weight

of the turbine and the number of exhaust ends on a common shaft. Other factors include the blade tip speed and the turbine inlet pressure. The turbine cost estimates are based on a model developed by the Barber-Nichols company of Denver, Colorado (19). The generator cost is a direct function of the gross plant power produced (20).

The effect of variations in working fluid molecular weight and georesource temperature on turbine and generator capital costs is shown in Figure 8.6. The turbine cost increases with increasing molecular weight at a particular georesource temperature. However, the turbine cost decreases with increasing georesource temperature for a given molecular weight. Only axial flow turbines have been considered in the present study.

8.4.4 cooling tower cost

The cooling towers considered in this study are wet cooling towers of the mechanical draft type. Figure 8.7 shows the cooling tower cost as a function of georesource temperature and working fluid molecular weight.

8.4.5 working fluid and cooling water pump cost

Figure 8.8 illustrates the working fluid and cooling water pumping costs associated with various molecular weight working fluids at various georesource temperatures. The isobutane cycle has the highest pumping costs, since the isobutane operating pressure is higher than other fluids at each georesource temperature.

8.5 Energy Conversion Efficiency

There are several parameters used to evaluate the efficiency of the power cycle. The relationships between these various indicators

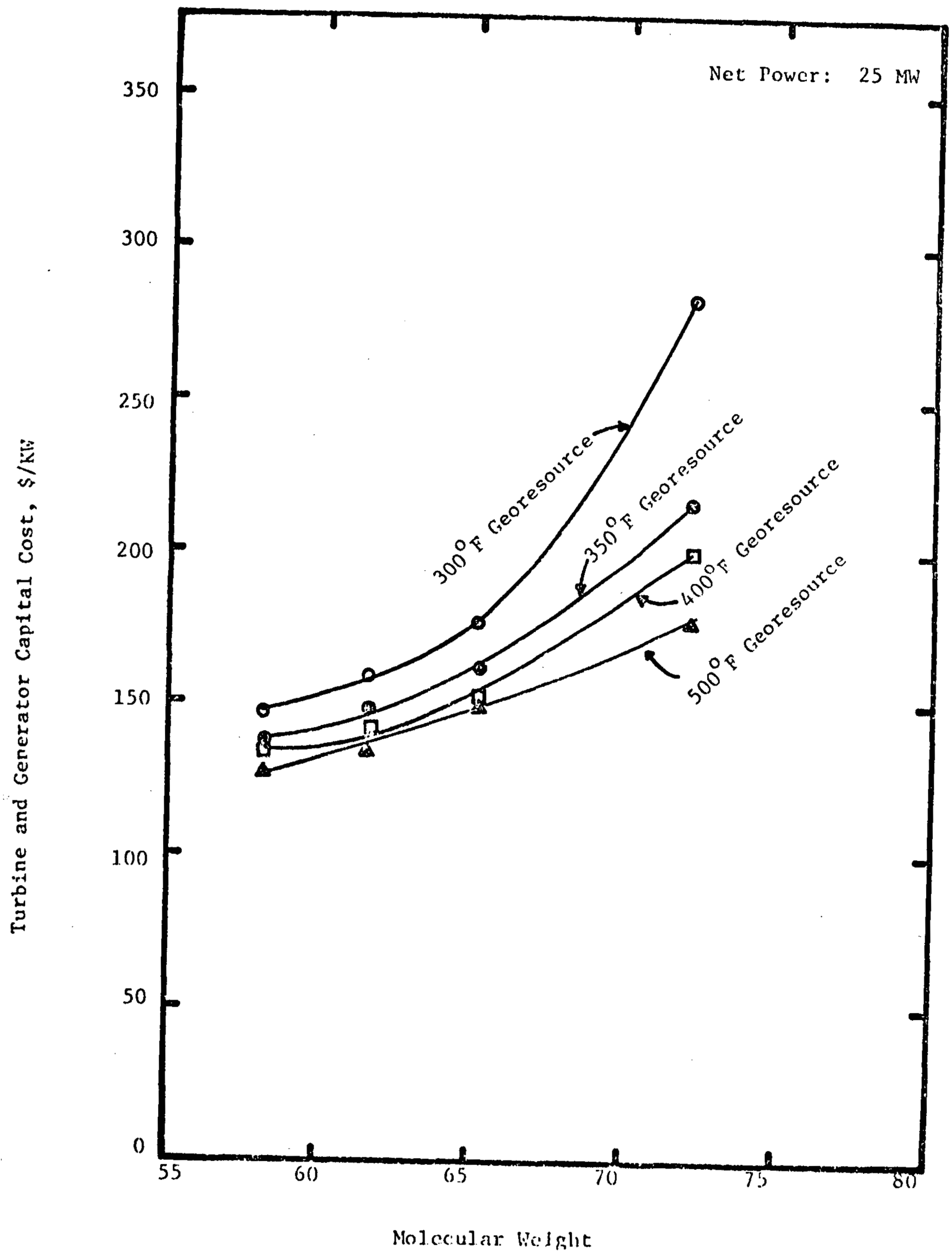

Figure 8.6 Turbine and Generator Capital Cost Versus Georesource Temperature and Molecular Weight

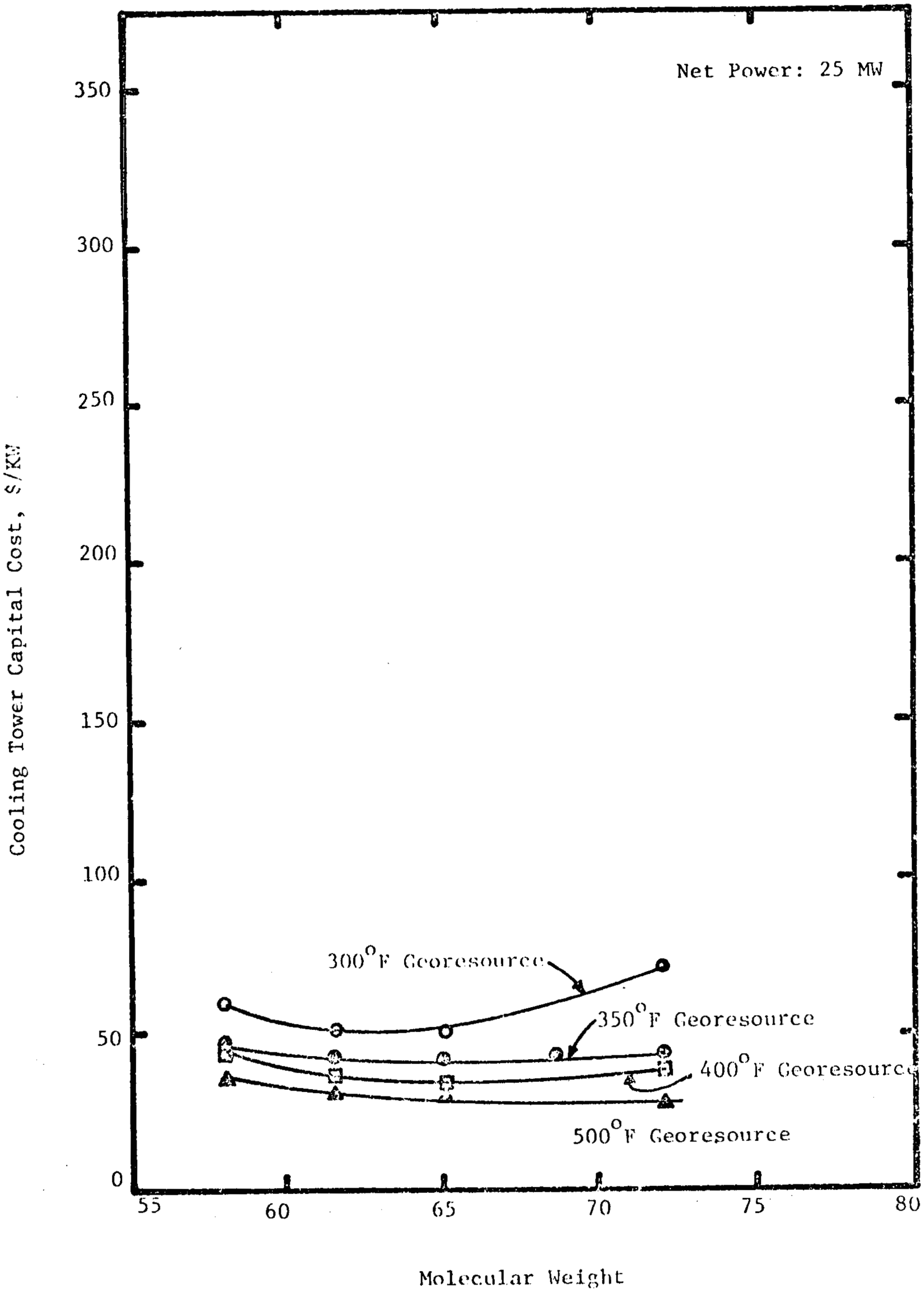

Figure 8.7 Cooling Tower Capital Cost Versus Georesource Temperature and Molecular Weight

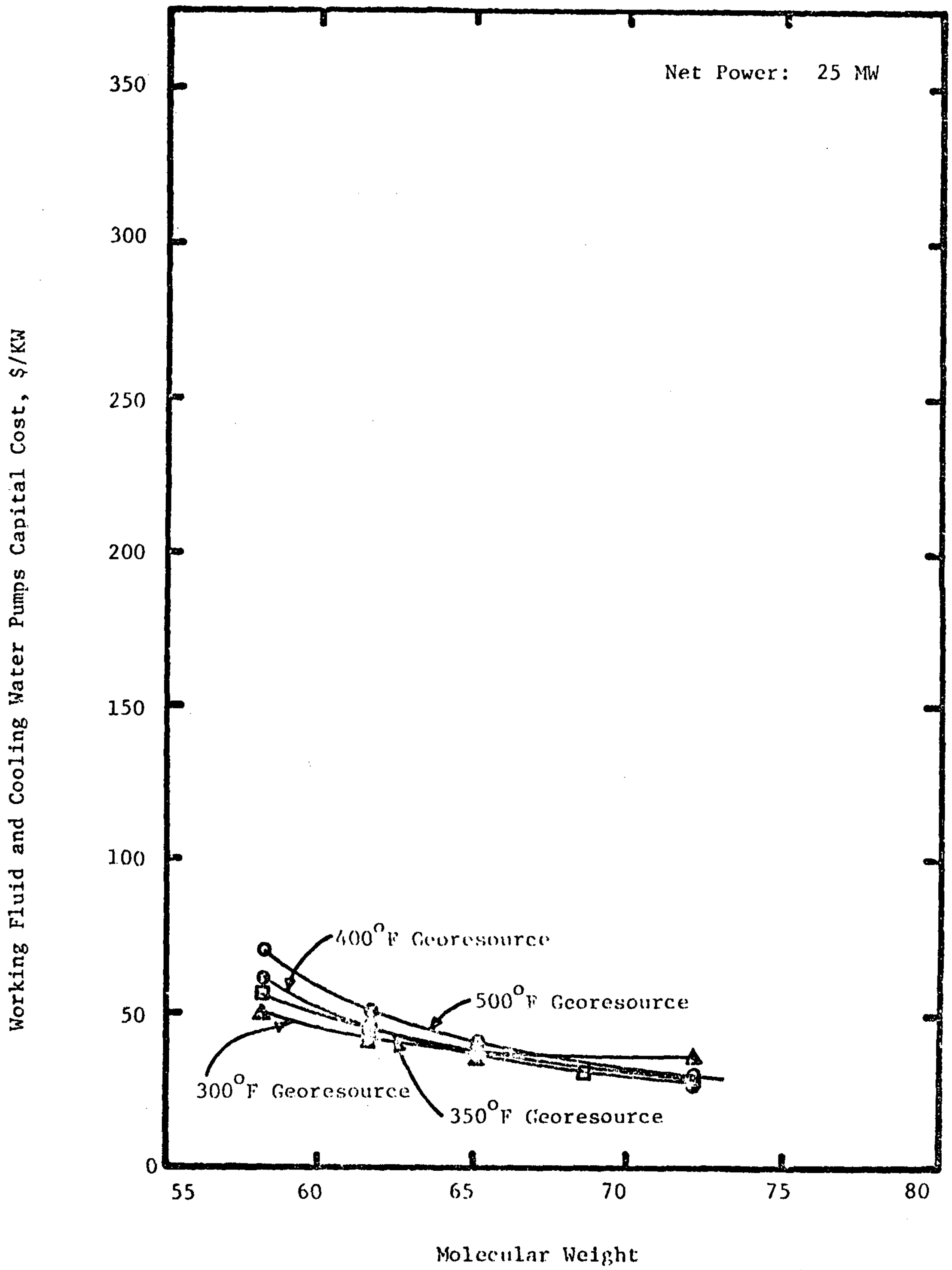

Figure 8.8 Working Fluid and Cooling Water Pumps Capital Cost Versus Georesource and Molecular Weight

were detailed previously (2). In order to maximize the ability to compare the results of this parameter sensitivity study with the results of other work, the most commonly used efficiency indicators are described below.

8.5.1 <u>resource thermal utilization efficiency</u>

Figure 8.9 illustrates the effects of variations in molecular weight and georesource temperature on the net resource thermal utilization efficiency (W_{NP}/Q_R). The important points to note are:

(1) The net thermal utilization efficiency for a given working fluid increases with increasing the georesource temperature. Since lower brine and cooling water flow rates are required at higher georesource temperatures, which result in decreased parasitic power losses, thus increasing the net plant work per unit mass of brine.

(2) For subcritical pressure cycles, the net thermal utilization efficiency decreases with increasing working fluid molecular weight while the opposite trend occurs for supercritical pressure cycles (molecular weight of 58-61 at 400°F and 58-65 at 500°F). The behavior for subcritical cycles occurs in part because the brine heat exchanger duty in the boiling range is larger for the higher molecular weight fluids, forcing the brine exit temperature to be larger (the bubble point temperature is essentially the same for each working fluid considered). The behavior for supercritical cycles occurs in part because the brine heat exchanger operating pressure decreases with molecular weight, leading to smaller logarithmic mean temperature difference, with the net result that

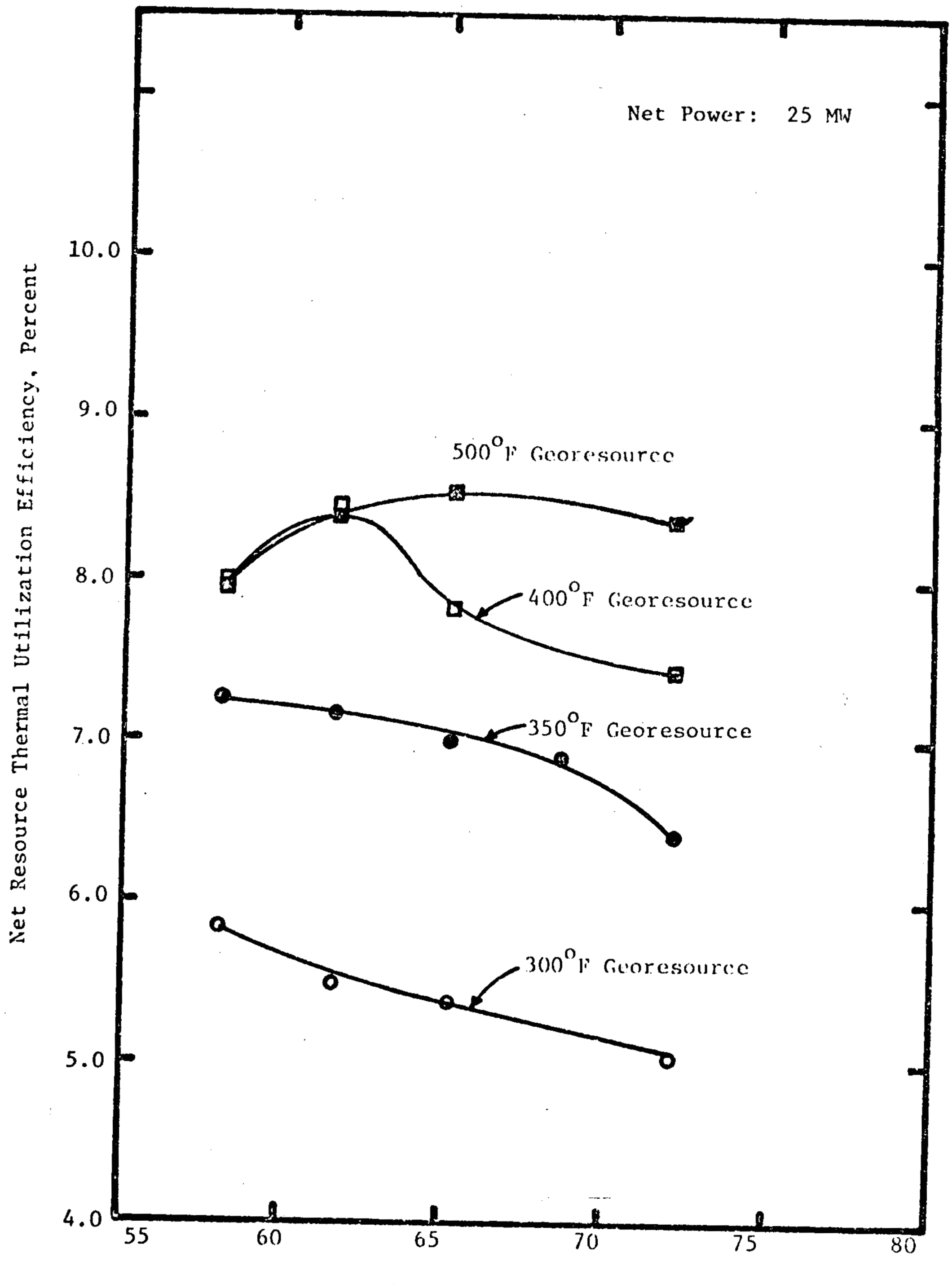

Figure 8.9 Net Resource Thermal Utilization Efficiency Versus Georesource Temperature and Molecular Weight

the net work per unit mass of brine is increased (reflected in Figure 8.9 in an increase in the net resource thermal utilization efficiency).

It can be noted that isobutane-isopentane mixture cycles at 400°F and 500°F have higher resource thermal utilization efficiencies than either the pure isobutane or isopentane cycle.

8.5.2 net cycle work/availability

Net cycle work to availability ratio defined here can also be called resource utilization efficiency. Milora and Tester (20) refer to this as the resource utilization factor. The term net cycle work/availability ratio, η_u, is used here to avoid confusion with the resource thermal utilization efficiency discussed earlier. It may be noted here that η_u can be determined for any geothermal energy conversion process and therefore process details are not required for intercomparisons of processes using this efficiency measure. Other efficiency measures, such as thermal efficiency, which is useful for intercomparing binary cycles but cannot be defined for total flow processes, are inadequate for broad intercomparisons of geothermal energy conversion processes.

Figure 8.10 illustrates the behavior of η_u for various working fluids at various georesource temperatures. The following points can be noted:

(1) The net cycle work/availability ratio for the working fluids studied has a maximum in the 350°F to 400°F georesource range.

(2) The net cycle work/availability ratio is greatest for

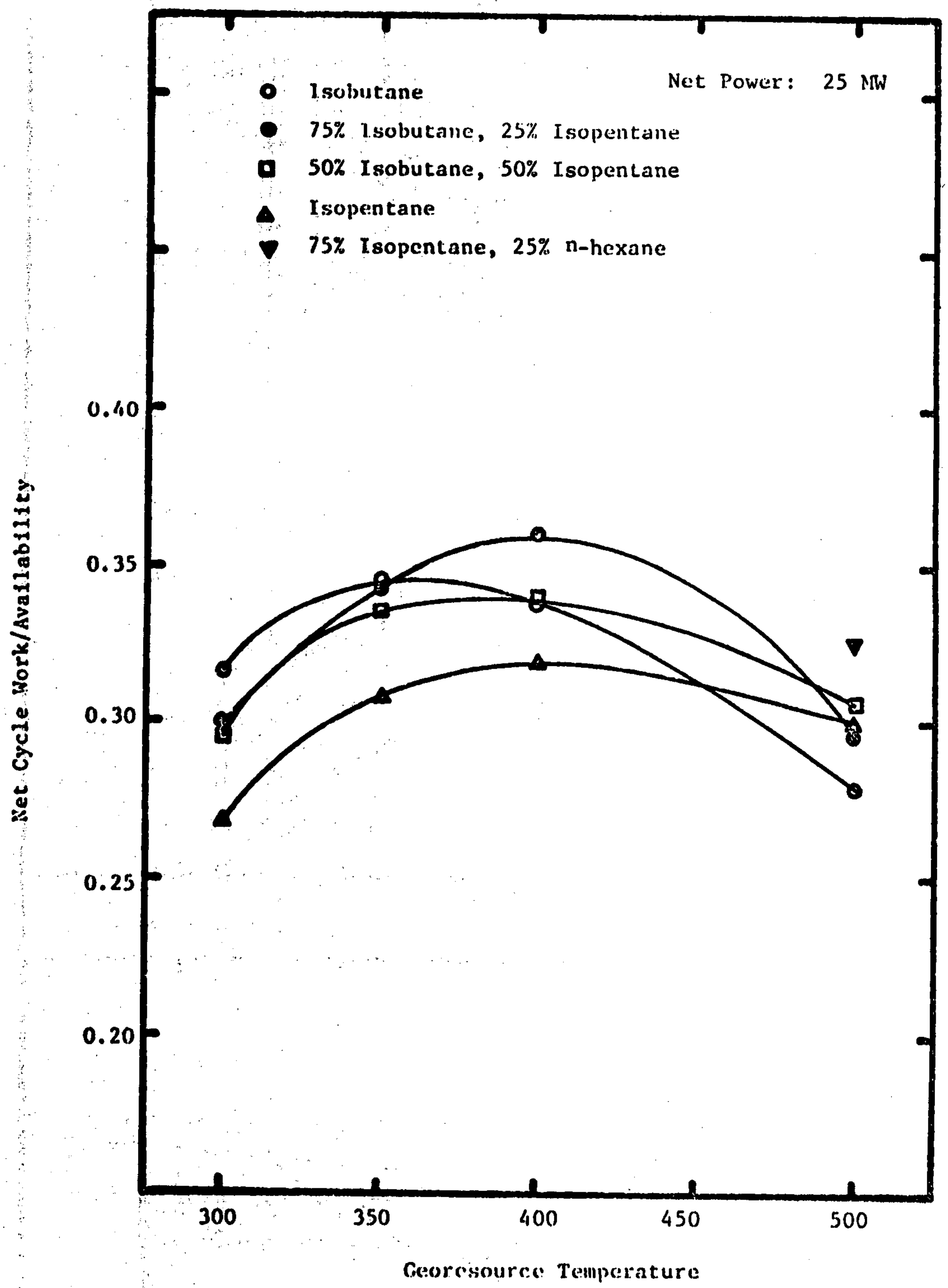

Figure 8.10 Net Cycle Work/Availability Versus Georesource Temperature and Molecular Weight

the 75% isobutane and 25% isopentane mixture, primarily due to the fact that this working fluid has the lowest brine flow rate at this georesource temperature which results in higher net cycle work per unit mass of brine.

(3) Since the availability at a specific georesource temperature is the same for any working fluid, the net plant work per unit mass of brine must be increased in order to achieve higher values of η_u. Therefore, smaller brine flow rates are desired for maximizing net cycle work/availability.

(4) The maximum value of η_u for isobutane for the economically optimized cycles considered here occurs at a georesource temerpature of 350°F, whereas *Milora and* Tester's maximum η_u for isobutane for thermodynamically optimized cycles occurs at a georesource temperature of 415°F (20). This indicates that economic factors must be included along with thermodynamic and process factors, to determine the optimum working fluid for a given georesource condition.

8.5.3 cycle net work per unit mass of brine

The cycle net work per unit mass of brine is another parameter which has been used as an optimization parameter, and is a measure of geothermal fluid resource utilization. Figure 8.11 illustrates the effect of variations in georesource temperature and working fluid molecular weight on net cycle work per pound of brine. Since the geothermal well system (or brine system) is a major cost element, the

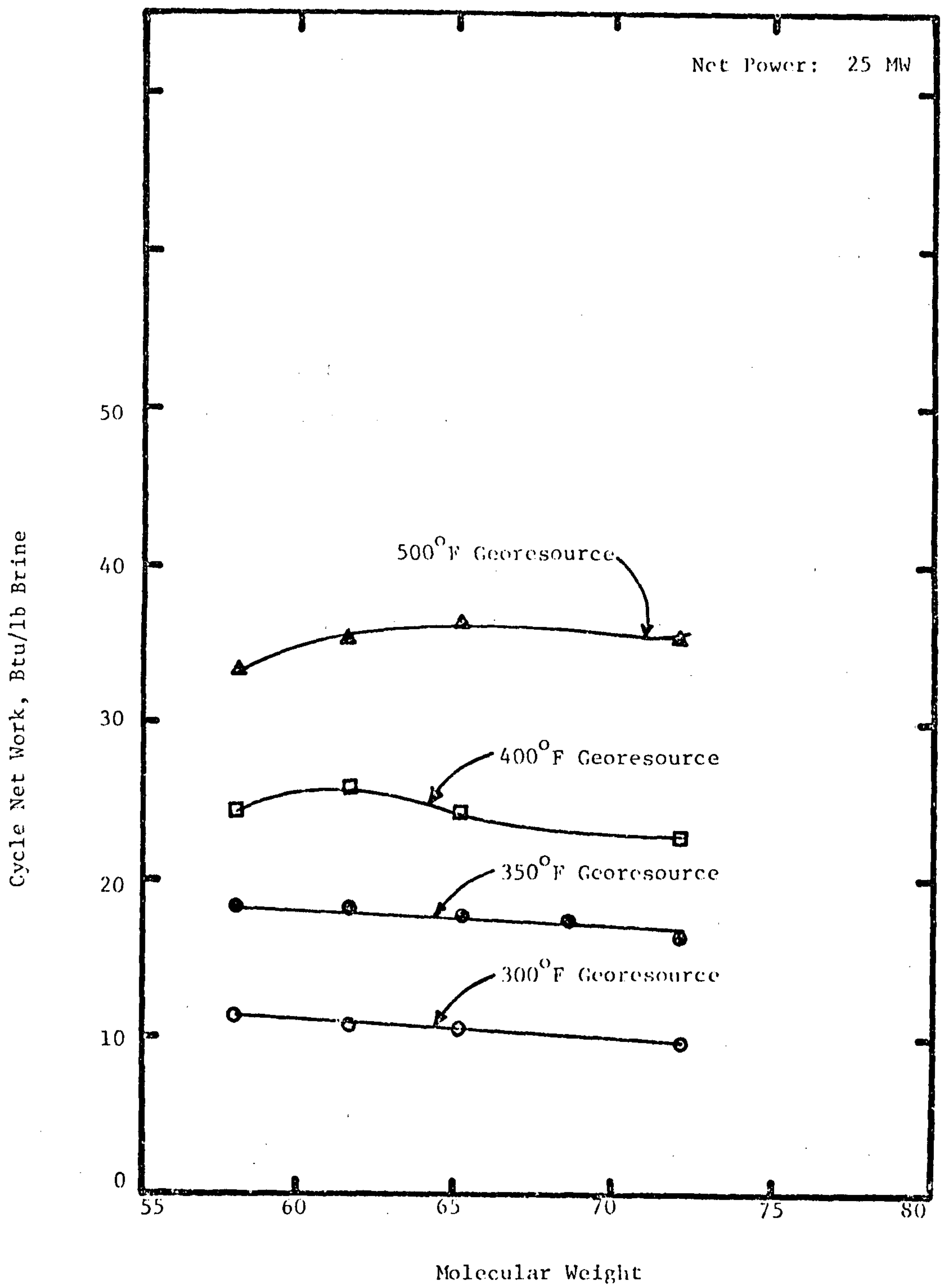

Figure 8.11 Cycle Net Work Per Unit Mass of Brine Versus Georesource Temperature and Molecular Weight

maximization of cycle net work per unit mass of brine results in the minimum brine system cost for a given cycle.

Since the cycle net plant work was fixed at 25 Mw for this study, it is apparent that cycles with minimum brine flow rate would yield maximum cycle net work per unit mass of brine at a specific georesource temperature. It can be noted in Figure 8.11 that for the 300°F and 350°F georesource temperatures isobutane yields the greatest net plant work per unit mass of brine. For the 400°F georesource a mixture (75% isobutane and 25% isopentane) yields the highest net plant work per unit mass of brine. At 500°F an equimolar (50-50) yields the maximum cycle net work per unit mass of brine. It is interesting to note that in agreement with the present work, Ingvarsson and Turner (21) report isobutane to give better performance than isopentane in the georesource temperature range of 300°-360°F. However, they report that isopentane yields better performance than isobutane in the georesource temperature range of 380°-400°F, whereas isopentane becomes superior to isobutane at a georesource temperature above 400°F according to the present work.

8.5.4 thermodynamic cycle efficiency

The thermodynamic cycle efficiency, W_N/Q_H, is a traditional measure of the performance of the working fluid and cycle. This efficiency is determined by the operating conditions of the cycle and the thermodynamic behavior of the working fluid. From the definition of thermodynamic cycle efficiency, it is obvious that for a given net plant output it can be increased by two fundamental ways: (1) increasing the net thermodynamic cycle work and (2) reducing the brine heat exchanger load.

Figure 8.12 shows the net thermodynamic cycle efficiency versus georesource temperature and molecular weight. It can be noted in Figure 8.12 that isobutane-isopentane mixtures yield higher efficiencies than either isobutane or isopentane for all georesource temperatures studied. The reasons for the behavior of the net thermodynamic cycle efficiency shown in Figure 8.12 will be made evident in the discussion on the working fluid enthalpy change in the turbines.

8.6 Near Optimum Cycle Operating Parameters

In order to understand more fully the impact of cycle operating conditions on the capital cost and performance of geothermal power cycles which use various working fluids, including mixtures, the following section details the priniciple cycle operating conditions used in the parameter sensitivity study.

8.6.1 turbine inlet pressure

The results of the capital cost optimization carried out to determine the near optimal turbine inlet pressure for the five working fluids (pure fluids and mixtures) at various georesource temperatures (300°F-500°F) are presented in Figures 8.13 and 8.14. The turbine inlet pressure for near optimal performance can be correlated as follows:

$$\begin{aligned} P_T = & -652.2 - 13.50\,(M.W.) + 9.81\,(T_g) \\ & + 0.1796\,(M.W.)^2 - 0.00386\,(T_g)^2 \\ & - 0.0833\,(M.W.)\,(T_g) \end{aligned}$$

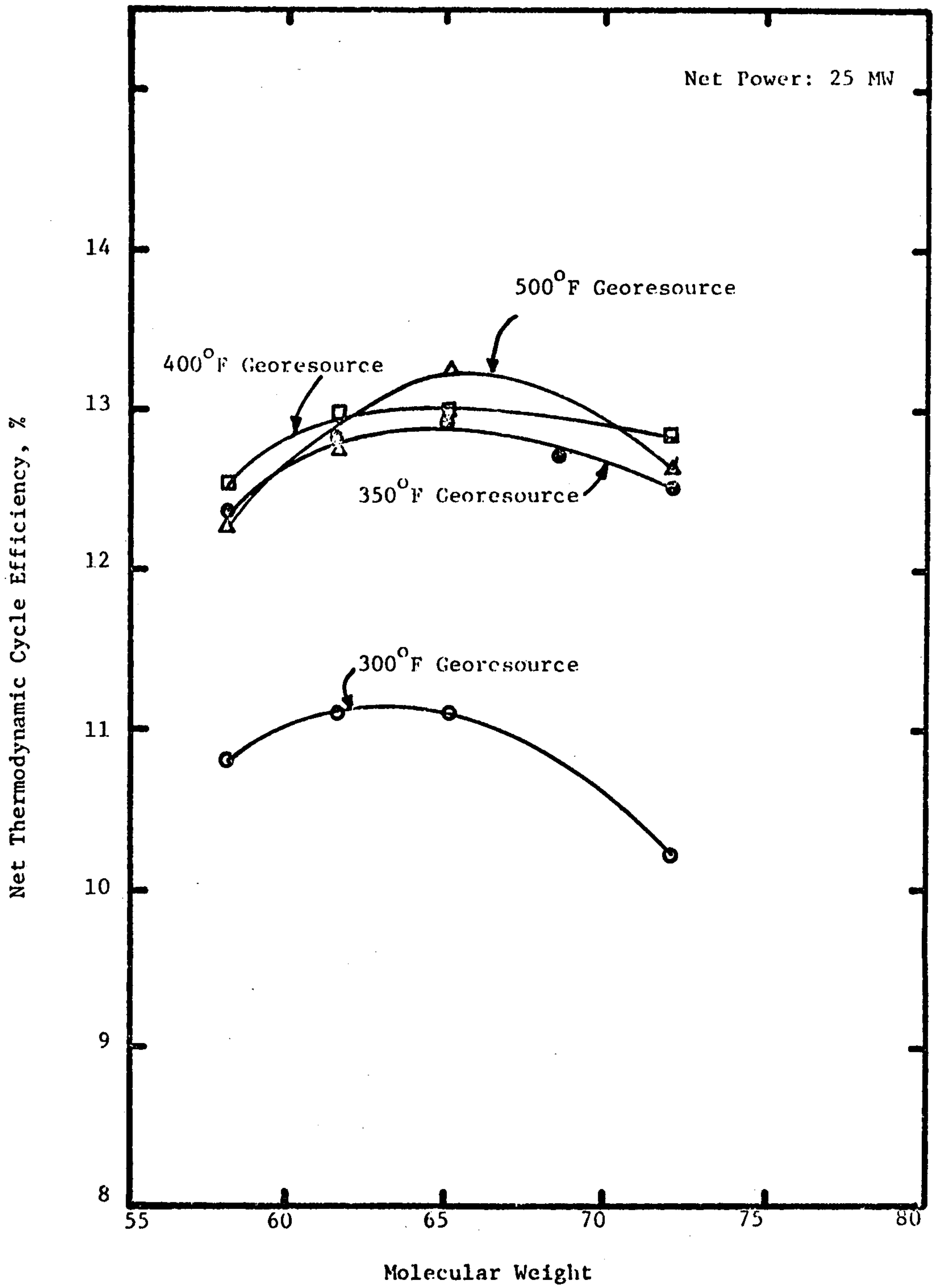

Figure 8.12 Net Thermodynamic Cycle Efficiency, Versus Georesource Temperature and Molecular Weight

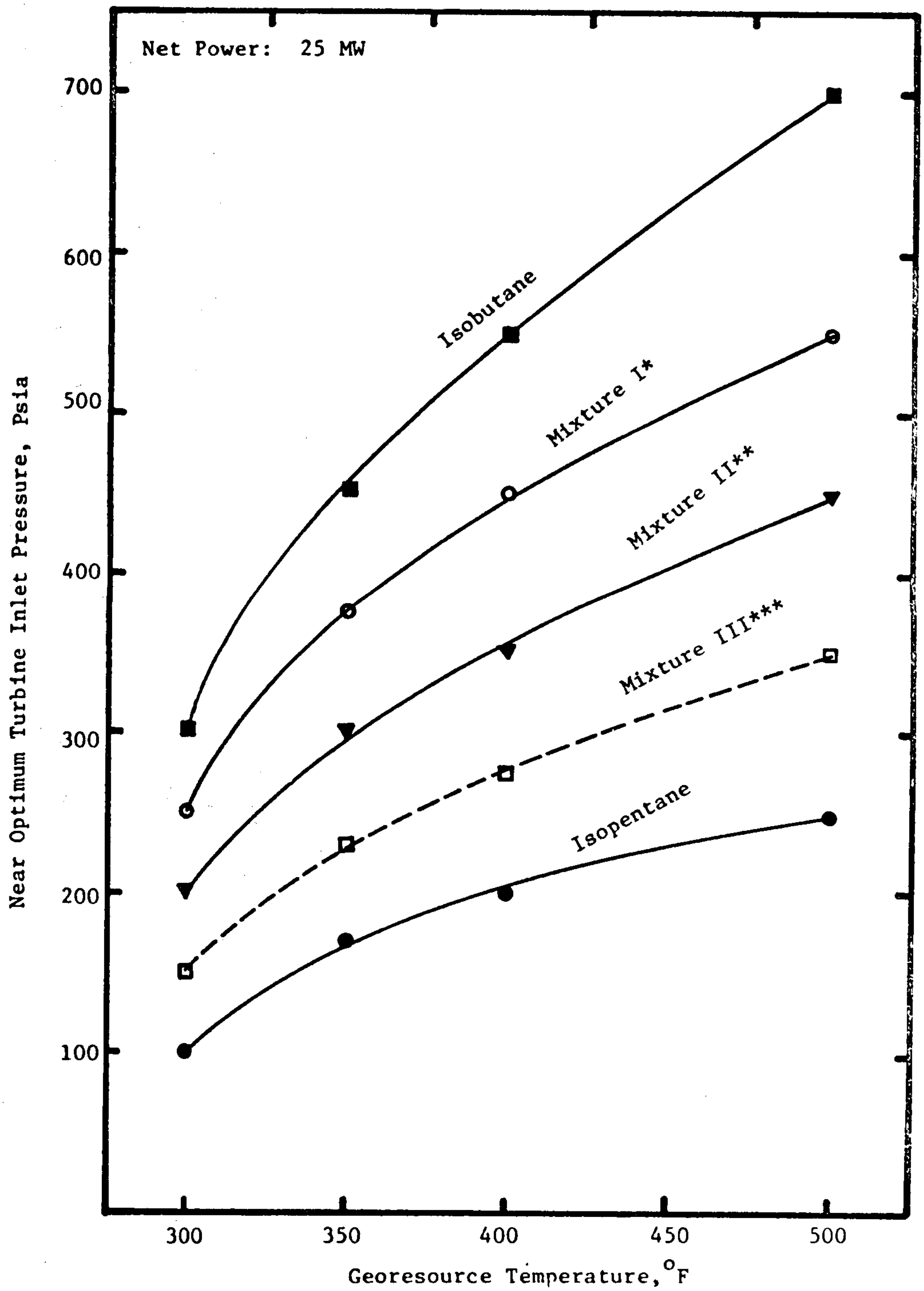

*Mixture I: 75 Mole % Isobutane - 25 Mole % Isopentane
**Mixture II: 50 Mole % Isobutane - 50 Mole % Isopentane
***Mixture III: 25 Mole % Isobutane - 75 Mole % Isopentane

Figure 8.13 Near Optimal Turbine Inlet Pressure Versus Molecular Weight and Georesource Temperature

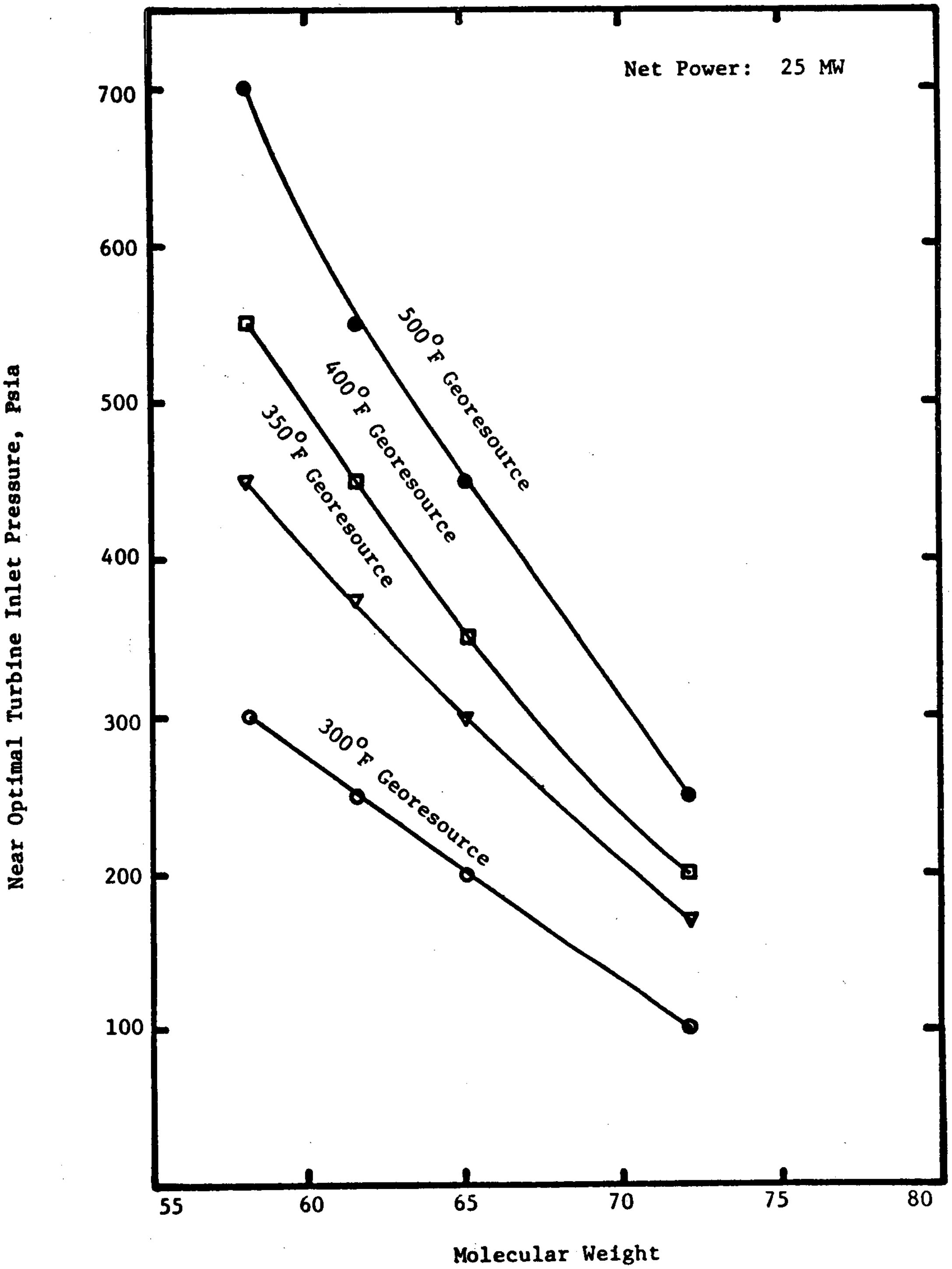

Figure 8.14 Near Optimal Turbine Inlet Pressure as a Function of Georesource Temperature and Molecular Weight

where M.W. = hydrocarbon working fluid molecular weight

P_T = turbine inlet pressure, psia

T_g = temperature of the geothermal resource, °F

The near optimal turbine inlet pressure increases with increasing georesource temperature and decreasing working fluid molecular weight. The increase in turbine inlet pressure with increasing georesource temperature is smaller for the higher molecular weight working fluids. Another result to note is the fact that the turbine inlet pressures of all three isobutane-isopentane mixture working fluids lie between the pure component turbine inlet pressures.

8.6.2 <u>turbine inlet temperature and enthalpy change in turbine</u>

Figures 8.15 and 8.16 illustrate the effects of molecular weight and georesource temperature on the turbine inlet temperature and working fluid enthalpy drop in the turbine. The following points can be noted:

(1) The turbine inlet temperature and enthalpy drop in the turbine both increase with increasing georesource temperature. This is due principally to the fact that as higher georesource temperatures are considered, there is a trade-off between decreased heat exchanger size (due to increased LMTD) and increased cycle thermodynamic efficiency (due to increased turbine inlet temperature). Because a higher working fluid temperature at the turbine inlet results in a greater enthalpy drop in the turbine, a lower working fluid flow rate also results.

(2) The turbine inlet temperature for a given molecular weight mixture is greater than the straight line interpolation of pure

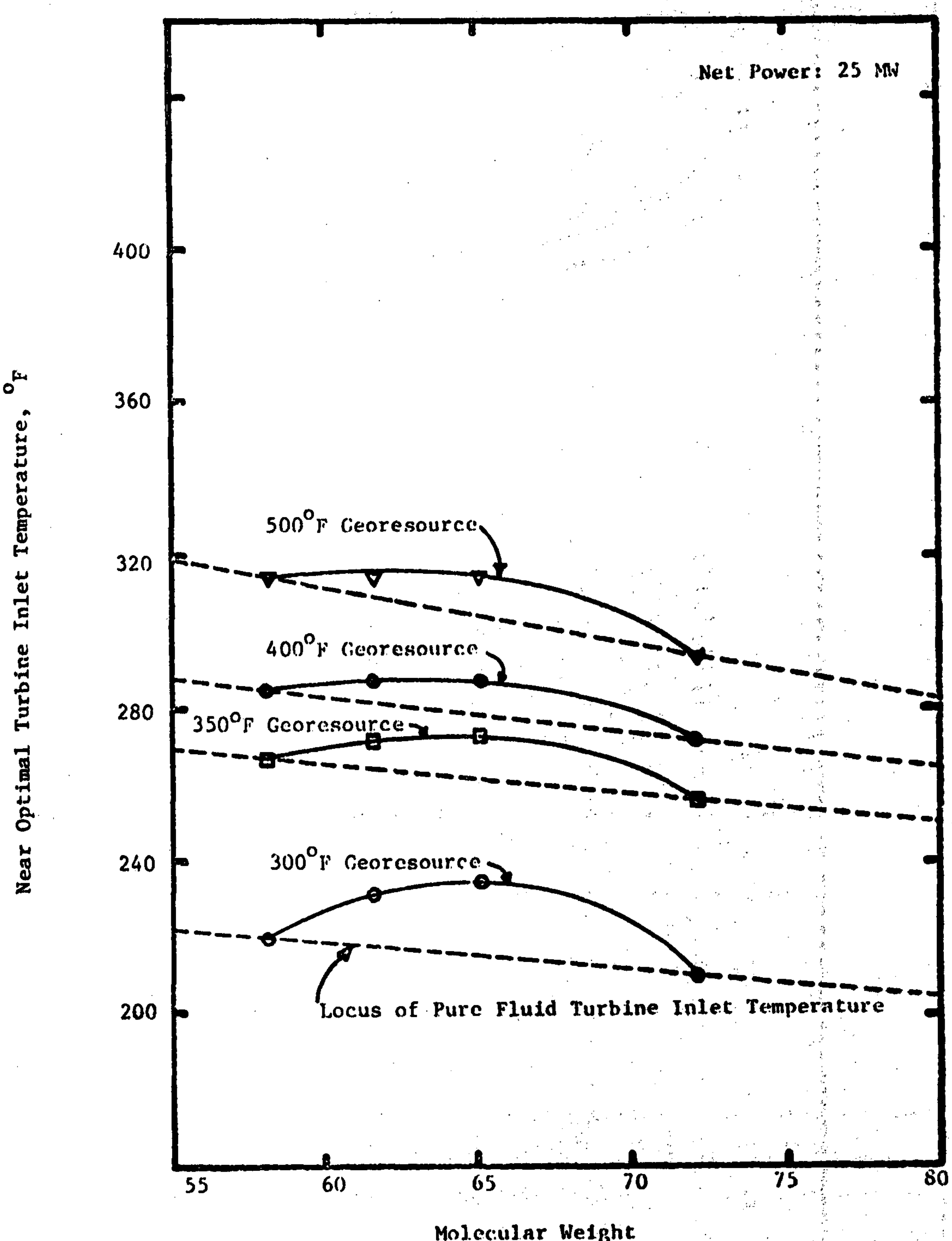

Figure 8.15 Near Optimal Turbine Inlet Temperature as a Function of Georesource Temperature and Molecular Weight

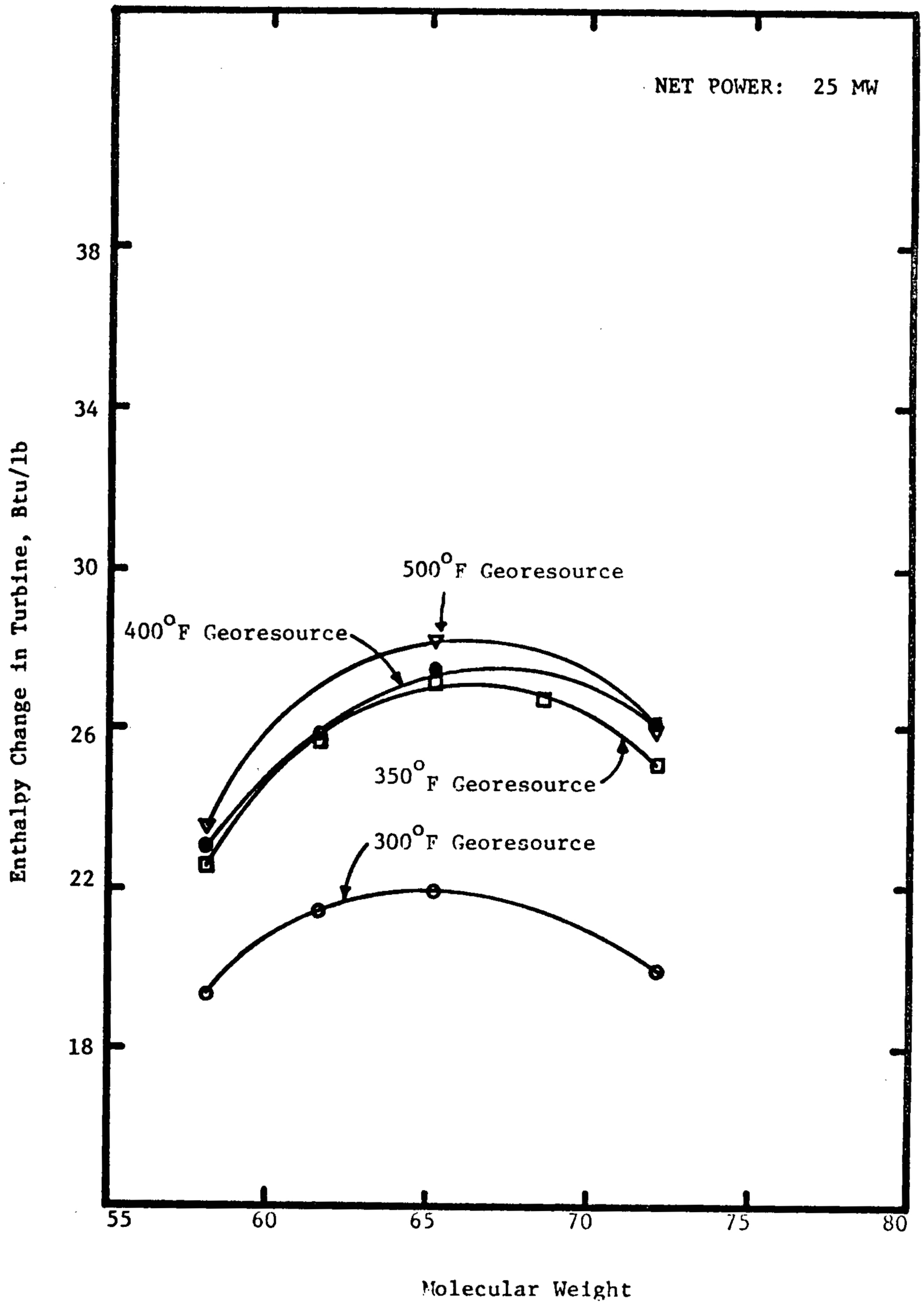

Figure 8.16 Enthalpy Change in Turbine Versus Georesource Temperature and Molecular Weight

fluid turbine inlet temperatures (shown as dotted lines in Figure 8.15. The enthalpy drop in the turbine behaves in an analogous manner (Figure 8.16).

A comparison between mixture and pure fluid cycle state points is given in Figure 8.17 on a superimposed temperature-enthalpy diagram for isobutane and the 50% isobutane-50% isopentane mixture cycles for the case of a 300 °F georesource temperature. The turbine inlet temperature and enthalpy for the mixture are both considerably higher than for isobutane. However, the mixture has greater superheat and a higher enthalpy than isobutane at the turbine exit. Because the gain at the turbine entrance exceeds the loss at the turbine exit, the mixture cycle yields more gross turbine work per unit mass of working fluid than the isobutane cycle.

Some of the major differences between pure fluid and mixture cycles can be explained by reference to Figure 8.17. First, it can be noted that the vaporization and condensation of the mixture is very nonisothermal compared to the pure working fluid. Thus, for specified cooling water inlet and outlet temperatures, and fixed condenser LMTD (logarithmic mean temperature difference) in the condensing region, the mixture condensing curve would intersect the pure fluid condensing curve (usually near the midpoint). For the binary mixture of isobutane and isopentane, the turbine exit superheat would be greater than for isobutane and less than for isopentane. Thus, the overall condenser LMTD for the binary mixture would be between the pure fluid cycle condenser LMTD's. This behavior of the condenser LMTD's will be verified subsequently. With respect to the brine heat exchanger, the near optimal LMTD for isopentane is lower than

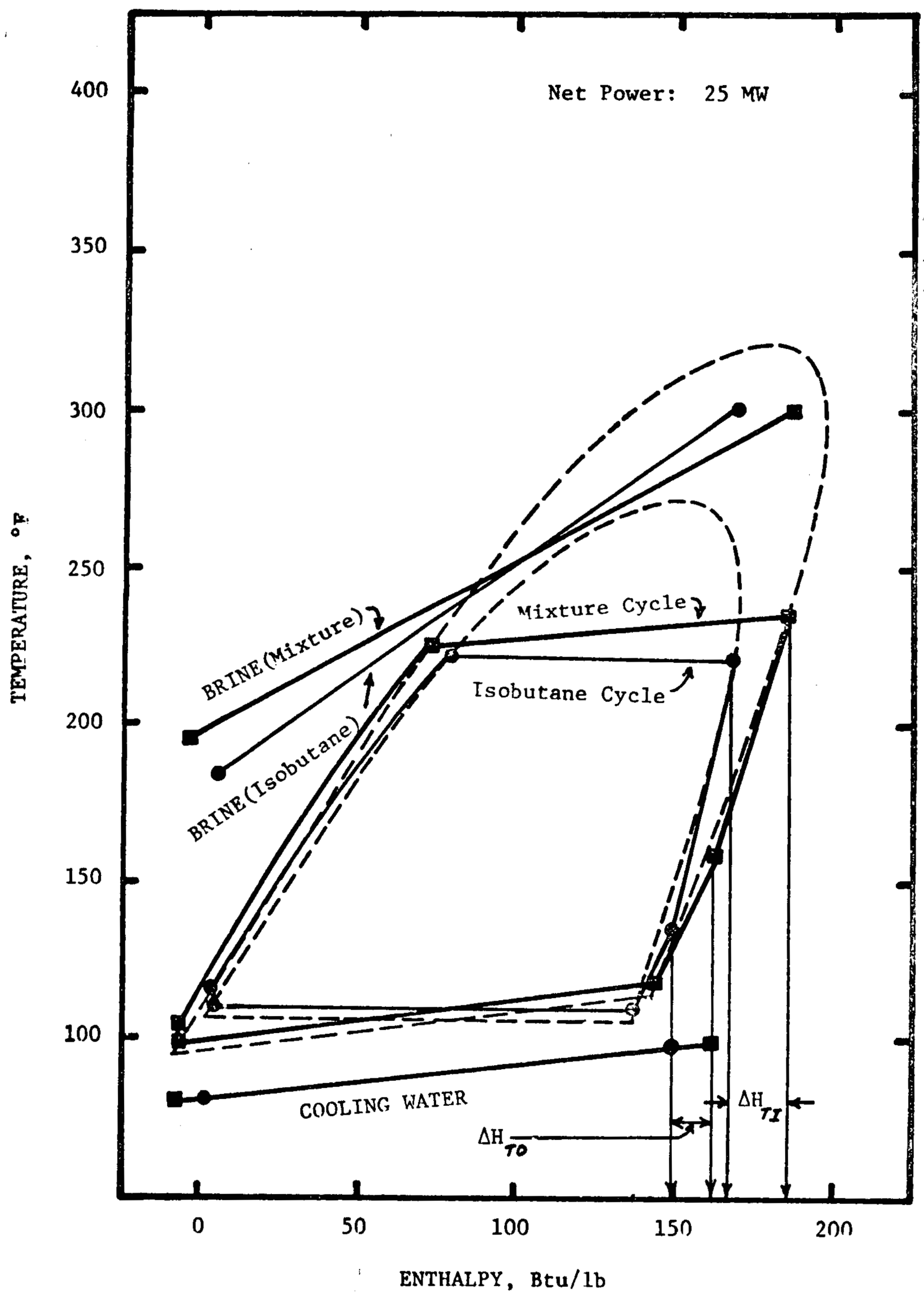

Figure 8.17 Superimposed Temperature-Enthalpy Diagram of Isobutane and Mixture (50% isobutane-50% isopentane) Cycle

for isobutane. This is because the turbine inlet pressure to achieve a given turbine inlet temperature is smaller for isopentane that isobutane (by a factor of about one third), leading to lower brine heat exchanger cost per unit area and a smaller LMTD for the isopentane cycle. This lower cost per unit heat transfer surface area for the brine heat exchanger also allows a larger brine exit temperature for the economic optimum for the isopentane cycle. For binary mixtures of isobutane and isopentane, the near optimal brine heat exchanger LMTD's and brine exit temperatures fall between the pure fluid cycle values. It is interesting to note that the bubble point temperature of the working fluid in the brine heat exchanger is virtually independent of working fluid composition (within a few degrees F) for a given georesource temperature (see Tables 8.1-8.4). The fact that the isobutane-isopentane mixture vaporization curve is nonisothermal then yields a larger enthalpy at the turbine inlet than would be obtained for pure isobutane (see Figure 8.17). It was noted previously with reference to Figure 8.17 that the mixture has a larger enthalpy than isobutane at both the turbine inlet and exit, but the enthalpy drop in the turbine is greater for the mixture because the enthalpy difference is greater at the turbine inlet. Similarly, isopentane has a larger enthalpy than the mixture at both the turbine inlet and exit but because the difference is greater at the turbine exit, the enthalpy drop for the mixture is greater than for pure isopentane.

8.6.3 brine heat exchanger and condenser temperature differences

The cost optimization studies for the geothermal binary cycle (without preheater) demonstrate that optimal brine heat exchanger and condenser LMTD's (for counter current flow) vary with georesource

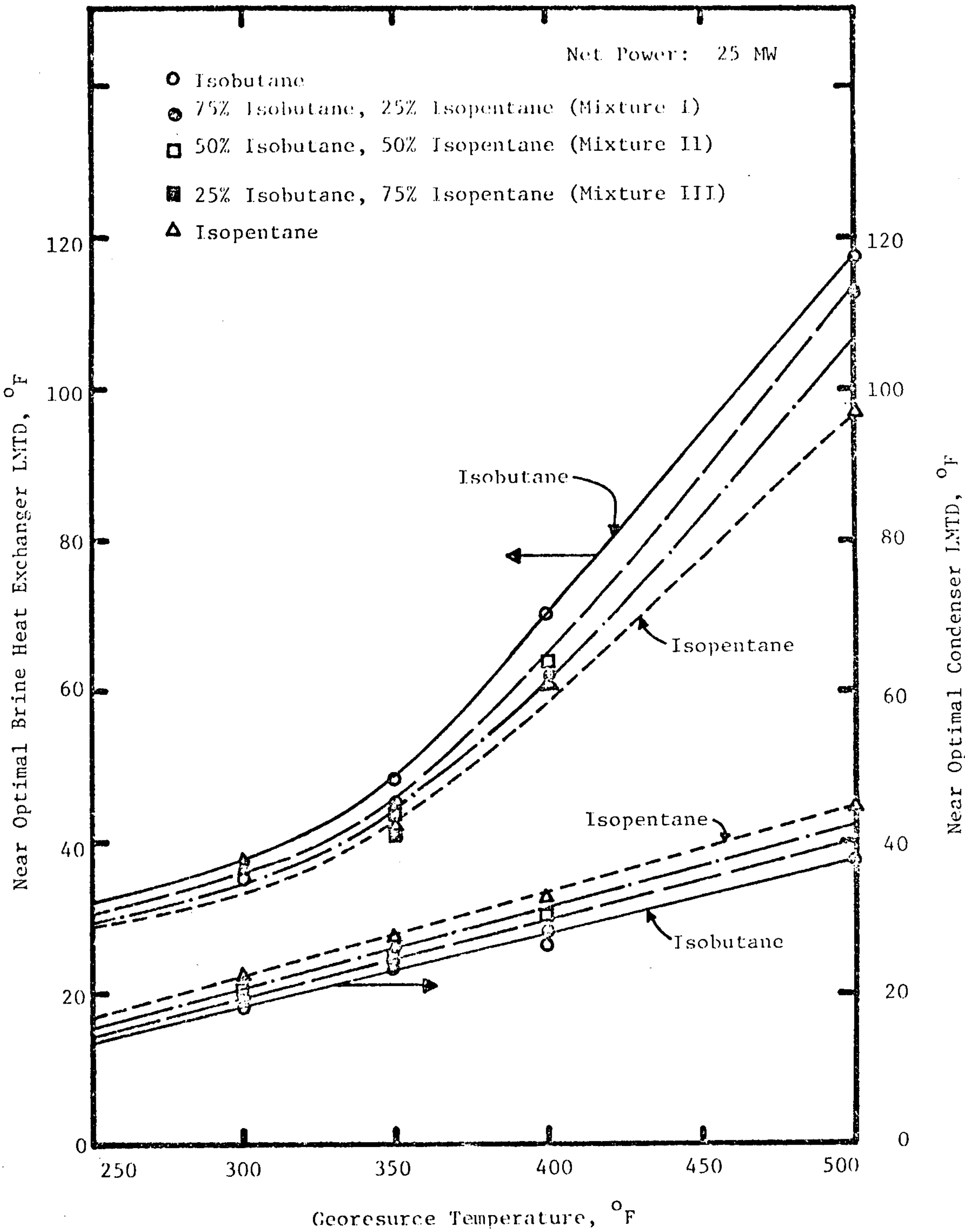

Figure 8.18 Brine Heat Exchanger and Condenser LMTD's as a Function of Georesource Temperature and Molecular Weight

temperature and molecular weight as in Figure 8.18. The major factors leading to the results in Figure 8.18 were explained in the previous subsection. The parameters which directly affect the exchanger LMTD's are the inlet and exit approach temperatures and the pinch point (or minimum) temperature difference. Since the approach temperature at the brine inlet (DTHWI) is fixed for a specified turbine inlet pressure, while the approach temperature at the brine exit is a function of the minimum approach temperature or pinch temperature difference (DTHWO), it is obvious that the pinch temperature difference is the parameter controlling the brine heat exchanger LMTD. On the other hand, the condenser LMTD can be controlled by the approach temperature at the working fluid dew point (DTCWO)or the approach temperature at the working fluid bubble point (DTCWI). The approach temperature at the working fluid dew point (DTCWO) is the pinch point temperature difference for pure fluids and mixtures for which the working fluid temperature drop is less than the cooling water temperature rise in the condensing region. The approach temperature at the working fluid bubble point (DTCWI) is the pinch point temperature difference for mixtures for which the working fluid temperature drop is greater than the cooling water temperature rise in the condensing region.

Figure 8.19 shows the effect of georesource temperature on the brine heat exchanger pinch temperature difference for isobutane, isopentane and three mixture working fluids. It can be noted that the pinch point temperature curves for isopentane and mixtures containing at least 50% isopentane are concave increasing functions of georesource temperature, whereas the pinch temperature curves for isobutane and the mixture containing 75% isobutane are concave below 400°F and

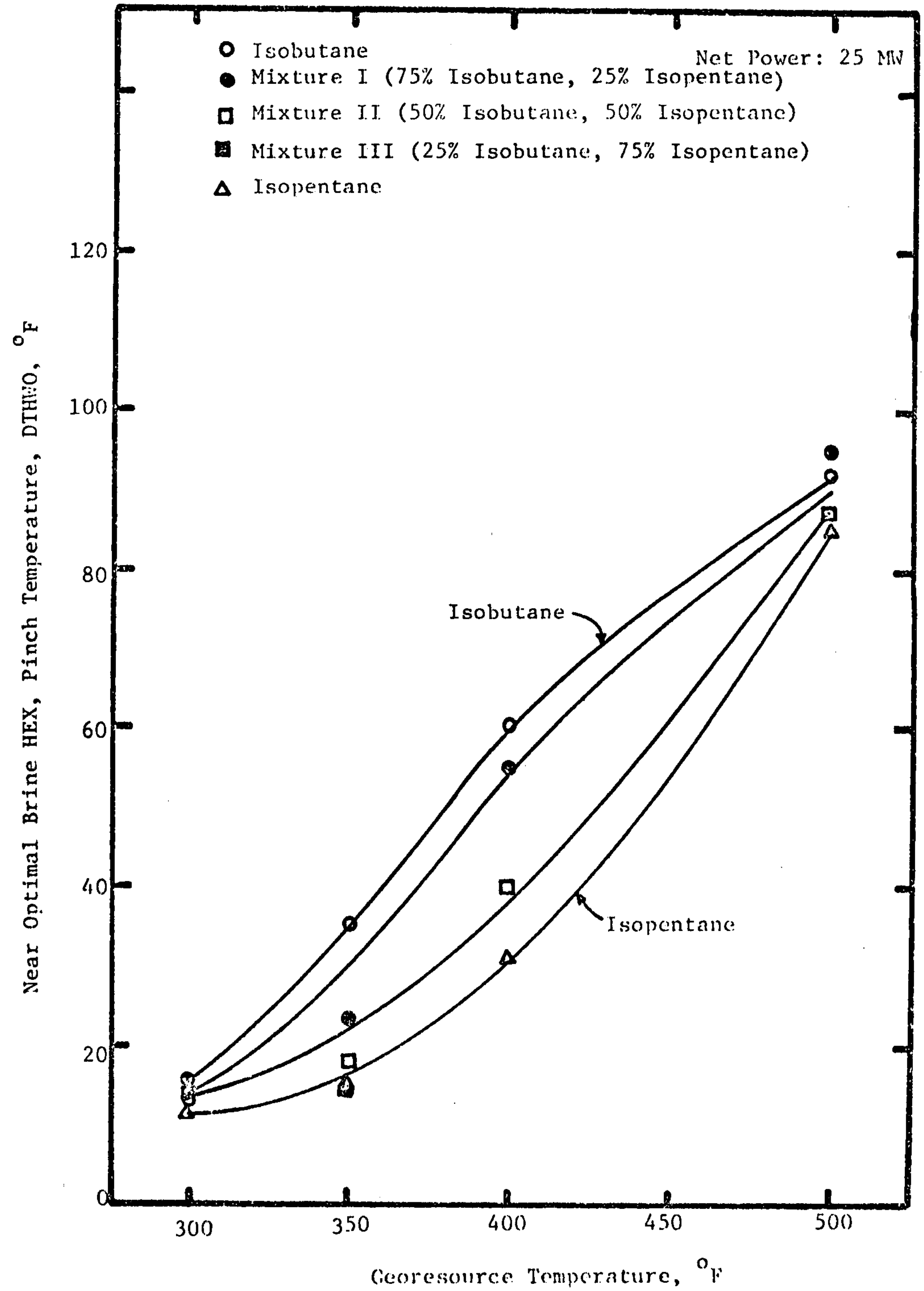

Figure 8.19 Brine Heat Exchanger Pinch Temperature DTHWO Versus Georesource Temperature and Molecular Weight

convex above 400°F. This is due to the fact that above 400°F, georesource, the isobutane and 75% isobutane - 25% isopentane cycles are supercritical. For subcritical cycles the pinch point occurs very near the working fluid bubble point in the brine heat exchanger. The pinch point occurs nearer to the brine outlet for supercritical cycles than for subcritical cycles. Because the working fluid temperature profile in the brine heat exchanger is more linear for supercritical cycles, the pinch point temperature difference plays a less dominant role in fixing the LMTD for supercritical cycles than subcritical cycles. This leads to the decreased slope of the pinch point temperature difference versus georesource temperature for supercritical cycles.

Figures 8.20 and 8.21 show the optimal condenser approach temperatures for the georesource temperature range of 300°F to 500°F for various working fluids. Both the approach temperature at the working fluid dew point, DTCWO, and the approach temperature at the cooling water inlet, DTCWI, increase almost linearly with increasing goeresource temperature for a given working fluid. For a specified working fluid and georesource temperature, the condenser pinch point temperature difference is the smaller of DTCWO and DTCWI. In most instances DTCWO is the pinch point temperature difference. It can be noted from Figure 8.20 that DTCWO values for mixtures are greater than the pure fluid values, from Figure 8.21 that DTCWI values for mixture are less than the pure fluid values and from Figures 8.18 that mixture cycle LMTD values generally fall between the pure fluid cycle LMTD values.

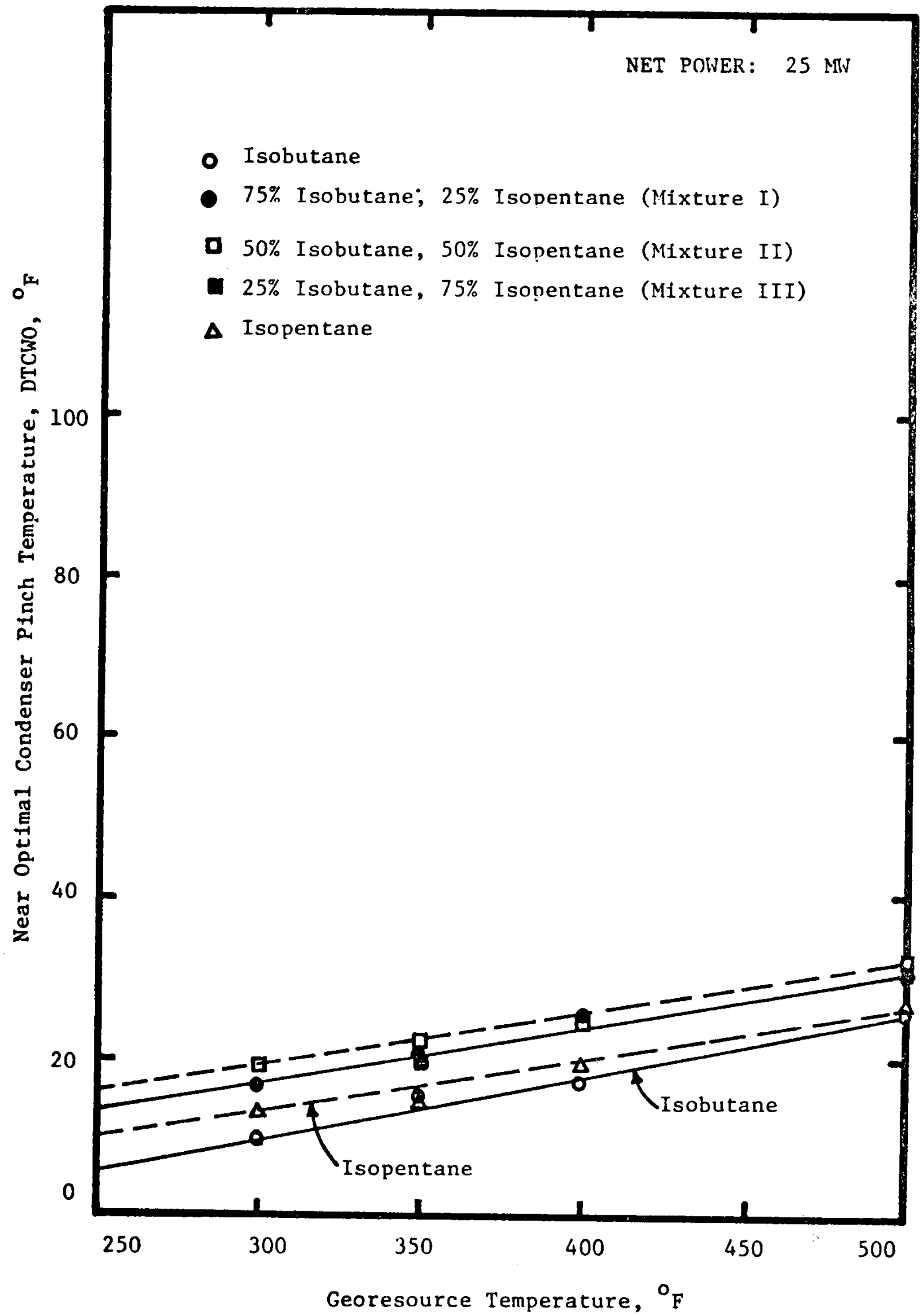

Figure 8.20 Near Optimal Condenser Pinch Temperature DTCWO Versus Georesource Temperature and Molecular Weight

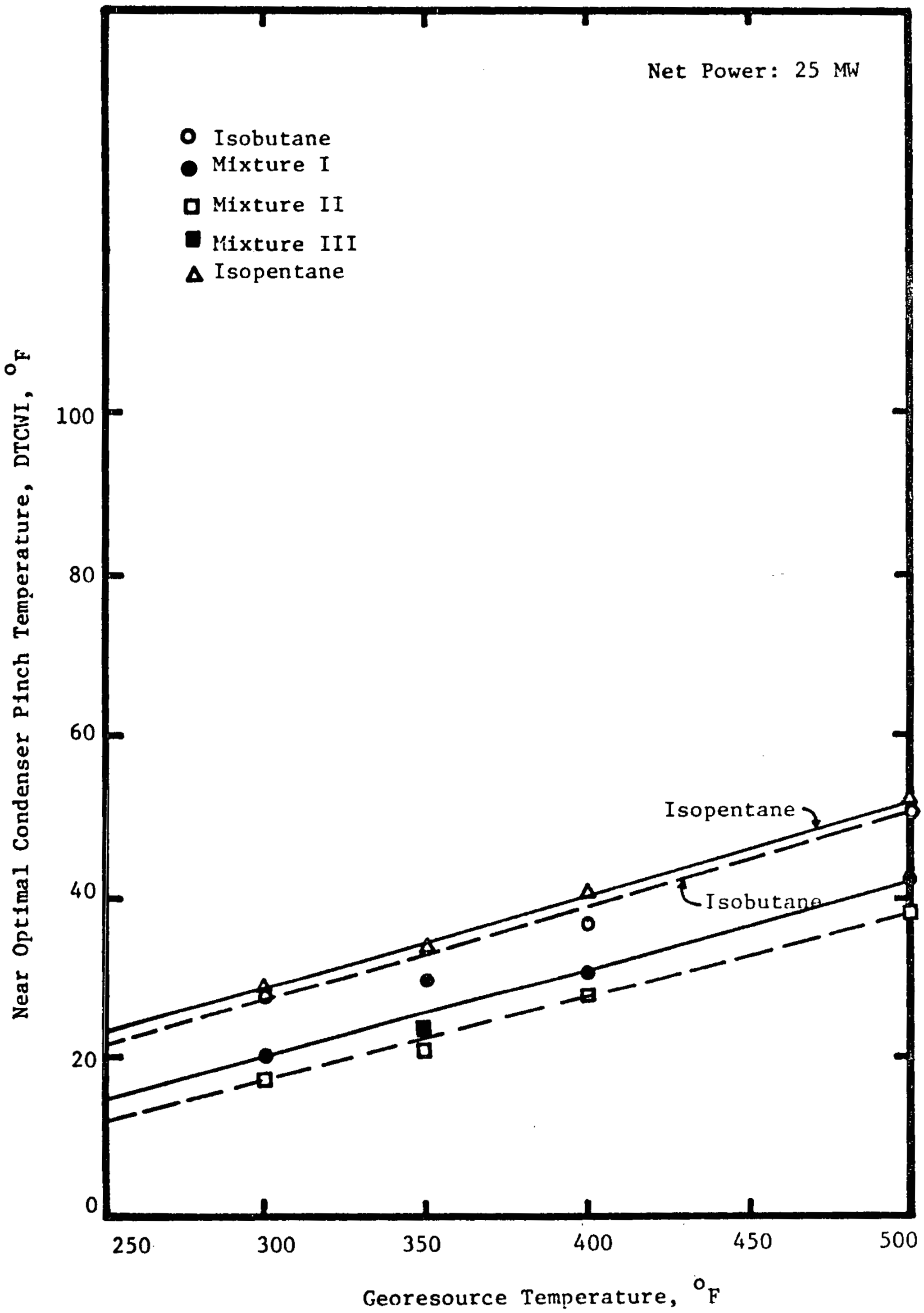

Figure 8.21 Near Optimal Condenser Pinch Temperature, DTCWI, as a Function of Georesource Temperature and Molecular Weight

8.6.4 condenser dew point pressure and temperature

The variations of condenser dew point pressure and temperature with increasing georesource temperature are plotted in Figure 8.22 for the optimized working fluid at each georesource temperature.

The dew point pressures and temperatures are almost linear between the 300° and 400°F georesource temperatures, but increase non-linearly above 400°F. The working fluid dew point temperature in the condenser is approximately equal to the sum of the cooling water exit temperature and the approach temperature at the dew point (DTCWO). The fact that the dew point temperature is approximately constant at 120°F for the optimized cycles in the 300°F to 400°F georesource range leads to the decreasing dew point pressure in this range by virtue of the fact that the optimum working fluid has an increasing molecular weight and therefore a decreasing dew point pressure at 120°F. For georesource temperatures above 400°F, the fact that the condenser LMTD and cooling water exit temperature for cost optimized cycles both increase leads to the upward trend in the working fluid dew point temperature and pressure in the condenser.

8.6.5 cooling water exit temperature

The cooling water exit temperature variation for the georesource temperature range of 300°-500°F is illustrated in Figure 8.23. The slope of the cooling water exit temperature curve for isopentane probably is greater than for isobutane because the amount of superheat at the turbine exit increases with increasing georesource temperature more rapidly for isopentane. When the superheat at the turbine exit is large, both a large condenser LMTD and a large approach temperature at the dew point (DTCWO) are possible.

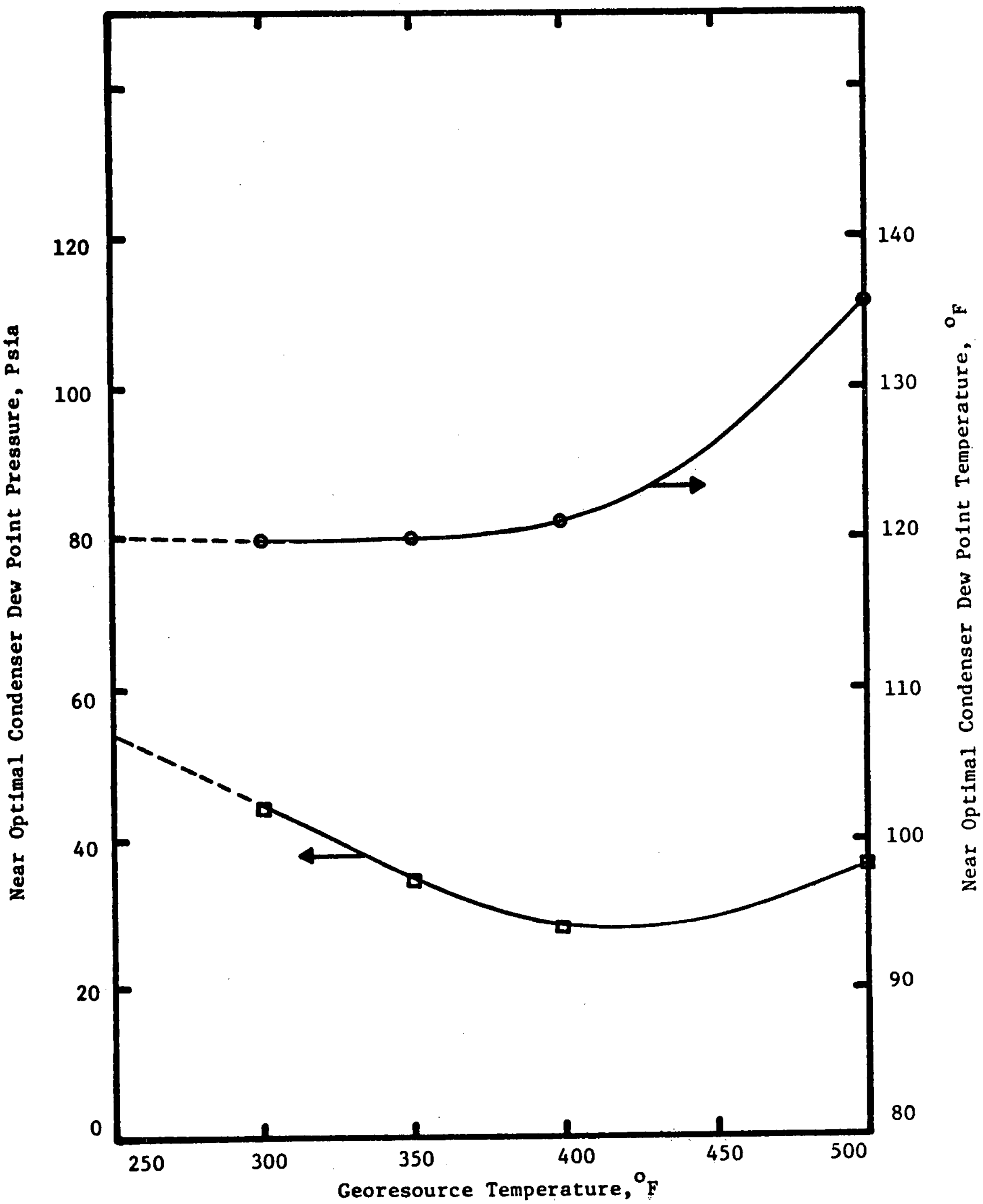

Figure 8.22 Near Optimal Condenser Dew Point Pressure and Temperature as a Function of Georesource Temperature

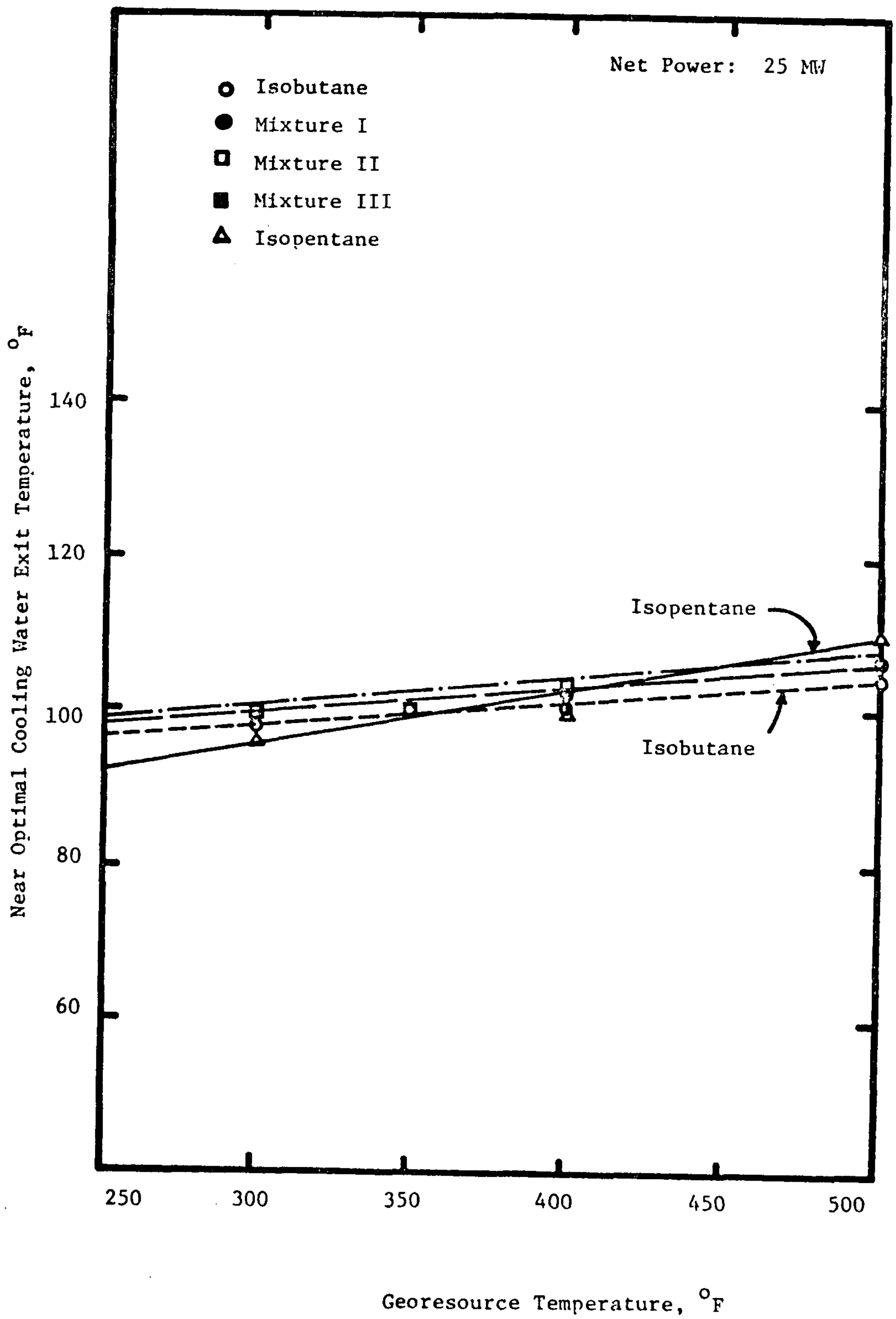

Figure 8.23 Near Optimal Cooling Water Exit Temperature Versus Georesource Temperature and Molecular Weight

8.6.6 brine heat exchanger and condenser duty

Figures 8.24 and 8.25 illustrate brine heat exchanger and condenser duty variations for various georesource temperatures versus hydrocarbon working fluid molecular weight. For Rankine cycles with efficiences as low as geothermal binary cycles, the heat exchanger duties (for a specified net work) are roughly inversely proportional to the net thermodynamic cycle efficiency. For the thermodynamic cycle, the net work (turbine plus cycle pump work), W_N, is

$$W_N = Q_H + Q_C$$

where Q_H is the brine heat exchanger duty and $-Q_C$ is the condenser duty. The net thermodynamic cycle efficiency, η, is then

$$\eta = \frac{W_N}{Q_H}$$

Thus, the following relations can be written for Q_H and Q_C,

$$Q_H = \frac{W_N}{\eta}$$

$$Q_C = W_N - Q_H = \frac{W_N}{\eta}(\eta - 1)$$

Thus, for specified W_N, Q_H is inversely proportional to η and if η is small, $-Q_C$ is roughly inversely proportional to η. This behavior of the brine heat exchanger and condenser duty is illustrated clearly in Figures 8.24 and 8.25 when these figures are compared with Figure 8.12 for the net thermodynamic cycle efficiency.

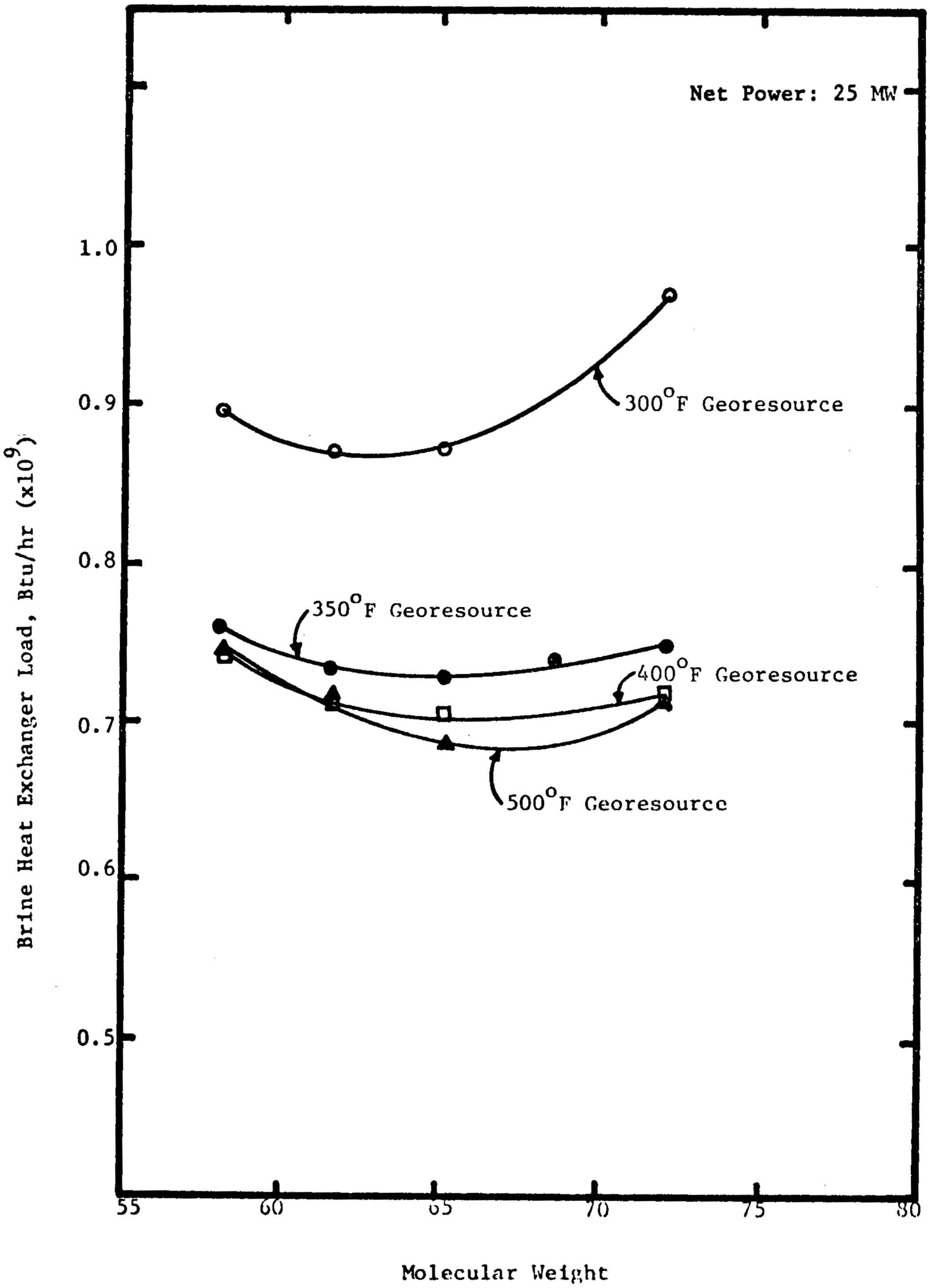

Figure 8.24 Brine Heat Exchanger Load Versus Georesource Temperature and Molecular Weight

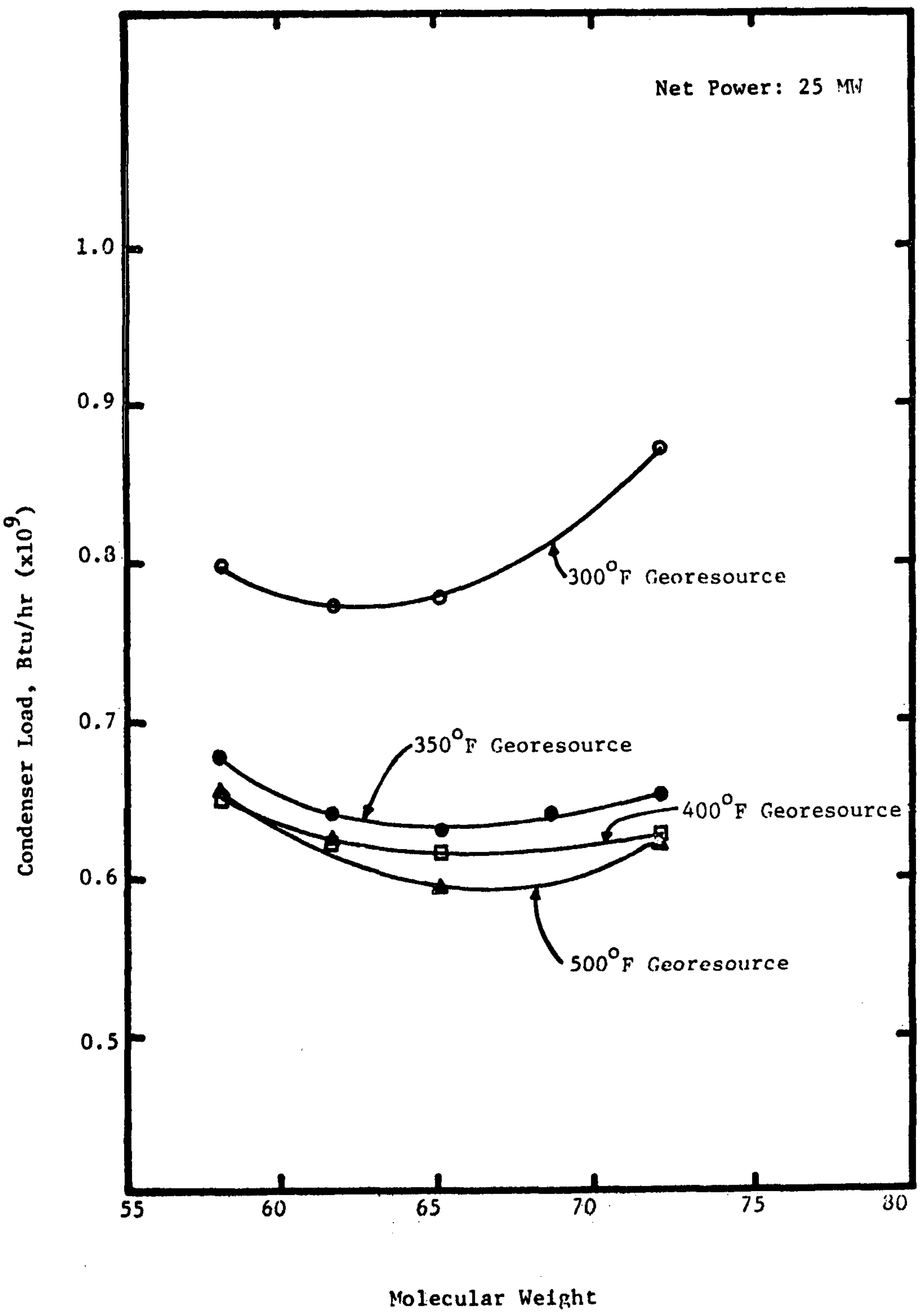

Figure 8.25 Condenser Load Versus Georesource Temperature and Molecular Weight

8.6.7 brine flow rate

Brine flow rates for various georesource temperatures are plotted versus hydrocarbon working fluid molecular in Figure 8.26. It can be noted that except for the 500°F georesource temperature, the brine flow rate increases with increasing molecular weight. This occurs because the brine heat exchanger pressure is smaller for the higher molecular weight working fluids, leading to lower heat exchanger cost per unit heat transfer surface area, thereby allowing smaller LMTD's and higher brine flow rates for the cost optimized cycles. At the 500°F georesource temperature, most of the difference between operating pressures for different working fluids is taken up by the LMTD variation, and the brine flow rate is nearly constant, whereas at 300°F, most of the difference is taken up by brine flow rate variation and the LMTD is nearly constant, as can be noted by consulting Figures 8.26 and 8.18.

Figure 8.27 shows the brine flow rate for near optimal working fluids versus georesource temperature. It can be seen from this plot that for georesource temperatures of 250°F or lower, brine flow rate requirements will increase tremendously. This is due mainly to the fact that the net extractable energy in the brine decreases sharply at lower georesource temperatures, so that large brine flow rates are needed to generate the specified power (25 MW in Figure 8.27).

8.6.8 working fluid to brine flow rate ratio

Figure 8.28 shows the effects of molecular weight and georesource temperature on the working fluid to brine flow rate ratio. For most georesource temperatures, the working fluid to brine ratio decreases

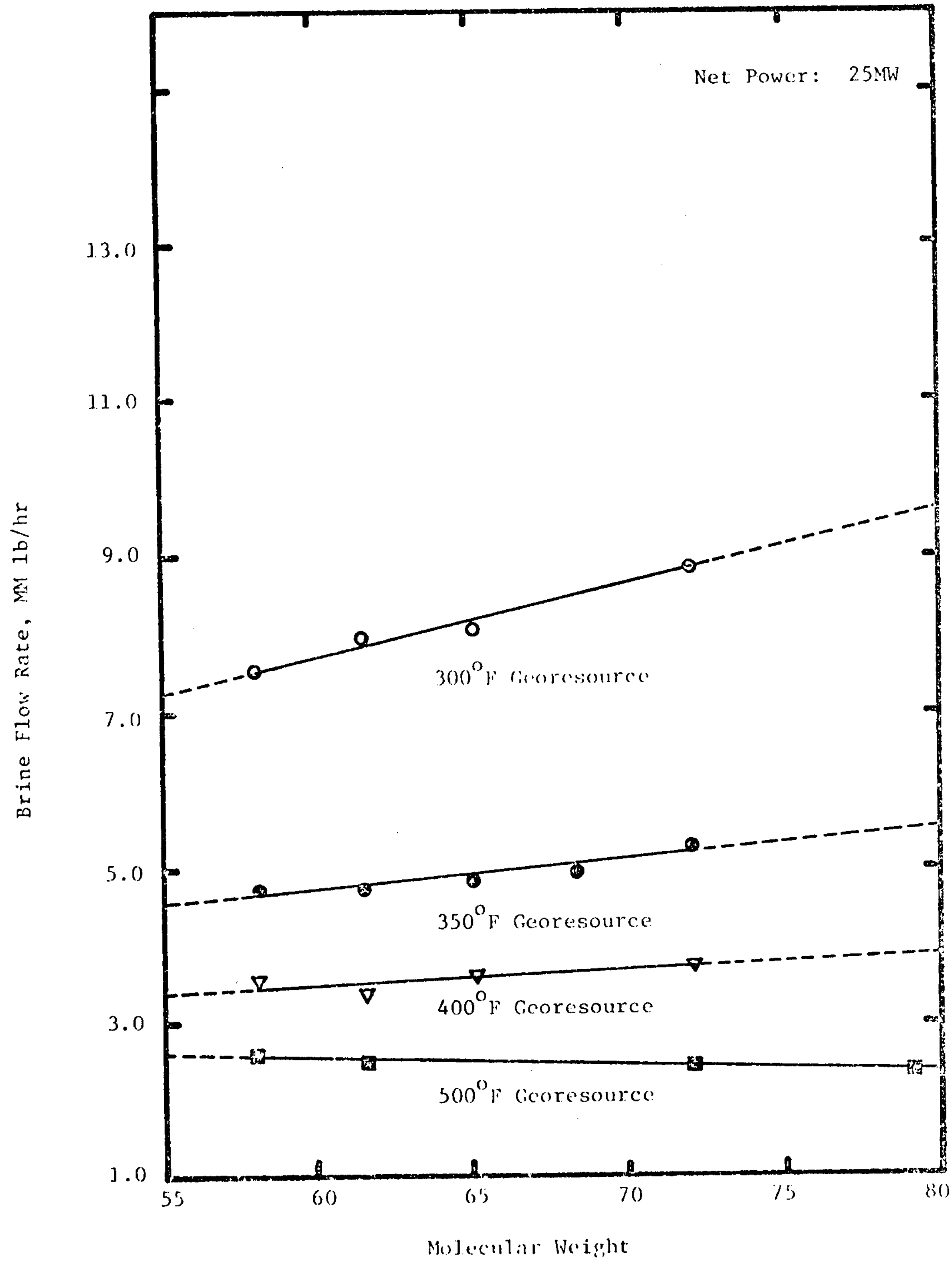

Figure 8.26 Brine Flow Rate as a Function of Georesource Temperature and Molecular Weight

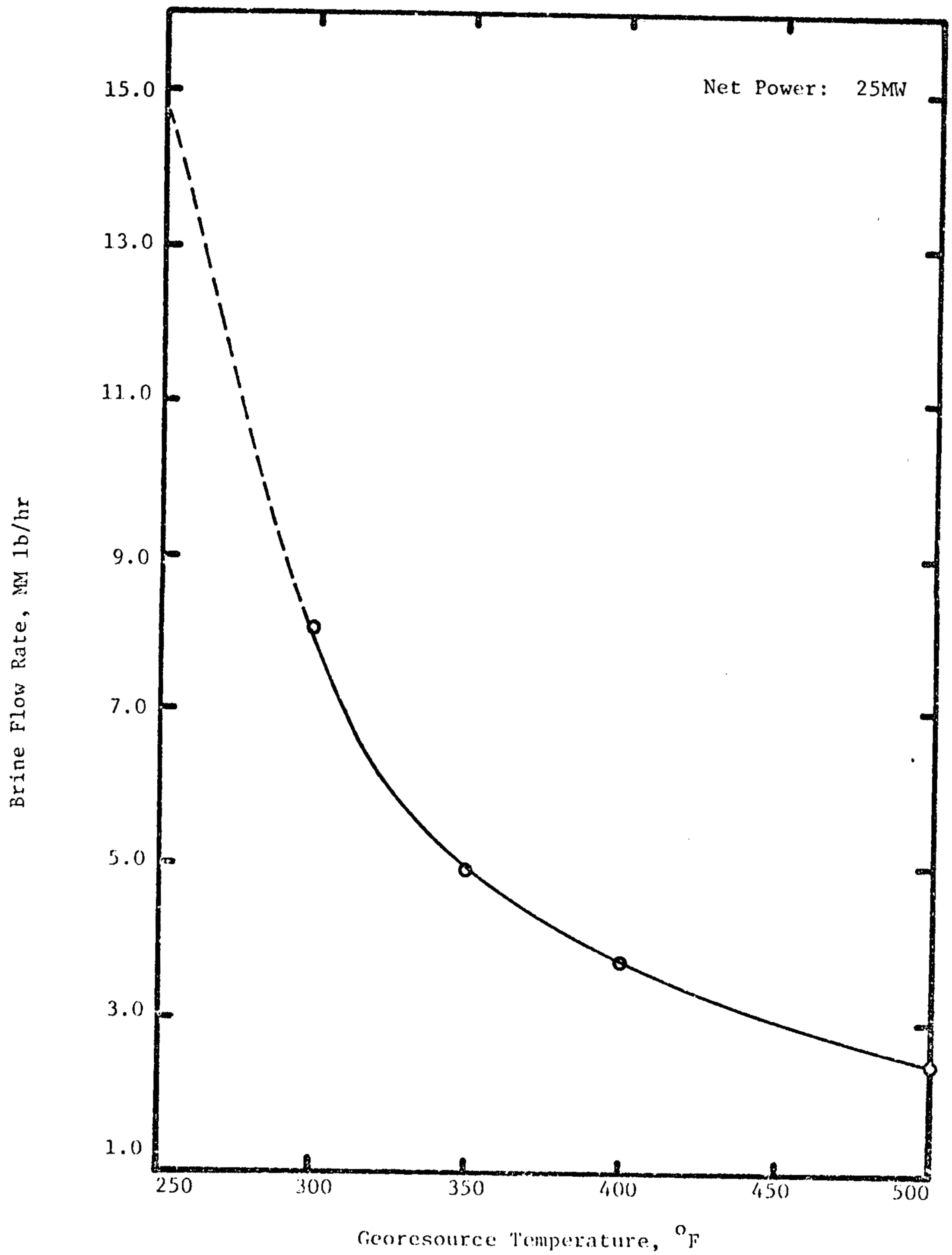

Figure 8.27 Brine Flow Rate (of Near Optimal Molecular Weight) as a Function of Georesource Temperature

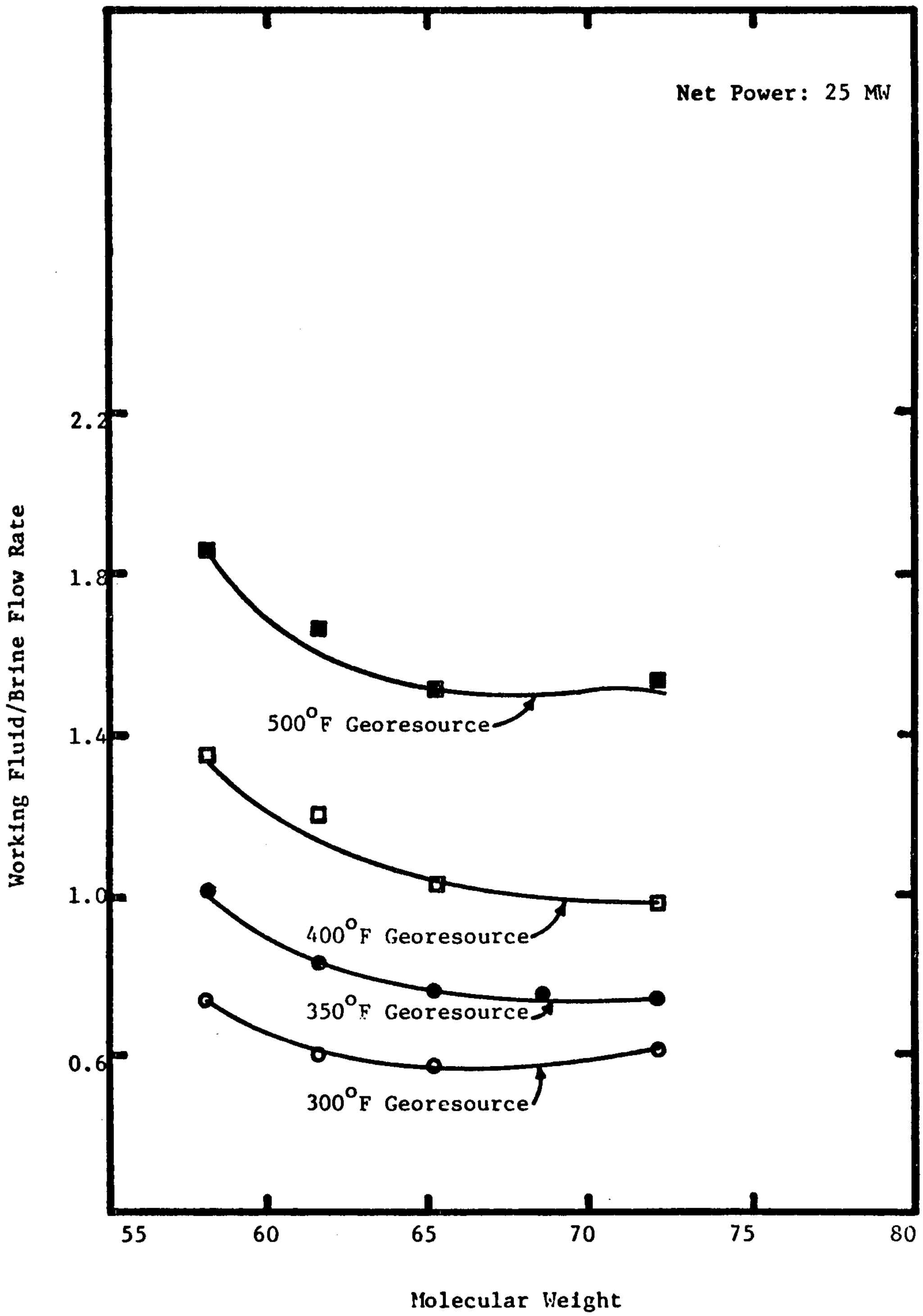

Figure 8.28 Working Fluid/Brine Flow Rate Versus Georesource Temperature and Molecular Weight

with increasing molecular weight. Even though the working fluid to brine ratio increases with increasing georesource temperature, the actual working fluid flow rates are comparatively lower at higher temperatures.

8.6.9 cooling water to brine flow rate ratio

Figure 8.29 illustrates the behavior of the cooling water to brine flow rate ratio versus hydrocarbon working fluid molecular weight for the georesource temperatures studied herein. The cooling water to brine ratio increases with increasing georesource temperature but shows somewhat erratic behavior with molecular weight. Except for the higher molecular weights for 300° and 400°F, the general trend seems to be that the ratio of cooling water to brine flow rate decreases with increasing working fluid molecular weight. The cooling water requirements are dependent upon the condenser duty and the cooling water temperature rise in the condenser, which in turn are dependent upon the condenser approach temperatures and cooling water exit temperature. Nonoptimal values of these parameters may contribute to the erratic behavior noted in Figure 8.29.

8.7 Working Fluid Selection

The calculations performed for isobutane, isopentane and isobutane-isopentane mixtures provide enough information for a preliminary correlation of near optimal working fluid characterization parameters (for the special case of the hydrocarbon working fluids and cost formulas utilized). The characterization parameters considered are the molar average molecular weight, MW, critical temperature, Tc, critical density, ρc, and acentric factor, ω. These quantities are calculated using the formulas

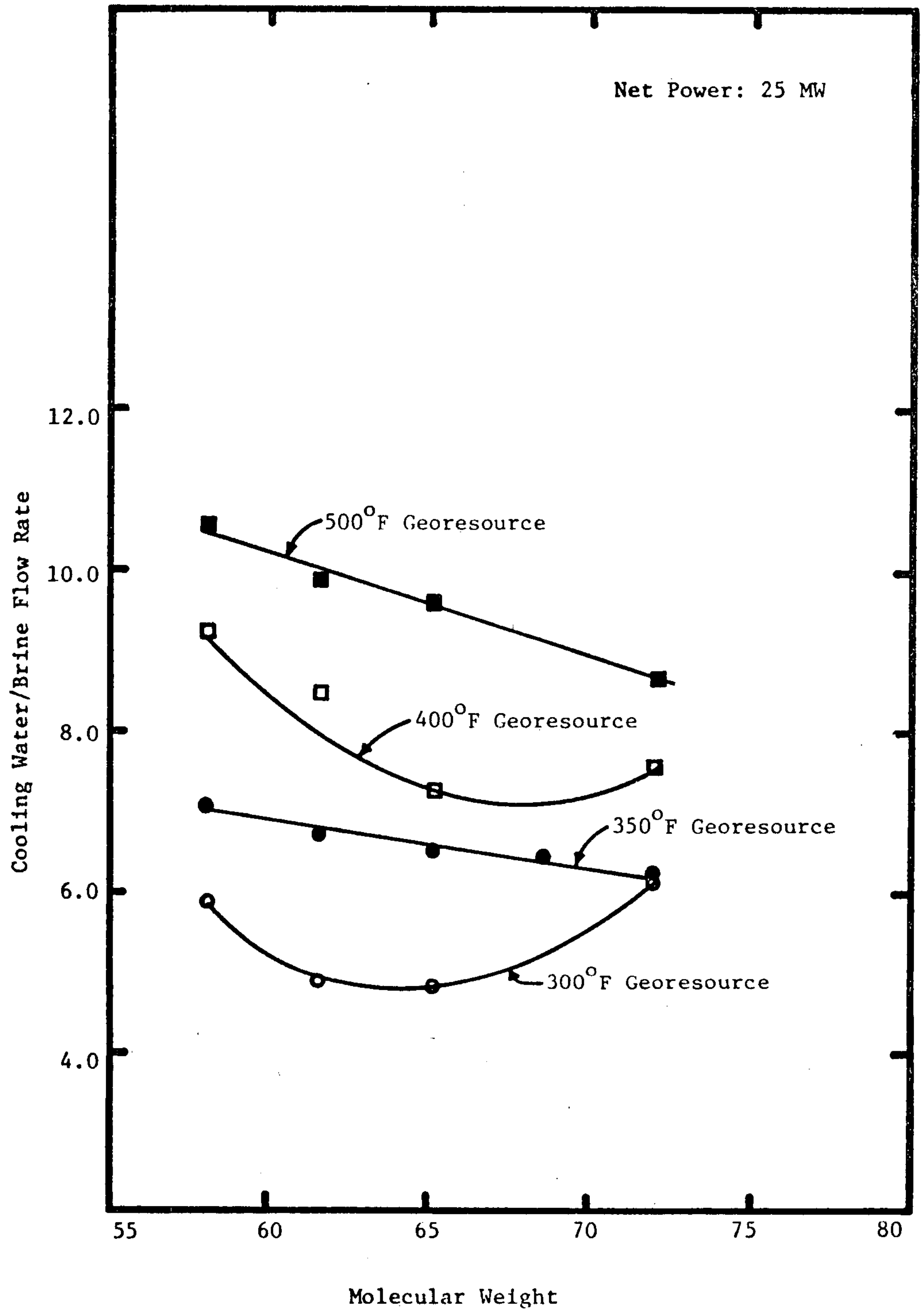

Figure 8.29 Cooling Water/Brine Flow Rate Versus Georesource Temperature and Molecular Weight

$$MW = \Sigma\ Z_i (MW)_i$$

$$T_c = \Sigma\ Z_i\ T_{c_i}$$

$$\rho_c = \Sigma\ Z_i\ \rho_{c_i}$$

$$\omega = \Sigma\ Z_i\ \omega_i$$

where $(MW)_i$, T_{c_i}, ρ_{c_i}, ω_i and Z_i are, respectively, the molecular weight, critical temperature, critical density, acentric factor and mole fraction of the ith component and the summations range over all components in the mixture (for a pure working fluid, there is only one term in the sum). Table 8.5 and Figures 8.30 and 8.31 show the values of these characterization parameters for the optimal working fluids determined in this study. Although Figures 8.30 and 8.31 can be used for working fluid selection and the previously discussed plots of parameters such as turbine inlet pressure can be used for operating conditions selection for geothermal binary cycles, caution should be exercised in such use of these results. The consideration of other classes of working fluids (such as halocarbons) will introduce additional factors (such as dipole moment effects) and the consideration of different equipment types and/or brine system and equipment cost formulas will cause translation and warping of the plots of the various parameters studied. Nevertheless, the study presented here provides perspective regarding the trends of the various parameters and the behavior of binary mixtures compared to pure fluids.

Table 8.5 Near Optimal Working Fluid Parameters for Georesource Temperature Range 300°F-500°F

Georesource Temperature (°F)	Compound	Molecular Weight	Pseudo Critical Density (lb mole/ft^3)	Pseudo Critical Temperature (°F)	Pseudo Accentric Factor
300	iC_4H_{10} = 50% iC_5H_{12} = 50%	65.13	0.2200	322.0	0.2045
350	iC_4H_{10} = 25% iC_5H_{12} = 75%	68.64	0.2113	345.5	0.2152
400	iC_4H_{10} = 15% iC_5H_{12} = 85%	70.04	0.20789	354.9	0.2216
500	iC_5H_{12}	72.15	0.2027	369.0	0.2260

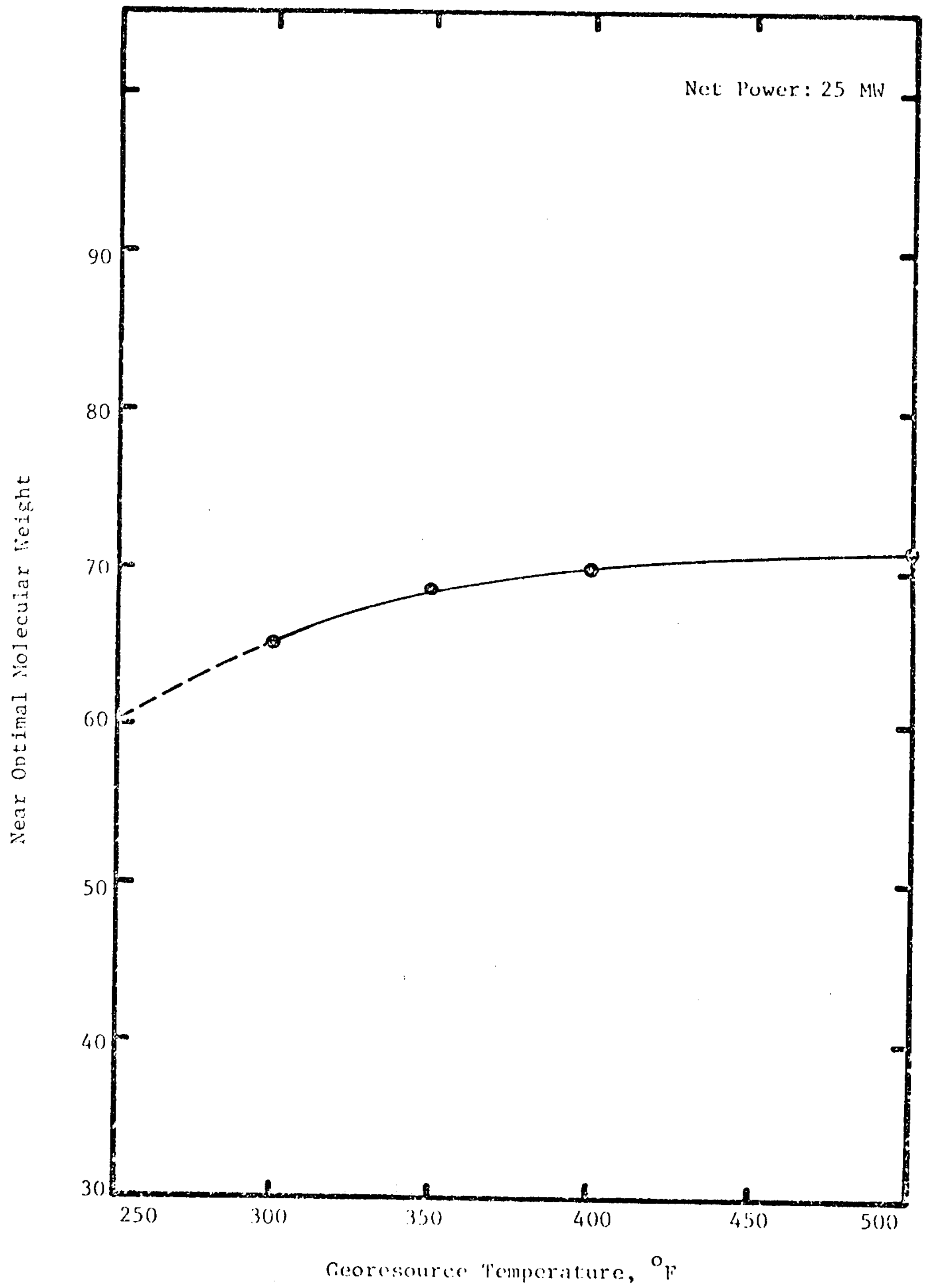

Figure 8.30 Molecular Weight as a Function of Georesource Temperature

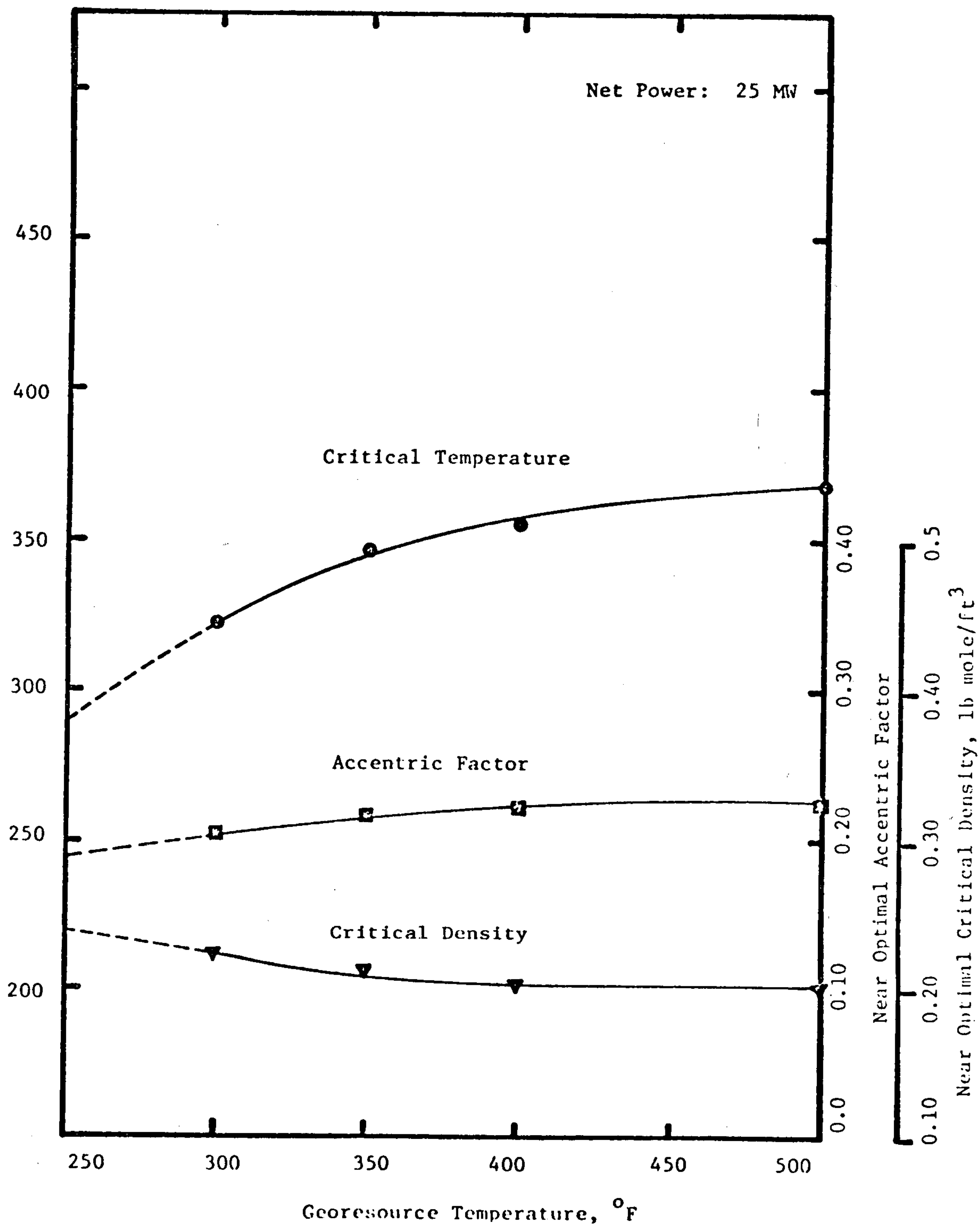

Figure 8.31 Critical Temperature, Critical Density and Accentric Factor as a Function of Georesource Temperature

9.0 PRELIMINARY STUDIES OF THE SENSITIVITY OF CYCLE DESIGN CALCULATIONS TO VARIATIONS IN THERMODYNAMIC PROPERTIES CORRELATIONS

Because there are a number of different correlations of the thermodynamic properties of working fluids, it is important to know the sensitivity of cycle design calculations to variations in the correlations used in the calculations. Eskesen (22) found that there were relatively small differences in the state conditions of isobutane in a binary cycle when the calculations were performed using the Martin-Hou equation of state with parameters determined by Milora (20) and the modified BWR equation of state (1, 23).

Because three sets of MBWR equation parameters for isobutane have been reported by the authors of this report, a preliminary study was performed in this work to evaluate the sensitivty of isobutane cycle calculations to variations in the MBWR parameters for this important working fluid. The three sets of MBWR parameters for isobutane are (a) the specific parameters published (23) in 1973, (b) the parameters obtained from the generalized correlation published (23) in 1973 and (c) the specific parameters determined (24) in 1977. The 1977 parameters (24) most accurately describe the properties of isobutane. The generalized parameters are the least accurate for prediction of pure isobutane behavior. However, for the prediction of mixture behavior, interaction parameters have been determined only for the 1973 GMBWR (generalized modified Benedict-Webb-Rubin) equation (1, 23). The thermodynamic properties computer program presented in Report ORO-4944-2 (1) utilizes the generalized parameters for mixture properties predictions and provides the option of use of the generalized or specific parameters for pure fluid calculations. The 1973 and 1977 MBWR parameters for isobutane are given in Table 9.1. The GMBWR parameters for isobutane can be calculated using the generalized correlation (1,23).

The calculations performed initially in this study were unoptimized conventional geothermal binary cycle calculations for a 300°F georesource using the same turbine inlet conditions and heat exchanger approach temperatures to determine differences in other operating conditions, equipment sizes and capital cost. The results of these calculations are summarized in Table 9.2. Because most workers have used the 1973 specific MBWR parameters in their calculations, the most important comparison of results in Table 9.2 is for the 1973 and 1977 specific parameters. It can be noted that the differences in operating conditions, equipment sizes and capital cost are small. However, comparisons for a georesource temperature of 350°F, with comparison of optimized cycles are planned for future work, to better analyze the sensitivity of cycle calculations to equation of state parameter variations.

From this preliminary study, the tentative conclusion is reached that the use of the specific MBWR parameters for isobutane published in 1973 yields geothermal binary cycle simulations which are essentially equivalent to the use of the MBWR parameters determined in 1977. The use of the MBWR parameters

Table 9.1. MBWR Parameters for Isobutane Reported in 1973 and 1977.

MBWR Equation of state parameters	Parameter Values in British Engg. System of Units	
	1973	1977
B_o	1.87890	2.026152731
A_o	37264.0	38980.20150
$C_o \times 10^{-8}$	101.413	106.58145088
γ	7.11486	9.213784536
b	8.58663	6.707625908
a	47990.7	38864.3892
α	4.23987	6.877265605
$c \times 10^{-8}$	406.763	328.2196701
$D_o \times 10^{-10}$	85.3176	147.0459327
$d \times 10^{-4}$	2168.63	618.3034445
$E_o \times 10^{-10}$	8408.60	8981.524117

Table 9.2. Comparison of Isobutane Cycle Calculations for a 300°F Georesource Using Different MBWR Equation of State Parameters.

	1973 Specific Parameters	1977 Specific Parameters
Net Power, MW	25.	25.
Brine Inlet Temperature, °F	300.	300.
Brine Exit Temperature, °F	176.6	179.7
Cooling Water Inlet Temperature, °F	80.	80.
Cooling Water Exit Temperature, °F	98.	98.
Turbine Inlet Temperature, °F	220.	220.
Turbine Inlet Pressure, psia	300.	300.
Turbine Outlet Temperature, °F	140.3	141.0
Turbine Outlet Pressure, psia	82.4	82.3
Enthalpy at Turbine Inlet, Btu/lb	170.9	171.6
Enthalpy at Turbine Outlet, Btu/lb	151.7	152.3
Enthalpy Drop in Turbine, Btu/lb	19.22	19.32
Net Thermodynamic Efficiency	10.6	10.6
Heat Transfer Surface Area, $ft^2 x10^{-3}$		
(1) Brine Heat Exchanger	105.4	102.0
(2) Condenser	205.7	204.9
Brine Flow Rate, $lb/hr x10^{-5}$	73.4	74.8
Cooling Water Flow Rate, $lb/hr x10^{-5}$	455.6	451.9
Working Fluid Flow Rate, $lb/hr x10^{-5}$	54.8	54.5
Capital Cost, $/kw	1348.	1348.

determined from the generalized correlation is not recommended for pure isobutane cycle calculations. However, at the present time, the generalized parameters should be used for mixture working fluids. Improved simultaneous correlation of pure isobutane and isobutane-isopentane mixture working fluids will be sought in future research.

10.0 CONCLUSIONS

A computer simulation program has been developed which permits detailed evaluation of geothermal binary cycles. The complex interactions between the process parameters within the power conversion cycle reaffirm the need for a simulation program in order to properly evaluate the wide range of possible operating modes. Since changing a single parameter, such as heat exchanger LMTD or turbine inlet pressure, requires corresponding changes in other cycle process equipment units, the effect of operating condition changes on total power cost and the thermodynamic efficiency is extremely complex.

The cycle operating conditions for maximum thermodynamic efficiency (Btu per pound of geothermal brine) are considerably different than the cycle operating conditions which provide minimum system plant cost ($ per kilowatt).

Using strictly thermodynamic cycle analysis, the thermodynamic efficiency is maximized through the utilization of a high pressure supercritical cycle. For a 400°F geothermal resource, approximately 55 Btu/lb of brine could be conceivably recovered using a set of cycle operating conditions which included a 1000 psia turbine inlet pressure. However, the use of higher pressure equipment results in increasing process capital cost. When minimum total system cost is the desired goal, a different set of cycle operating conditions is required. The minimum cost system includes a 500 psia turbine inlet pressure and recovers only 35 Btu per pound of brine, a considerably lower thermodynamic efficiency. Hence, the selection of cycle operating pressure must be a compromise between the desire to maximize thermodynamic efficiency and minimize power cost.

Minimizing the geothermal brine exit temperature simultaneously aids both power conversion goals, thermodynamic efficiency and minimum cost. Therefore, the brine exit temperature can be a useful parameter to cycle optimization studies.

Minimum capital cost usually occurs when the amount of superheat at both turbine inlet and exit is minimized. Minimizing the working fluid superheat at the turbine inlet means that the brine heat exchanger is optimized. Excessive superheat available in the turbine exit requires increased condenser heat transfer area. Since desuperheating the working fluid in a condenser is not efficient from a heat transfer viewpoint, the sensitivity of the condenser surface requirement to turbine exit superheat is an important consideration.

Although the major portion of the Phase II effort was directed toward development of the computer simulation, parameter sensitivity studies were included in the computer program debugging plan. These preliminary sensitivity studies were directed toward identification of the advantages and disadvantages of mixtures as cycle working fluids. It should be noted that mixtures are the rule rather than the exception when hydrocarbon systems are under consideration. The cost of obtaining reagent-grade purity in the hydrocarbon working fluid is prohibitive.

Evaluations to date indicate that working fluid mixtures can be tailored for particular geothermal resource temperatures in order to increase resource utilization; turbine inlet pressures and heat exchanger LMTD's must be optimized for each mixture composition. In addition, increasing the cooling water temperature rise above 20°F appears to enhance mixture cycles to a greater extent than pure fluid cycles. Also, mixtures offer the possibility of adjusting the mixture composition and behavior to match changes in the geothermal resource. These factors will be studied in more detail in future work.

11.0 REFERENCES

1. Fish, L.W. and Starling, K.E., "HSGC, A Mixture Thermodynamic Properties Computer Program", University of Oklahoma Report ORO-4944-2, December 1975.

2. Iqbal, K.Z., Yieh, D., Fish, L.W. and Starling, K.E., "Resource Utilization Improvement of Geothermal Binary Cycles-Phase I", University of Oklahoma Report ORO-4944-3, December, 15, 1975.

3. Starling, K.E. et.al., "Resource Utilization Efficiency Improvement of Geothermal Binary Cycles-Phase-II", University of Oklahoma Report ORO-4944-5, December, 1976.

4. McAdams, W.H., Heat Transmission, McGraw-Hill Book Company, New York, N.Y., 1954.

5. Suratt, W.B. and Hart, G.K., "Study and Testing of Direct Contact Heat Exchangers for Geothermal Brines", DSS Engineers, Fort Lauderdale, Florida, August 1976.

6. Sheinbaum, I., "Direct Contact Heat Exchangers in Geothermal Power Production", AICHE-ASME Heat Transfer Conference, San Francisco, California, August 11-13, 1975.

7. Blanding, F.H. and Elgin, J.C., Trans. A.I.Ch.E., 38, 305, 1942.

8. Sideman, S., "Advances in Chemical Engineering", 6, 20, Academic Press, New York, 1966.

9. Sakiadis, B.S. and Johnson, A.I., Ind. Eng. Chem., 46, 1229, 1954.

10. Letan, R. and Kehat, E., A.I.Ch.E. Jour., 11, 804, 1965.

11. Suratt, W.B. and Hart, G.K., "Study and Testing of Direct Contact Heat Exchangers for Geothermal Brines", DSS Engineers, Fort Lauderdale, Florida, January 1977.

12. Bokyo, L.D. and Kruzhilin, G.N., Int. J. Heat Mass Trans., 10, 361, 1967.

13. Perry, J.H. and Chilton, C.H., Chemical Engineers Handbook, 5th ed., McGraw-Hill Book Co., pp. 10-14, 1973.

14. Tong, L.S., Boiling Heat Transfer and Two-Phase Flow, pp. 123-126, John Wiley and Sons, New York, 1965.

15. TRW Systems Inc., "Ocean Thermal Energy Conversion Baseline System Concept", Final Report #NSF-C958, Volume 5, June 1975.

16. Starling, K.E. et.al., "Resource Utilization Efficiency Improvement of Geothermal Binary Cycles", University of Oklahoma Report ORO-4944-4, June 15, 1975-June 15, 1976.

17. Himmelblau, D.M., Applied Nonlinear Programming, McGraw-Hill Book Co., 1972.

18. Hsu, C.C., "Use of the Flexible Tolerance Method for Determination of Optimum Operating Conditions for Geothermal Binary Cycles, Including Mixture Cycles", Master's Thesis, University of Oklahoma Report ORO-4944-6, December 1977.

19. Nichols, K.E., "Turbine Prime Mover Cost Model Empirical Equation, P.O. 11Y-49428V", Barber-Nichols Engineering Co., Awada, Colorado, March, 1975.

20. Milora, S.L. and Tester, J.W., Geothermal Energy as a Source of Electric Power, MIT Press, 1975.

21. Ingvarsson, I.J. and Turner, S.E., "Working Fluid and Cycle Selection Criteria for Binary Geothermal Power Plants with Resource Temperature in the Range of 220-400°F", TREE-1108, Idaho National Engineering Laboratory, Idaho, April, 1977.

22. Eskesen, J.H., "Study of Practical Cycles for Geothermal Power Plants", Contract No. E (11-1)-2619, General Electric Co., Schenectady, New York, April 1976.

23. Starling, K.E., Fluid Thermodynamic Properties for Light Petroleum Systems, Gulf Publishing Co., Houston, Texas, 1973.

24. Starling, K.E., Goin, K.M. and Kumar, K.H., "Thermodynamic Properties of Isobutane Using a Modified BWR Equation of State", University of Oklahoma Report ORO-5249-2, December, 1977.

APPENDIX A

DESIGN BASIS ENGINEERING PARAMETERS

As noted previously, the geothermal power plant can be divided into six primary process areas. Prior to detailed investigation of the sensitivity of various process parameters on thermodynamic or economic performance indicators, it is necessary to define all of the arbitrary process parameters used in the basic plant specification. The design basis specifications are simply a list of specific process parameters which were utilized in the project evaluation. Since there is no recommended set of design basis plant specifications yet developed by the geothermal industry to aid economic comparison, the selected process design parameters for each major process item are representative of available process equipment.

A 25 Mw net output was chosen as the base plant design. In order to meet this particular power output rating whole evaluating process alternatives, several key parameters are varied, including brine flow rate, cooling water flow rate, and working fluid flow rate.

The basic design parameters used in this study to define each major cycle process unit are detailed in Table A.1.

Table A-1

DESIGN BASIS ENGINEERING PARAMETERS

I. Brine Heat Exchanger

Type and Material of Construction:

shell and tube
horizontal
carbon steel construction

Shell:

single pass
ASME design pressure = 1.25 x max. operating pressure

Tube Bundle:

1.0 inch tube outside diameter
14 B.W.G.
1.4063 inch tube pitch
single pass

Other Selected or Assumed Parameters:

brine in tube side
working fluid in shell side
minimum allowable pinch point ΔT = 10°F
working fluid fouling factor = 0.0001
brine fouling factor = 0.002
velocity of brine through tubes = 7.0 ft/sec

Heat Transfer Coefficient Correlations:

1-phase	:	Dittus-Boelter	(1)
2-phase	:	Chen's boiling cor	(2)

Pressure Drop Correlations:

1-phase	:	Kern	(3)
2-phase	:	Degance	(4)

Friction Factor Correlations:

1-phase	:	Moody	(5)
2-phase	:	Starczewski	(6)

II. Condenser

Type and Material of Construction:

Shell and tube
horizontal
carbon steel construction

Table A-1 (continued)

Shell:

single pass
ASME design pressure = 1.25 x max. operating pressure

Tube Bundle:

1.0 inch tube outside diameter
14 B.W.G.
1.4063 inch tube pitch
single pass

Other Selected or Assumed Parameters:

cooling water in tube side
working fluid in shell side
minimum allowable pinch point ΔT = 10°F
working fluid fouling factor = 0.0001
cooling water fouling factor = 0.001
cooling water velocity through tubes = 7.0 ft/sec.

Heat Transfer Coefficient Correlations:

1-phase	:	Dittus-Boelter (1)
2-phase	:	Nusselt's top tube formula (1,7)

Pressure Drop Correlations:

1-phase	:	Kern	(3)
2-phase	:	Degance	(4)

Friction Factor Correlations:

1-phase	:	Moody	(5)
2-phase	:	Starizewski	(6)

III. Turbine

axial flow type
specific speed = 80
efficiency of turbine-generator = 86%

Design Correlations:

turbine diameter, specific diameter, turbine wheel tip speed, RPM (8, 9)

IV. Generator

efficiency of generator = 98%

V. Working Fluid Pump

multi-stage centrifugal type
pump efficiency = 85%

Table A-1 (continued)

VI. Brine System

equal number of brine production and reinjection (or dry) wells
well casing diameter = 8.0 in.
brine flow rate per well = 500,000 lb/hr
brine pump efficiency = 85%
total brine system piping per 25 MW net power output = 5000 ft.

VII. Cooling System

mechanical draft cooling towers
wet bulb temperature range = 35-80°F
cooling temperature range ΔT = 10°-32°F
approach temperature = 8°F $\rightarrow$ variable
rating factor (R.F.) = 0.5 - 1.6
Design correlation : (10)

Tower Unit (TU)= GPM x R.F.
Fan Horsepower = 0.0125 BHP/TU
assumed value of R.F. = 1.0

Table A-2

DESIGN BASIS COST PARAMETERS

I. Power Plant

The factored estimate method described by Milora (11) and modified later (12) has been used:

$$C_t = \sum_i C_{ei}(1 + \sum_i f_i)(1 + \sum_j \overline{f}_j)$$

C_t = total capital investment in 1976 dollars

C_e = cost of major equipment (eg., heat exch., condenser, etc.).

f_i = factors for estimation of direct expenses, such as piping, control, etc.

$\overline{f}_j$ = factors for estimation of indirect expenses, such as fees, escalation, etc.

Cost Estimation Factors for Power Plant Used in GE04

installation	0.50
instrument/control	0.15
piping/insulation	0.75
electrical	0.10
bldgs/structures/concrete	0.15
fire control	0.05
environment	0.05
land/improvement	0.10
start up	0.05
auxiliaries	0.10
Total Direct $(1 + \Sigma f_i)$	3.00
engineering/legal	0.15
contingency	0.10
working capital	0.15
environmental/safety	0.10
overhead/escalation	0.15
Total Indirect $(1 + \Sigma \overline{f}_j)$	1.65
TOTAL	4.95

I-a Heat Exchanger and Condenser

Cost Correlation:

$$\ln(\$/ft^2) = A \ln (P_{shell}) - B \qquad (13)$$

where

for tube side pressure of 200-300 psia, A=0.4383, B=0.1297
for tube side pressure of 300-1000 psia, A=0.4092, B=0.3744
for tube side pressure of 1000-2000 psia, A=0.3461, B=1.046

Table A-2 (continued)

Note: The cost of condenser in ($\$/ft^2$) is same for shell side pressures $\leq$ 50 psia.

I-b Turbine

Turbine cost based on Barber-Nichols Company (14, 13)

$$C_{tur} = (1.04\, N_e - 0.04\, N_e^2) f_p (2.4858 \times 10^3\, n_s\, f_u\, D_T^{2.1}) + 4.7494 \times 10^2\, D_T^3 + 1.9248 \times 10^3\, D_T^2$$

where

C_{tur} = turbine cost in dollars
N_e = number of exhaust ends
n_s = number of internal stages (Pr/stage $\approx$ 0.7)
D_T = last stage pitch diameter
f_u = cost multiplier for tip speed, V_T, ft/sec.
f_p = cost multiplier for inlet pressure

$$f_u = -2.469 + 0.009\, V_T - 7.991 \times 10^{-6}\, V_T^2 + 2.446 \times 10^{-9}\, V_T^3$$

$$f_p = 6.2857 \times 10^{-5}\, P_{max} + 0.9707$$

Note: The equation for C_{tur} is considered to be valid for h/D_T (last stage blade height to pitch diameter) values up to 0.11.

I-c Generator

Cost equation is a function of generator net plant output (11,13)

$$C_G = 44893.4\, (MW_e)^{0.7}$$

where

C_G = generator cost in dollars
MW_e = net electrical output of the unit in mega watts

Note: This equation is applicable to power levels of 1 MW_e to 100 MW_e.

I-d Working Fluid Pump

Cost correlation is a function of pump power rating (11, 13)

$$\ln (\$) = 0.8751 \ln (MW_e) + 11.0$$

Table A-2 (continued)

where
MW_e = working fluid pump power rating in mega watts.

I-e Cooling Tower

Cost of Cooling Tower in dollars = 3.33 TU (10)

II. Brine System

The factored estimate method described by Milora (11) has been used:

$$C_B = \eta_w C_w (1 + f_w)(1 + f_I^*)$$

C_B = total brine system capital investment

C_w = cost of a geothermal production and/or reinjection well

η_w = number of wells required for a particular size plant

f_w = factor which accounts for piping from the wellhead to the power plant

f_I^* = indirect cost factors, eg., costs associated with drilling exploratory holes, contingencies, etc.

Cost Estimation Factors for Brine System used in GEO4

piping (wellhead to plant)	0.24
Total Direct (1t f_w)	1.24
land acquisition (leasing, legal fees)	0.19
drilling exploratory holes (1 out of 4 successful)	0.14
surface exploration (geophysical-geochemical)	0.10
contingency	0.13
Total Indirect (1 + f_I^*)	1.56
TOTAL	1.934

well cost:
a well cost (C_w) of $500,000/well was used with a brine flow rate of 500,000 lb/hr per well.

REFERENCES

1. McAdams, W.H., Heat Transmission, 3rd ed. McGraw-Hill Book Company, New York, 1954.

2. Tong, L.S., Boiling Heat Transfer and Two-Phase Flow, John Wiley and Sons Inc., New York, 1965.

3. Kern, D.Q., Process Heat Transfer, McGraw-Hill Book Company, New York, 1950.

4. Degance, A.C., Atherton, R.W., Chemical Engineering, March 23, 1970.

5. Moody in Parker, J.D. et.al., Introduction to Fluid Mechanics and Heat Transfer, Addison-Wesley Pub., p. 232, 1969.

6. Starczewski, J., Hydrocarbon Processing, p. 147, June, 1971.

7. Short, B.E., and Brown, H.E., 27, "General Discussion on Heat Transfer", London ASME, New York (1951).

8. Anderson, J.H., Report No. NSF/RANN/SE/GI-34979/7316, University of Massachussets, May, 1973.

9. Anderson, J.H., Report No. NSF/RANN/SE/GI-34979/7317, University of Massachussetts, June, 1973.

10. West, H.H., "Private Communication, Energy Analysts Inc., Norman Oklahoma, 1977.

11. Milora, S.L. and Tester, J.S., Geothermal Energy as a Source of Electric Power, MIT Press Cambridge, Mass., 1976.

12. Starling, K.E. et.al., "Resource Utilization Efficiency Improvement of Geothermal Binary Cycles", ORO-4944-5, University of Oklahoma, June 15-December 15, 1976.

13. Starling, K.E., et.al., "Resource Utilization Efficiency Improvement of Geothermal Binary Cylces", ORO-4944-3, University of Oklahoma, June 15-December 15, 1975.

14. Nichols, K.E., "Turbine Prime Mover Cost Model Empirical Equation, P.O. 11Y-49428V", Barber-Nichols Engineering Co., Awada, Colorado, March, 1975.

APPENDIX B

Sample Computer Output

Basis: 500°F Georesource

Working Fluid: Isopentane

```
   TCW9      TCW10      THW11      THW12      PCW9      PCW10      PHW11      PHW12
 80.0000   110.0000   500.0000   222.5000   60.0000    46.1520   700.0000   678.2530

   EFFT       EFFC      EFFHWP     EFFCWP     VELHW      VELCW
  0.8600     0.8500     0.8500     0.8500     7.0000     7.0000

  DPWF12     DPWF35     DPWF56     DPWF78     DPWF81
  0.0        2.2693     0.0        0.0       31.2279

  DPLIQS     DPLIQT     DPSTPH     DP2TUB      DP2S       DPC4      DPCW4
 14.3779     5.9927    16.6542     0.0314    16.6542     2.1851    11.1496

  DTWF12     DTWF56     DTWF78     DTHWI      DTHWO      DTCWI      DTCWO
  0.0        0.0        0.0      206.0000    75.0000    52.0000    26.0000

  DT81      DTEV2       DTS2        DT41       DT51       DTC5
 10.0000     0.2000     8.0000     5.0000     1.0000     7.0000

  DISEV      DISCND     DISCR2     TPICH1     TPICH2      FRAC      FRACND      DMWF
  0.0        0.0        0.0        1.3913     1.4362     0.1250     0.2500   200.0000

  CBRINE      COSTU      DPCTP       DPFC       DPFE      WLFACT     RF
  1.0000     3.3300    25.0000     0.2000     0.2000     1.0000     1.0000

   PWF2       PWF4      DELTAP     STRESS      COR       PIPLCW     PIPLHW      VMIN
250.0000    30.0000     0.500013500.0000     0.0      1000.0000 5000.0000     0.9000

  DITUBE     DCTUBE     FATUBE     TPITCH     ASURF      BSPACE     SPACEB     CCNDTW
  0.0695     0.0833     0.0038     1.4063     0.2183    20.0000    30.0000    93.0000

 NTPASS  NEXHAS    NSTAGE    ND       NID       MIW   NTUBEC  NTUBEV   NWPRCD     NWREIN          GC
     1       1        0      10        5         4       0       0   0.0        0.0          0.41700D 09

  FOULEV     FOULC      FOULHW     FOULCW     TCRUST     GRADIN      FWP       SSPEED
  0.0001     0.0001     0.0020     0.0010     0.0        0.0        0.0       80.0000

   DEQFI(I), I=1,ND
       0.5000     0.1500     0.7500     0.1000     0.1500     0.0500     0.0500     0.1000     0.0500     0.1000

   DIEQF(I), I=1,NID
       0.1500     0.1000     0.1500     0.1000     0.1500

   DIWEL(I), I=1,MIW
       0.1900     0.1400     0.1000     0.1300

    MHW           FPWELL        DPMAXE          DPMINE          DPMAXC         CPMINE                  IHWP
 0.240790D 07     138.88          0.0             0.0             0.0            0.0                     1

 DTPHI     DTPHO      VELWFT     DISPH      HEFFEC     TPICH      NTUBPH     NOPT
 0.0       0.0        1.0000     0.0        1.0000     1.4063        0          0

    WBASE     FIXCHG      OPCHG      FLOAD      PRMAX       EPSW      EPSDPW     EPSDPP
    25.00       0.18       0.01       0.85       0.92   0.10D-03   0.50D-01   0.50D-01

IPROC  IRESRS
  1      1

   EPSO           EPSV           FUGERR           EPSS          STEP           DMAX
 0.10000D-06    0.20000D-06    0.20000D-06    0.10000D-05     1.0000         3.0000

  NC NPHASE      ITHM        ITMAX        IPRNT       NPRINT       NCOS       IDPRNT
  2    4         30          9            0           0            1          0

COMP               IDCOM  CMW        TC            ACF        CD        PC         TBP
ISOPENTANE           3    72.1460   369.0000      0.2260     0.2027   490.4000    82.4000
CI      27.6234     -0.315040D-01    0.469884D-03  -0.582830D-07    0.102985D-10  -0.294850D-15    0.871908
ISOBUTANE            2    58.1200   274.9600      0.1830     0.2373   529.1000    11.0300
CI      13.2866      0.366370D-01    0.349631D-03   0.536100D-08   -0.298111D-10   0.538662D-14    0.609350
CKIJ     0.0008

   Z(ISOPENTANE       ) =     0.999990

   Z(ISOBUTANE        ) =     0.100000D-04
```

****SUMMARY OF GEO-4 INPUT****

TEMPERATURE (DEG F)		
INLET COOLING WATER	TCW9	80.0000
OUTLET COOLING WATER	TCW10	110.000
INLET BRINE	THW11	500.000
OUTLET BRINE	THW12	222.530
CRUSTAL OR AMBIENT	TCRUST	0.0
PRESSURES (PSIA)		
INLET COOLING WATER	PCW9	60.0000
OUTLET COOLING WATER	PCW10	46.1520
INLET BRINE	PHW11	700.000
OUTLET BRINE	PHW12	678.253
WORKING FLUID AT BHE OUTLET	PWF2	250.000
WORKING FLUID AT CONDENSER INLET	PWF4	30.0000
TEMPERATURE DIFFERENCES (DEG F)		
WORKING FLUID (WF)		
BHE OUTLET AND TURBINE INLET	DTWF12	0.0
COND OUTLET AND CYC PUMP INLET	DTWF56	0.0
CYC PUMP OUTLET AND BHE INLET	DTWF78	0.0
BRINE HEAT EXCHANGER (BHE)		
BRINE INLET MIN APPROCH	DTHWI	206.000
INTERNAL PINCH POINT	DTHWO	75.0000
SECTION 1&3-EACH SUBSECTION	DT81	10.0000
SECTION 2-EACH SUBSECTION	DTEV2	0.200000
SECTION 2-BRINE AND WF	DTS2	8.00000
PRE-HEATER		
PRE-HEATR INLET MIN APPROACH	DTPHI	0.0
PRE-HEATR OUTLET MIN APPROACH	DTPHO	0.0
CONDENSER (COND)		
COOLING WAT INLET MIN APPROCH	DTCWI	52.0000
COOLING WAT OUTLET MIN APPROCH	DTCWO	26.0000
SECTION 1-EACH SUBSECTION	DT41	5.00000
SECTION 2-EACH SUBSECTION	DT51	1.00000
SECTION 2-WF AND WALL	DTC5	7.00000
PRESSURE DIFFERENCES (PSIA)		
WORKING FLUID (WF)		
BHE OUTLET AND TURBINE INLET	DPWF12	0.0
CONDENSER (TOTAL)	DPWF35	2.26930
COND OUTLET AND CYC PUMP INLET	DPWF56	0.0
CYC PUMP OUTLET AND BHE INLET	DPWF78	0.0
BHE (TOTAL)	DPWF81	31.2279
BHE WF INLET AND BUBBLE POINT INSIDE BHE	DPLIQS	14.3779
DEW POINT AND BUBBLE POINT INSIDE BHE	DPSTPH	16.6542
SAME AS ABOVE	DP2S	16.6542
COND INLET AND DEW POINT INSIDE COND	DPC4	2.18510

BHE BRINE INLET AND		
WF BUBBLE POINT	DPLIQT	5.99270
BHE BRINE INLET AND		
WF DEW POINT	DP2TUB	0.3140000D-01
COOLING WATER AT COND INLET		
AND COOLING WATER AT WORKING		
FLUID DEW POINT	DPCW4	11.1496
BHE MAXIMUM ALLOWABLE	DPMAXE	0.0
BHE MINIMUM ALLOWABLE	DPMINE	0.0
COND MAXIMUM ALLOWABLE	DPMAXC	0.0
COND MINIMUM ALLOWABLE	DPMINC	0.0
INCREMENT FOR UP-DATING TURBINE		
OUTLET PRESSURE	DELTAP	0.500000
PRESSURE DROP IN COOLING TOWER	DPCTP	25.0000

EQUIPMENT SPECIFICATIONS

TURBINE		
EFFICENCY	EFFT	0.860000
NO OF EXHAUSTS	NEXHAS	1
NO OF STAGES	NSTAGE	0
WHEEL SPECIFIC SPEED	SSPEED	80.0000
MIN OUTLET VAPOR MOLE FRAC	VMIN	0.900000
PUMPS		
CYCLE-EFFICIENCY	EFFC	0.850000
BRINE-EFFICIENCY	EFFHWP	0.850000
COOLING WATER-EFFICENCY	EFFCWP	0.850000
BRINE HEAT EXCHANGER (BHE)		
SHELL INSIDE DIAMETER (FT)	DISEV	0.0
ONE-HALF OF (SHELL ID -		
TUBE BUNDLE OD) (FT)	FRAC	0.125000
BAFFLE SPACING (FT)	BSPACE	20.0000
NO OF TUBES	NTUBEV	0
WORKING FLUID FOULING FACTOR		
(HR SQFT DEG F/BTU)	FOULEV	0.1000000D-03
BRINE FOULING FACTOR		
(HR SQFT DEG F/BTU)	FOULHW	0.2000000D-02
BRINE VEL IN TUBES (FT/SEC)	VELHW	7.00000
PRESSURE DROP FACTOR	DPFE	0.200000
PRE-HEATER		
SHELL INSIDE DIAMETER (FT)	DISPH	0.0
NO OF TUBES	NTUBPH	0
WF VELOCITY IN TUBES (FT/SEC)	VELWFT	1.00000
PRE-HTR EFFECTIVENESS (FRAC.)	HEFFEC	1.00000
CONDENSER (COND)		
SHELL INSIDE DIA.(SEC. I).. FT.	DISCND	0.0
SHELL INSIDE DIA.(SEC.II).. FT.	DISCP2	0.0
ONE-HALF OF (SHELL ID -		
TUBE BUNDLE OD) (FT)	FRACND	0.250000
BAFFLE SPACING (FT)	SPACEB	30.0000
NO OF TUBES	NTUBEC	0
WORKING FLUID FOULING FACTOR		
(HR SQFT DEG F/BTU)	FOULC	0.100000D-03
COOLING WATER FOULING FACTOR		
(HR SQFT DEG F/BTU)	FOULCW	0.100000D-02
COOLING WATER VELOCITY IN		
TUBES (FT/SEC)	VELCW	7.00000
PRESSURE DROP FACTOR	DPFC	0.200000

```
WELLS
   TOTAL BRINE FLOW RATE(LB/HR)     MHW         0.240794D 07
   BRINE FLOW RATE/WELL(LB/SEC)     FPWELL       138.880
   NO OF PRODUCTION                 NWPROD      0.0
   NO OF REINJECTION                NWREIN      0.0
   THERMAL GRADIENT(DEG F/1000 FT) GRADIN  0.0
   WELL FACTOR                      WLFACT       1.00000
TUBES
   INSIDE FLOW AREA(SQFT)           FATUBE      0.379400D-02
   PITCH (IN)                       TPITCH       1.40625
   PITCH, IN. (PRE-HEATER)          TPICH        1.40625
   PITCH, IN. (CONDENSER  I)        TPICH1       1.39130
   PITCH, IN. (CONDENSER II)        TPICH2       1.43620
   INSIDE SURFACE AREA(SQFT)        ASURF       0.218340
   MATERIAL THERMAL CONCUCTIVITY
     (BTU FT/HR SQFT DEG. F)        CONDTW       93.0000
   NO OF PASSES                     NTPASS                 1
   INSIDE DIAMETER (FT)             DITUBE      0.6950000D-01
   OUTSIDE DIAMETER (FT)            DOTUBE      0.8333330D-01
CORROSION ALLOWANCE (IN)            COR         0.0
MAX ALLOWABLE STRESS (PSI)          STRESS       13500.0
COOLING WATER PIPING LENGTH (FT)    PIPLCW       1000.00
BRINE PIPING LENGTH (FT)            PIPLHW       5000.00
REQUIRED PLANT NET POWER (MW)       WBASE        25.0000

PROGRAM CONTROL
---------------
CONVERGENCE CRITERION
   DENSITIES                        EPSD        0.1000000D-06
   FLASH                            EPSV        0.2000000D-06
   FUGACITY                         FUGERR      0.2000000D-06
   SERCH                            EPSS        0.1000000D-05
   WF PRESSURE DROP                 EPSDPW      0.5000000D-01
   PLANT POWER                      EPSW        0.1000000D-03
   COOLING WATER AND BRINE
     PRESSURE DROP                  EPSDPP      0.5000000D-01
ITERATION
   MINIMUM NO FOR PHASE             NPHASE                 4
   MAXIMUM NO FOR THERMODYNAMIC
     SUBROUTINES                    ITNM                  30
   MAXIMUM NO FOR TURBINE AND
     BRINE FLOW RATE                ITMAX                  9
PRINT CONTROLS
   IPRNT  .NE. 0-HSGC DETAILS       IPRNT                  0
   NPRINT .NE. 0-HSGC SUMMARY TAB NPRINT                   0
   NCOS   .NE. 0-HXR PROPERTIES     NCOS                   1
   IDPRNT .NE. 0-HXR PROPERTIES
     EACH CYCLE CALCULATION         IDPRNT                 0
OPTIMIZATION CONTROL
   NOPT .LT. 0-BRINE FLOW AND
             PRESSURE DROPS
        .EQ. 0-GEO31 TYPE CALC
        .GT. 0-(SAME AS .LT.0)      NOPT                   0
MAX MOLAR DENSITY (LB-MOLE/CUFT)    DMAX         3.00000
INTITIAL FALSE POSITION STEP SIZE STEP           1.00000
WF FLOW RATE DECREMENT (LB/HR)      DMWF         200.000
BHE TYPE(1=SHELL-TUBE,2=DIR CON)    IPROC                  1
RESOURCE TYPE ( 1=BRINE,
```

```
   2= ANY OTHER TYPE )                  IRESRS                 1
BRINE PUMP REQUIREMENT (0=NO)           IHWP                   1
MAX PSEUDO-REDUCED PRESSURE             PRMAX     0.920000
INCREMENT FOR WORKING FLUID             DMWF       200.000

COST DATA
---------
NO OF MAJ EQ DIR COST FACTORS           ND                    10
NO OF MAJ EQ INDIR COST FACTORS         NID                    5
NO OF WELL INDIRECT COST FACTORS        MIW                    4
GATHERING SYSTEMS FACTOR                FWP       0.0
DIRECT COST FACTORS FOR MAJ EQ          DEQFI
   INSTALLATION                                   0.500000
   INSTRUMENT/CONTROL                             0.150000
   PIPING/INSULATION                              0.750000
   ELECTRICAL                                     0.1000000D 00
   BLDGS/STUCTURES/CONCRETE                       0.150000
   FIRE CONTROL                                   0.5000000D-01
   ENVIRONMENTAL                                  0.5000000D-01
   LAND/IMPROVEMENTS                              0.1000000D 00
   START-UP                                       0.5000000D-01
   AUXILIARIES                                    0.1000000D 00
INDIRECT COST FACTORS FOR MAJ EQ        DIEQF
   ENGINEERING/LEGAL                              0.150000
   CONTINGENCY                                    0.1000000D 00
   WORKING CAPITAL                                0.150000
   ENVIRONMENTAL/SAFETY                           0.1000000D 00
   OVERHEAD/ESCALATION                            0.150000
INDIRECT COST FACTORS FOR WELLS         DIWEL
   LAND ACQUISITION                               0.190000
   EXPLORATORY DRILLING                           0.140000
   SURFACE EXPLORATION                            0.1000000D 00
   CONTINGENCY                                    0.130000
FIXED CHARGE FACTOR                     FIXCHG    0.180000
OPERATING AND MAINTENANCE FACTOR        OPCHG     0.1000000D-01
OPERATING TIME FACTOR                   FLOAD     0.850000
UNIT COST OF BRINE                      CBRINE     1.00000
UNIT COST OF COOLING TOWER              COSTU      3.33000
RATING FACTOR FOR COOLING TOWER         RF         1.00000

COMPONENT DATA
--------------
NO OF COMPONENTS                        NC                     2
COMPONENT 1
   NAME-ISOPENTANE                      COMP
   MOLECULAR WEIGHT                     CMW        72.1460
   CRITICAL TEMPERATURE (DEG. R)        TC         828.690
   ACENTRIC FACTOR                      ACF       0.226000
   CRITICAL DENSITY(LB-MOLE/CUFT)       CD        0.202700
   CRITICAL PRESSURE(PSIA)              PC         490.400
   NORMAL BOILING POINT (DEG. R)        TBP        542.090
   MOLE FRACTION                        Z         0.999990
   IDEAL GAS POLYNOMIAL                 CI
     CI(1,1)=  27.6234         CI(1,2)=-0.3150400D-01
     CI(1,3)= 0.4698840D-03    CI(1,4)=-0.9828300D-07
     CI(1,5)= 0.1029850D-10    CI(1,6)=-0.2948500D-15
     CI(1,7)= 0.871908
COMPONENT 2
```

```
   NAME-ISOBUTANE                      COMP
   MOLECULAR WEIGHT                    CMW          58.1200
   CRITICAL TEMPERATURE (DEG. R)       TC           734.650
   ACENTRIC FACTOR                     ACF         0.183000
   CRITICAL DENSITY(LB-MOLE/CUFT)      CD          0.237300
   CRITICAL PRESSURE(PSIA)             PC           529.100
   NORMAL BOILING POINT (DEG. R)       TBP          470.720
   MOLE FRACTION                       Z           0.100000D-04
   IDEAL GAS POLYNOMIAL                CI
     CI(2,1)=  13.2866          CI(2,2)= 0.366370D-01
     CI(2,3)= 0.349631D-03      CI(2,4)= 0.536100D-08
     CI(2,5)=-0.298111D-10      CI(2,6)= 0.538662D-14
     CI(2,7)= 0.609350
INTERACTION PARAMETERS                 CKIJ
     CKIJ(1,2)= 0.800000D-03
```

***** SUMMARY OF GEO-4 SIMULATOR RESULTS *****

WORKING FLUID

COMPONENT	MOLE FRACTION
ISOPENTANE	1.0000
ISOBUTANE	0.0000

STATE POINT	LOCATION	TEMPERATURE (DEG.F)	PRESSURE (PSIA)	ENTHALPY (BTU/LB)	ENTROPY (BTU/LB-R)	VAPOR (MOLE FR.)	DENSITY (LB/FT3)
1	EVAPORATOR OUTLET	294.00	250.00	208.73	1.1922	1.0000	3.2976
2	TURBINE INLET	294.00	250.00	208.73	1.1922	1.0000	3.2976
3	TURBINE OUTLET	203.32	38.904	182.84	1.1986	1.0000	0.42016
3	DEW POINT	139.75	38.904	152.83	1.1511		
3	CONDENSER INLET	203.32	38.904	182.84	1.1986	1.0000	0.42016
4	DEW POINT	136.00	36.718	151.42	1.1502		
5	CONDENSER OUTLET	135.65	36.634	14.015	0.91949	0.0	36.469
5	BUBBLE POINT	135.85	36.634	14.131	0.91968		
6	CYCLE PUMP INLET	135.65	36.634	14.015	0.91949	0.0	36.469
7	CYCLE PUMP OUTLET	137.30	281.23	15.472	0.91985	0.0	36.590
8	EVAPORATOR INLET	137.30	281.23	15.472	0.91985	0.0	36.590
8	BUBBLE POINT	299.79	266.85	122.17	1.0771		

***** SUMMARY OF GEO-4 SIMULATOR RESULTS *****

BASIS = 1 HOUR AT 0.240790D 07 LB/HR BRINE

GROSS TURBINE WORK, MW-HR	=	27.989	NET THERMODYNAMIC EFFICIENCY, %	=	12.639
CYCLE PUMP WORK, MW-HR	=	1.5758	RESOURCE ENERGY EXTRACTION EFFICIENCY,%	=	66.063
COOLING WATER PUMP WORK, MW-HR	=	0.88773	NET THERMO. CYCLE RESOURCE UTIL. EFF.,%	=	8.3498
BRINE PUMP WORK, MW-HR	=	0.13485	PARASITIC POWER EFFICIENCY, %	=	94.653
COOLING TOWER FAN WORK, MW-HR	=	0.38972	NET WORK/AVAILABILITY, BTU/BTU	=	0.26436
NET THERMODYNAMIC CYCLE WORK, MW-HR	=	26.413	COOLING WATER FLOW RATE, LB/HR	=	0.207530 08
NET PLANT WORK, MW-HR	=	25.001	WORKING FLUID FLOW RATE, LB/HR	=	0.369060 07
HEAT INPUT TO EVAPORATOR, BTU	=	0.71323D 09	RATIO OF COOLING WATER TO BRINE	=	8.6188
HEAT REJECTED BY CONDENSER, BTU	=	0.62308D 09	RATIO OF WORKING FLUID TO BRINE	=	1.5327
TURBINE EFFICIENCY, %	=	86.000	COOLING WATER PUMP EFFICIENCY, %	=	85.000
CYCLE PUMP EFFICIENCY, %	=	85.000	BRINE PUMP EFFICIENCY, %	=	85.000
TURBINE DIAMETER, FT.	=	5.1489	COOLING WATER PIPE DIAMETER, FT.	=	1.8726
TURBINE WHEEL TIP SPEED, FT/SEC.	=	819.46	BRINE CARRYING PIPE DIAMETER, FT.	=	0.67629
TURBINE RPM	=	3065.7	LENGTH OF COOLING WATER PIPE, FT.	=	1000.0
SPECIFIC SPEED OF TURBINE	=	80.000	LENGTH OF BRINE PIPE, FT.	=	5000.0
SPECIFIC DIAMETER OF TURBINE	=	1.2894	CYCLE PUMP DISCHARGE PIPE DIAMETER, FT.	=	2.6466
LIQUID AT TURBINE OUTLET, WEIGHT %	=	0.0	BRINE INLET TEMPERATURE, DEG. F	=	500.00
LIQUID AT TURBINE OUTLET, VOLUME %	=	0.0	BRINE OUTLET TEMPERATURE, DEG. F	=	222.54

***** SUMMARY OF GEO-4 SIMULATOR RESULTS *****

NET 25.00 MW HORIZONTAL TUBE BRINE HEAT EXCHANGER SPECIFICATIONS

TUBE SIDE

TUBE OUTSIDE DIAMETER, IN.	=	1.0000
TUBE INSIDE DIAMETER, IN.	=	0.83400
TUBE PITCH (TRIANGULAR), IN.	=	1.4063
NUMBER OF TUBE PASSES	=	1
NUMBER OF TUBES	=	456
FLOW AREA, SQ.FT.	=	1.7301
VELOCITY THROUGH TUBES, FT/SEC.	=	7.0021

SHELL SIDE

SHELL INSIDE DIAMETER, FT.	=	2.6278
SHELL OUTSIDE DIAMETER, FT.	=	2.7170
EQUIVALENT DIA. FOR HEAT TRANSFER, FT.	=	0.98379D-01
EQUIVALENT DIA. FOR PRESSURE DROP, FT.	=	0.92016D-01
FLOW AREA, SQ.FT.	=	2.5361

		SECTION 1	SECTION 2	SECTION 3
WEIGHTED AVERAGE TUBE SIDE HEAT TRANSFER COEFFICIENT, BTU/HR-FT2-F	=	2551.7	3075.0	3246.9
WEIGHTED AVERAGE SHELL SIDE HEAT TRANSFER COEFFICIENT, BTU/HR-FT2-F	=	667.11	1634.9	854.73
WEIGHTED AVERAGE OVERALL HEAT TRANSFER COEFFICIENT, BTU/HR-FT2-F	=	241.20	305.03	268.33
WEIGHTED AVERAGE LOG MEAN TEMPERATURE DIFFERENCE, DEG.F	=	79.011	134.00	205.86
TOTAL HEAT TRANSFER SURFACE AREA, SQ.FT.	=	23662.	7762.2	39.547
LENGTH OF HEAT EXCHANGER TUBES, FT.	=	207.53	77.962	0.39721
TOTAL TUBE SIDE PRESSURE DROP, PSIA	=	15.605	5.8853	0.313680-01
TOTAL SHELL SIDE PRESSURE DROP, PSIA	=	14.241	16.624	0.19381

OVERALL WEIGHTED HEAT EXCHANGER LOG MEAN TEMPERATURE DIFFERENCE, DEGREES F = 96.878

OVERALL WEIGHTED HEAT EXCHANGER HEAT TRANSFER COEFFICIENT, BTU/HR-FT2-F = 258.65

***** SUMMARY OF GEO-4 SIMULATOR RESULTS *****

NET 25.00 MW HORIZONTAL TUBE CONDENSER SPECIFICATIONS

TUBE SIDE

		SECTION 1	SECTION 2
TUBE OUTSIDE DIAMETER, IN.	=	1.0000	1.0000
TUBE INSIDE DIAMETER, IN.	=	0.83400	0.83400
TUBE PITCH (TRIANGULAR), IN.	=	1.3913	1.4362
NUMBER OF TUBE PASSES	=	1	1
NUMBER OF TUBES	=	3496	3496
FLOW AREA, SQ.FT.	=	13.264	13.264
VELOCITY THROUGH TUBES, FT/SEC.	=	7.0007	7.0007

SHELL SIDE

		SECTION 1	SECTION 2
SHELL INSIDE DIAMETER, FT.	=	7.1986	7.4309
SHELL OUTSIDE DIAMETER, FT.	=	7.2414	7.4751
EQUIVALENT DIA. FOR HEAT TRANSFER, FT.	=	0.945360D-01	0.10620
EQUIVALENT DIA. FOR PRESSURE DROP, FT.	=	0.922560D-01	0.13356
FLOW AREA, SQ.FT.	=	21.631	24.300

		SECTION 1	SECTION 2
WEIGHTED AVERAGE TUBE SIDE HEAT TRANSFER COEFFICIENT, BTU/HR-FT2-F	=	1633.6	1519.3
WEIGHTED AVERAGE SHELL SIDE HEAT TRANSFER COEFFICIENT, BTU/HR-FT2-F	=	132.95	235.71
WEIGHTED AVERAGE OVERALL HEAT TRANSFER COEFFICIENT, BTU/HR-FT2-F	=	106.56	162.53
WEIGHTED AVERAGE LOG MEAN TEMPERATURE DIFFERENCE, DEG.F	=	58.096	42.442
TOTAL HEAT TRANSFER SURFACE AREA, SQ.FT.	=	18461.	73758.
LENGTH OF HEAT EXCHANGER TUBES, FT.	=	24.185	96.628
TOTAL TUBE SIDE PRESSURE DROP, PSIA	=	2.6957	11.135
TOTAL SHELL SIDE PRESSURE DROP, PSIA	=	2.1140	0.830250D-01

OVERALL WEIGHTED CONDENSER LOG MEAN TEMPERATURE DIFFERENCE, DEGREES F = 44.648

OVERALL WEIGHTED CONDENSER HEAT TRANSFER COEFFICIENT, BTU/HR-FT2-F = 151.33

SUMMARY OF GEO-4 SIMULATOR RESULTS

ESTIMATED CAPITAL COST BREAKDOWN OF MAJOR COMPONENTS
FOR A 25.00 MW GEOTHERMAL POWER PLANT MODULE

MAJOR EQUIPMENT	MM$ DIRECT	MM$ INSTALLED	PERCENT OF EQUIP CAP INV	PERCENT OF TOTAL CAP INV	$ PER KW TOTAL
TURBINE	0.4598	0.6897	4.48	3.08	18.39
GENERATOR	0.4273	0.6410	4.16	2.86	17.09
CYCLE PUMPS	0.0893	0.1340	0.87	0.60	3.57
EVAPORATOR ($16.01 PER SQ. FT.)	0.4557	0.6836	4.44	3.05	18.23
CONDENSER ($ 4.88 PER SQ. FT.)	0.4501	0.6752	4.38	3.01	18.00
COOLING WATER PUMPS	0.0541	0.0811	0.53	0.36	2.16
COOLING TOWER	0.1392	0.2088	1.36	0.93	5.57
MAJOR EQUIPMENT COST	2.0756	3.1133	20.20	13.88	83.02
SUPPORTING EQUIPMENT					
INSTALLATION	1.0378		10.10	6.94	41.51
INSTRUMENT/CONTROL	0.3113		3.03	2.08	12.45
PIPING/INSULATION	1.5567		15.15	10.41	62.27
ELECTRICAL	0.2076		2.02	1.39	8.30
BUILDING/STRUCTURES/CONCRETE	0.3113		3.03	2.08	12.45
FIRE CONTROL	0.1038		1.01	0.69	4.15
ENVIRONMENTAL	0.1038		1.01	0.69	4.15
LAND/IMPROVEMENT	0.2076		2.02	1.39	8.30
STARTUP	0.1038		1.01	0.69	4.15
AUXILIARIES	0.2076		2.02	1.39	8.30
SUPPORTING EQUIPMENT COST	4.1511		40.40	27.76	166.04
TOTAL DIRECT COST	6.2267		60.61	41.64	249.06
INDIRECT COST					
ENGINEERING/LEGAL	0.9340		9.09	6.25	37.36
CONTINGENCY	0.6227		6.06	4.16	24.91
WORKING CAPITAL	0.9340		9.09	6.25	37.36
ENVIRONMENTAL/SAFETY	0.6227		6.06	4.16	24.91
OVERHEAD/ESCALATION	0.9340		9.09	6.25	37.36
INDIRECT COST	4.0473		39.39	27.07	161.89
EQUIPMENT CAPITAL INVESTMENT	10.2740		100.00	68.71	410.95

WELLS	MM$ DIRECT	PERCENT OF TOTAL CAP INV	$ PER KW TOTAL
DRILLING/CASING (9.63WELLS)	2.4079	16.10	96.32
BRINE PUMPS	0.0104	0.07	0.42
GATHERING SYSTEM	0.5804	3.88	23.22
TOTAL DIRECT COST	2.9987	20.06	119.95
INDIRECT COST			
LAND ACQUISITION	0.5698	3.81	22.79
EXPLORATORY DRILLING	0.4198	2.81	16.79
SURFACE EXPLORATION	0.2999	2.01	11.99
CONTINGENCY	0.3898	2.61	15.59
INDIRECT COST	1.6793	11.23	67.17
WELL CAPITAL INVESTMENT	4.6780	31.29	187.12
TOTAL CAPITAL INVESTMENT	14.9520	100.00	598.07

OPERATING AND MAINTENANCE COST(CENTS/KWHR) 1.53

BASIS:
- OPER. + MAINT. RATE = 0.01
- FIXED CHARGE RATE = 0.18
- LOAD FACTOR = 0.85

-NET PLANT WORK (BTU/LB BRINE) -35.436
-NET PLANT WORK (BTU) -0.85327D 08
-NET PLANT WORK/AVAILABILITY (BTU/BTU) -0.26436

☆U.S. GOVERNMENT PRINTING OFFICE:1978 -740 -306/ 4260 REGION NO. 4